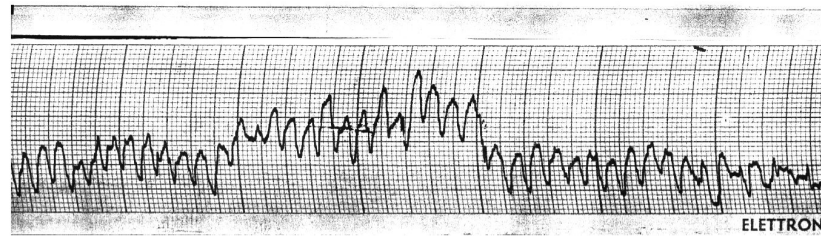
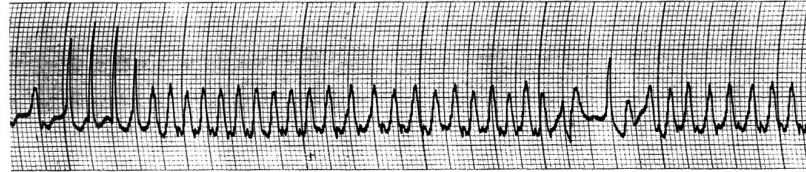


I



CARDIOLINE

II

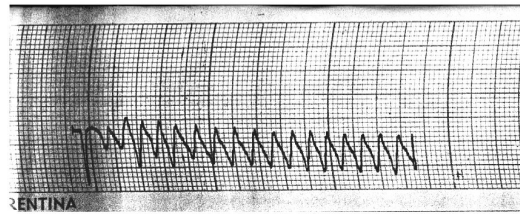


CARDIOLINE

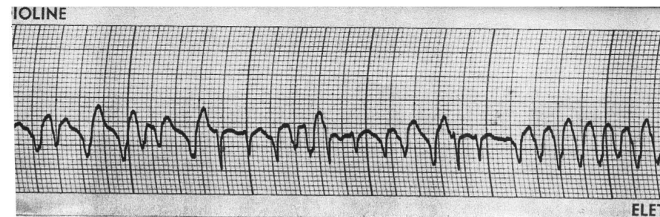
III



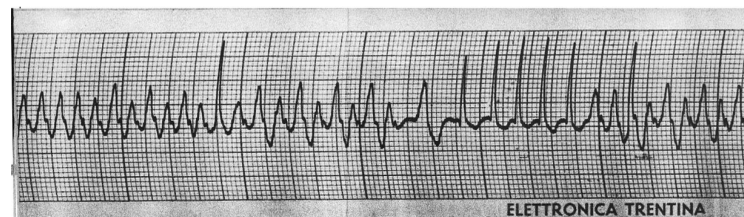
aVR



aVL

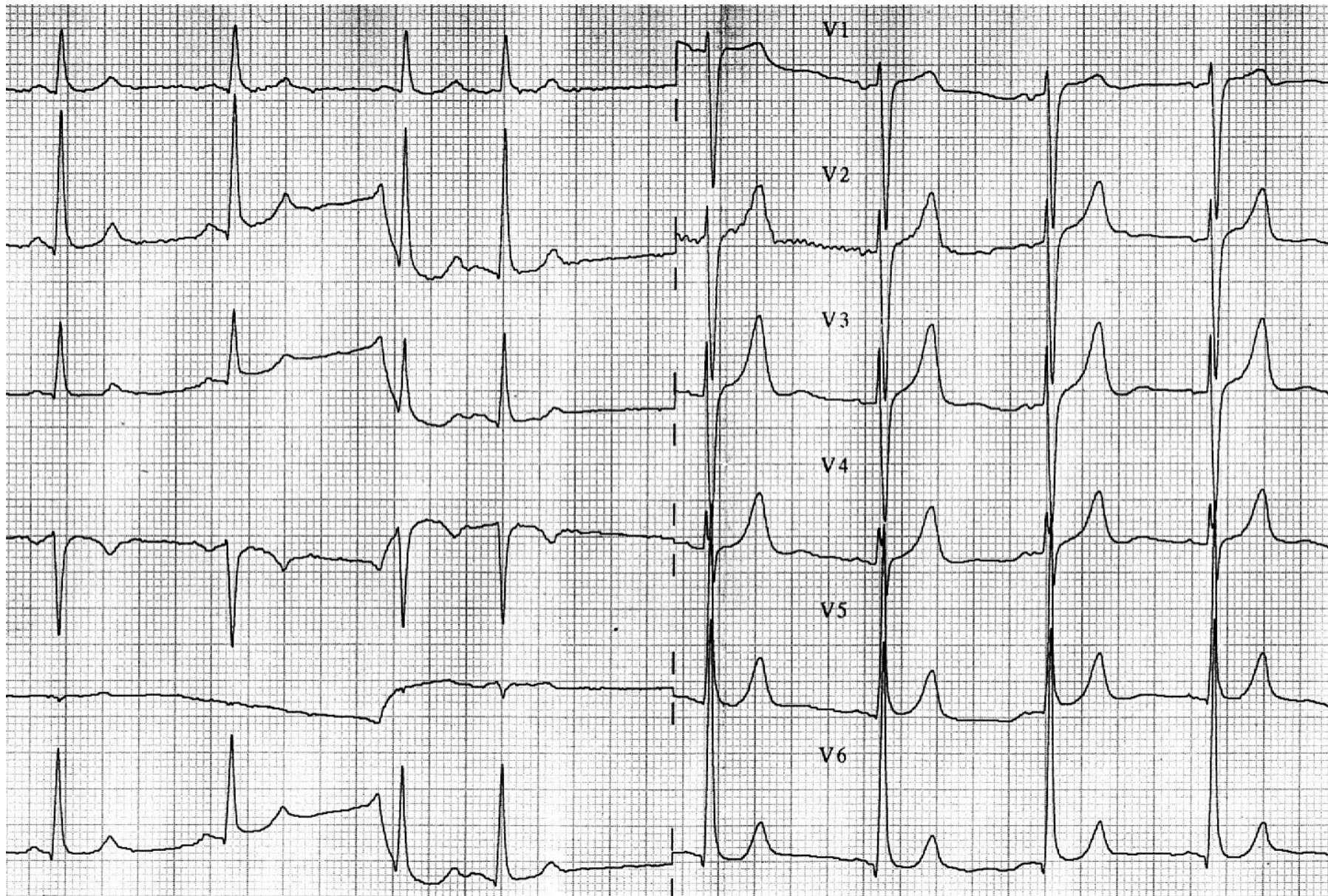


aVF

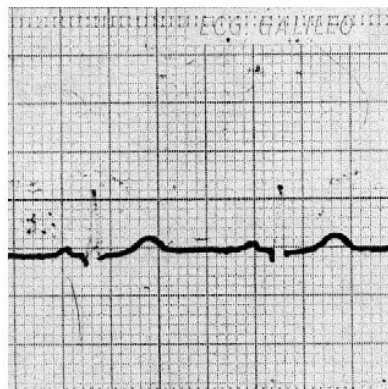


Another ICD for secondary prevention  
or  
a different analysis of ECG

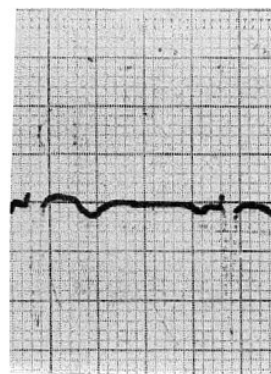




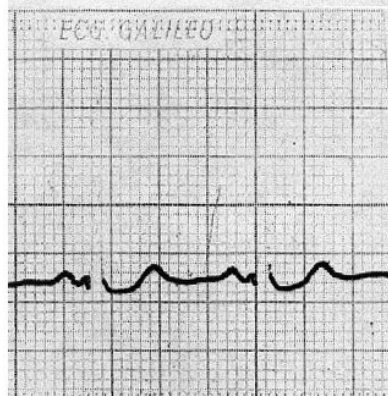
I



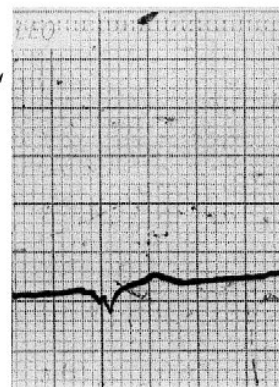
aVR



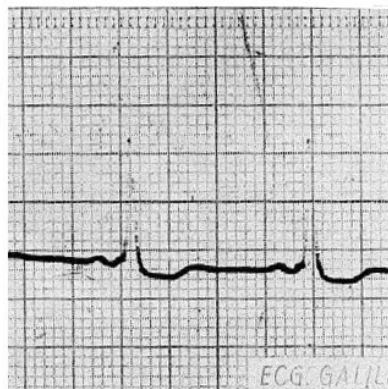
II



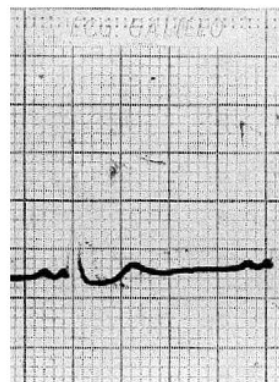
aVL



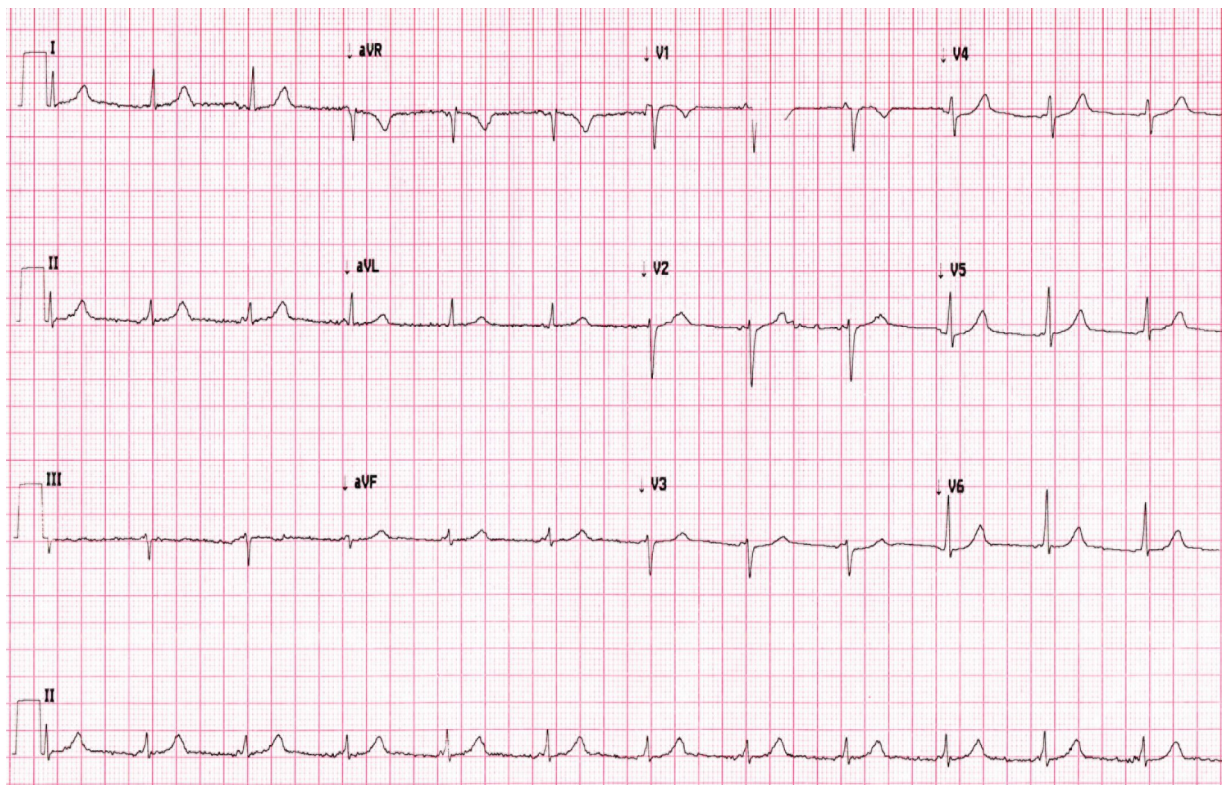
III



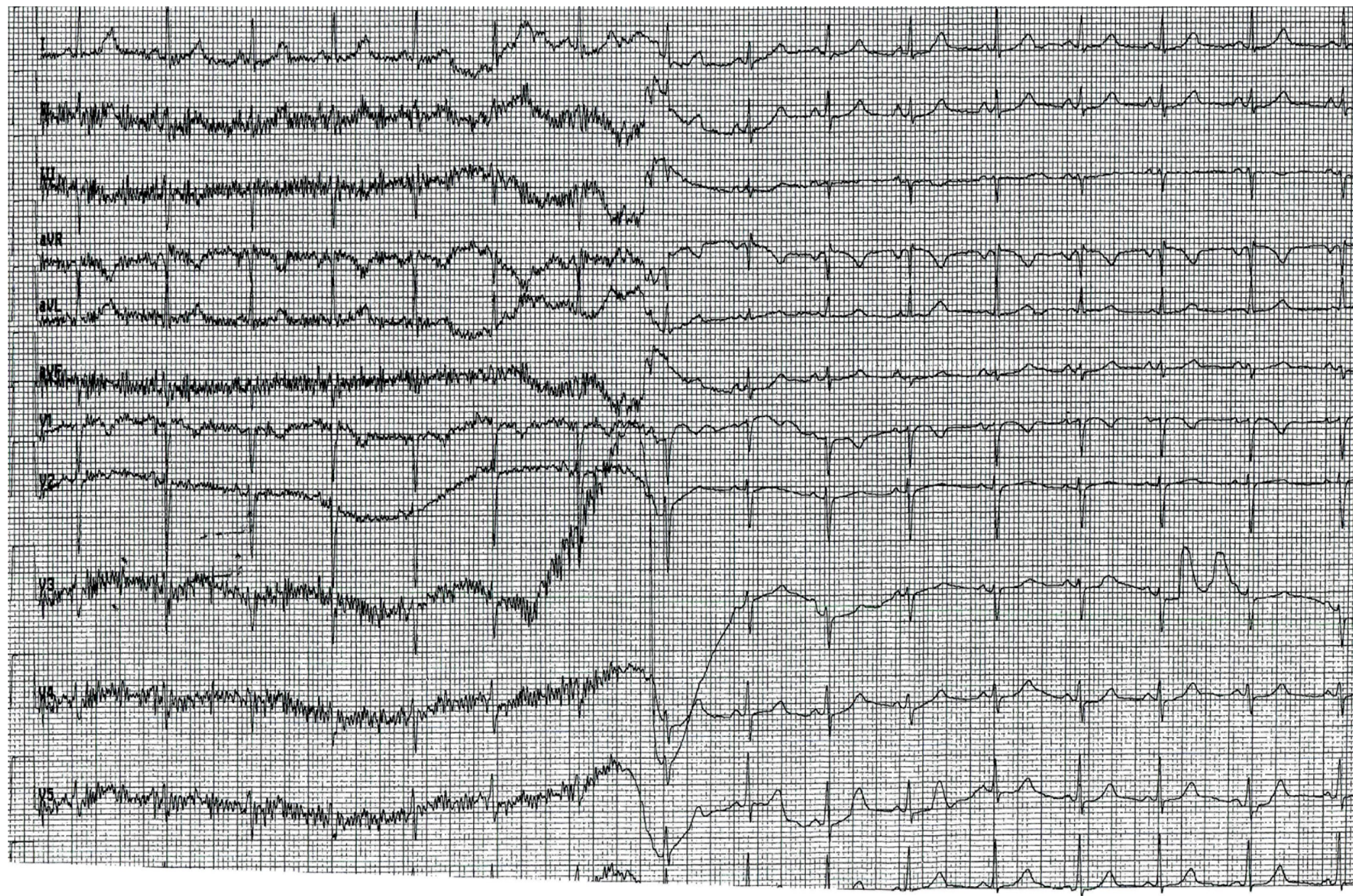
aVF



Some fatal arrhythmic  
syndrome can be cured  
with a single pulse of RF

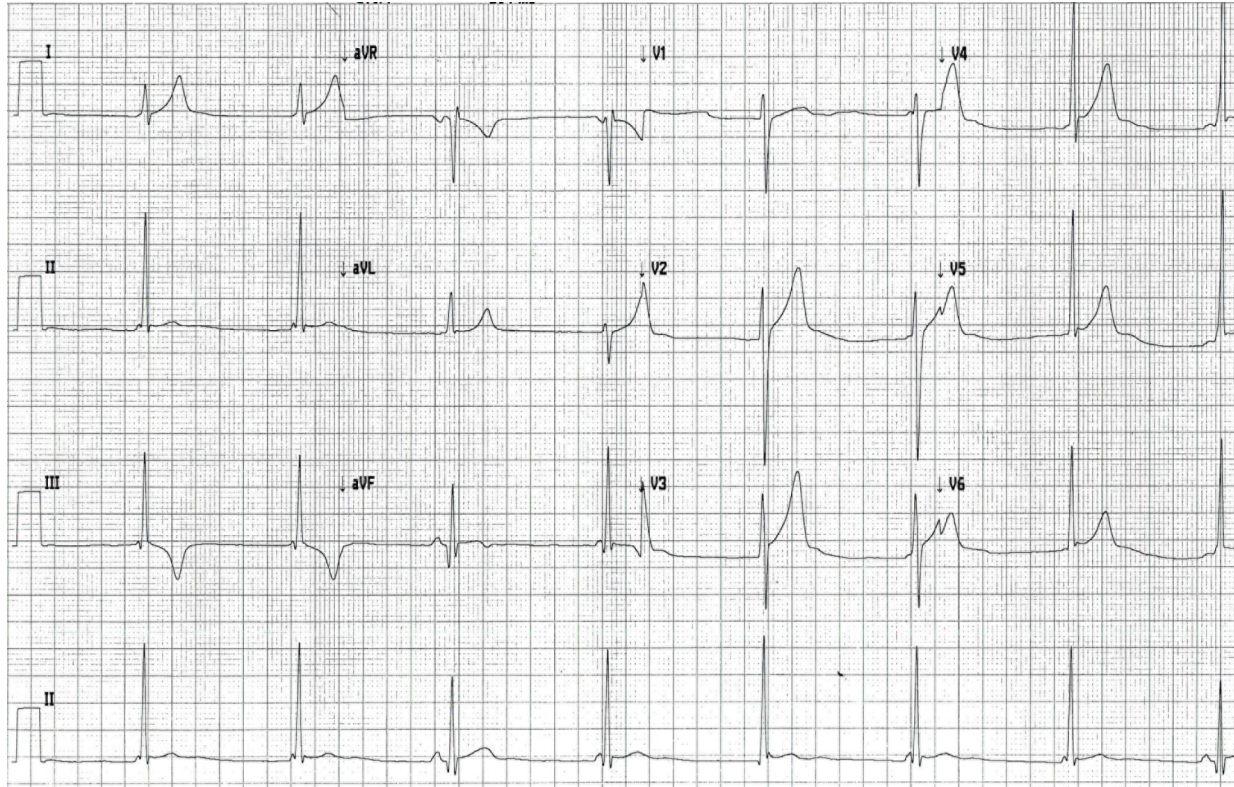










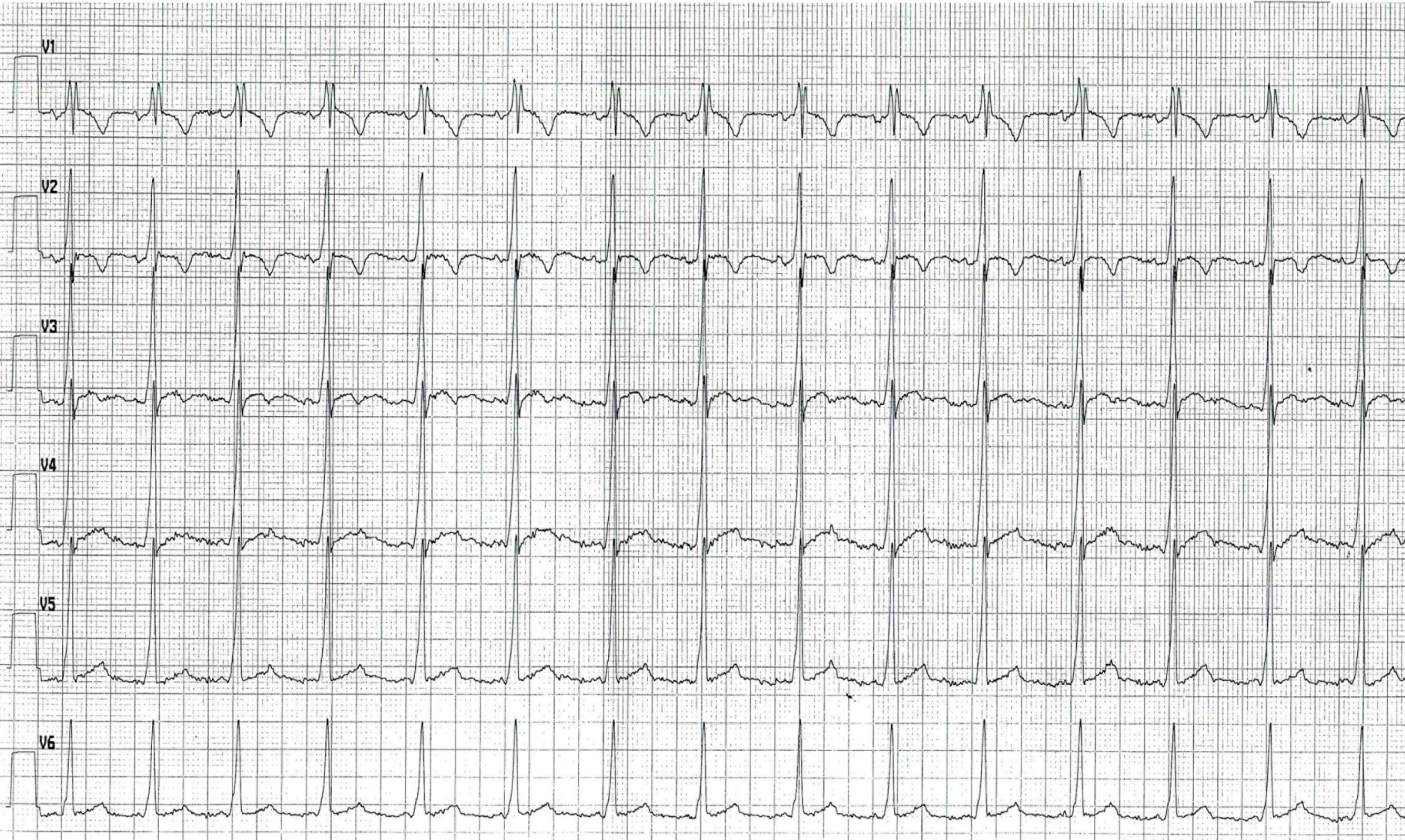




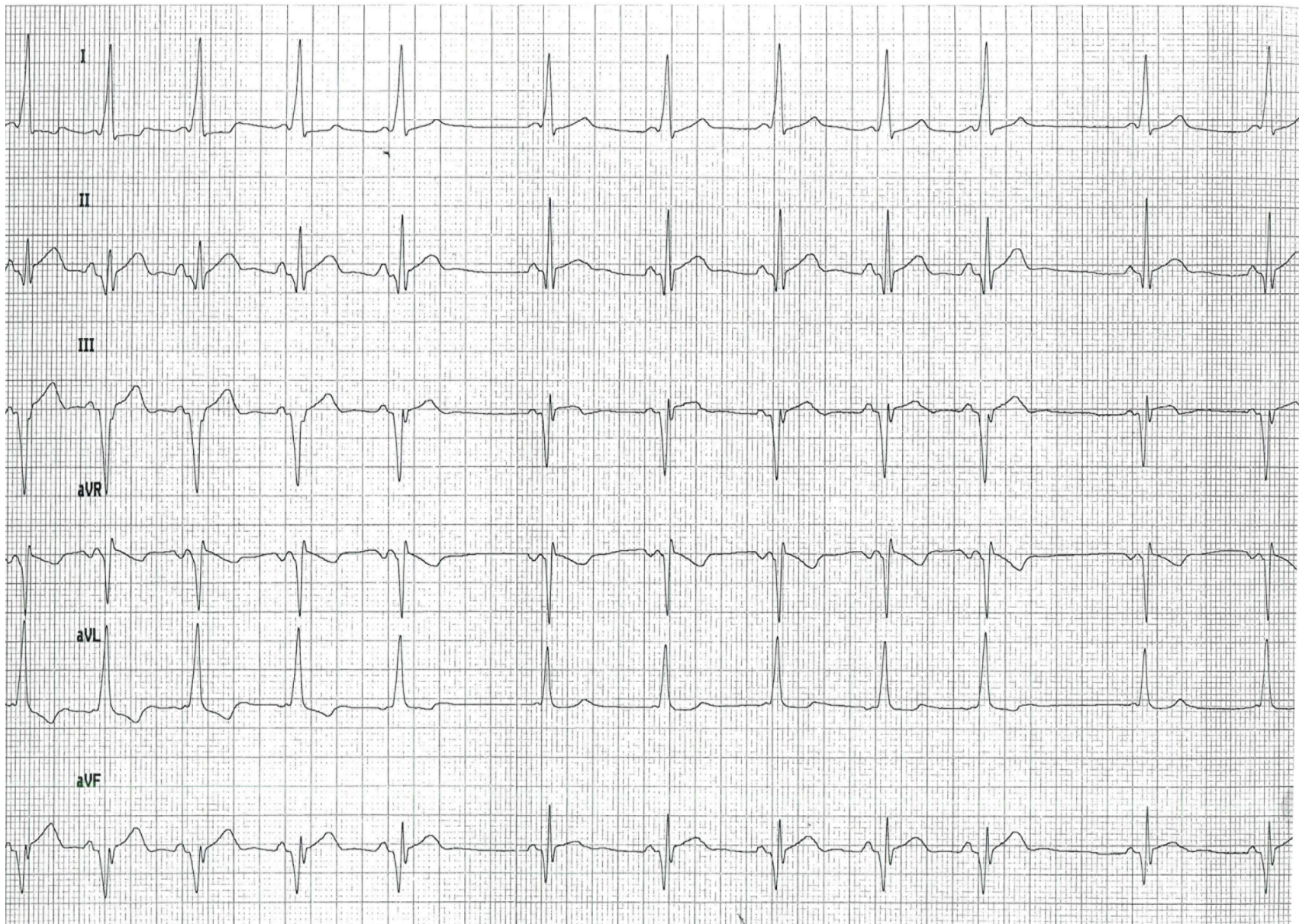
30-Set-2013 14:00:16

GAMB=ALTAIE

ID:  
Nato/a:  
anni,

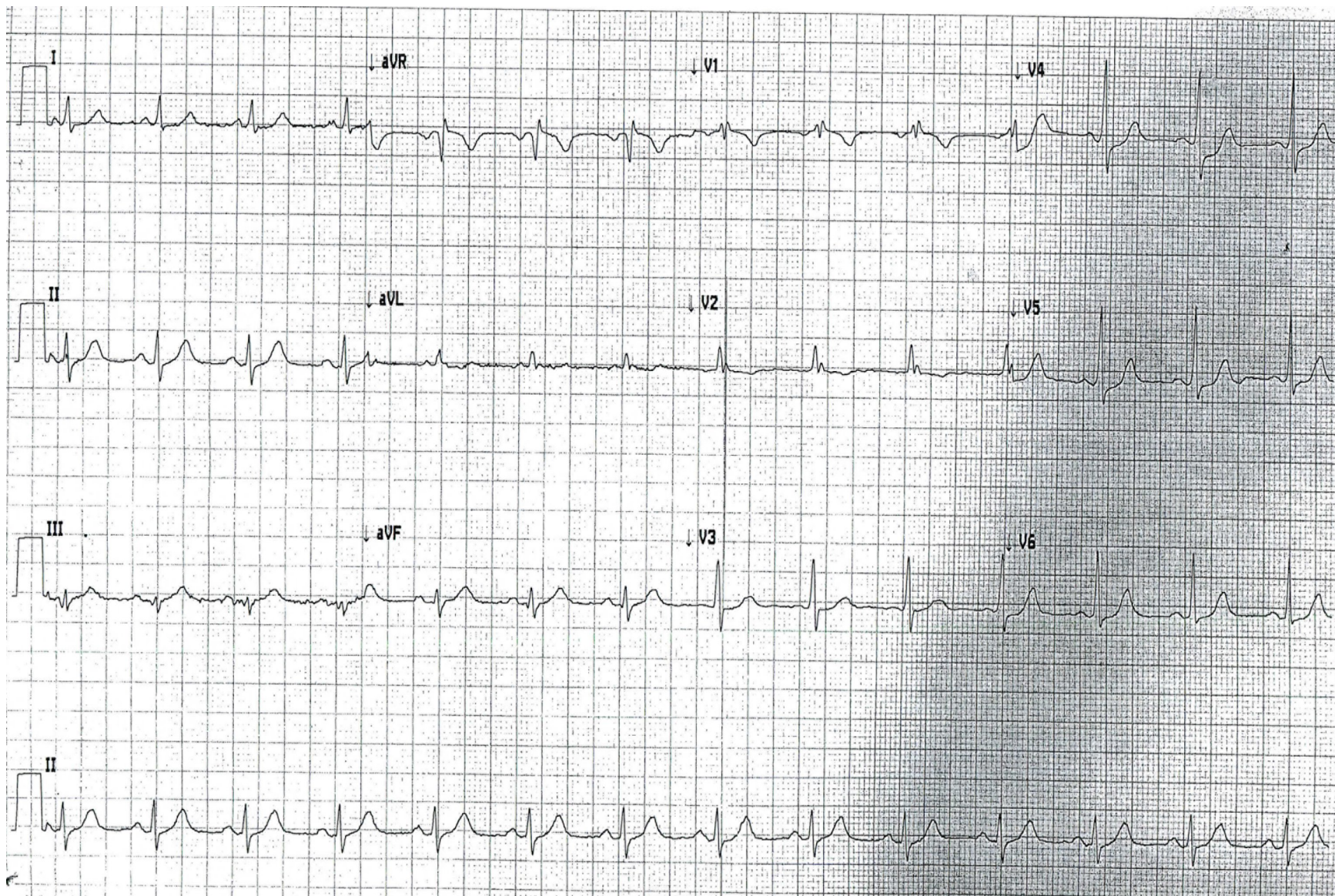




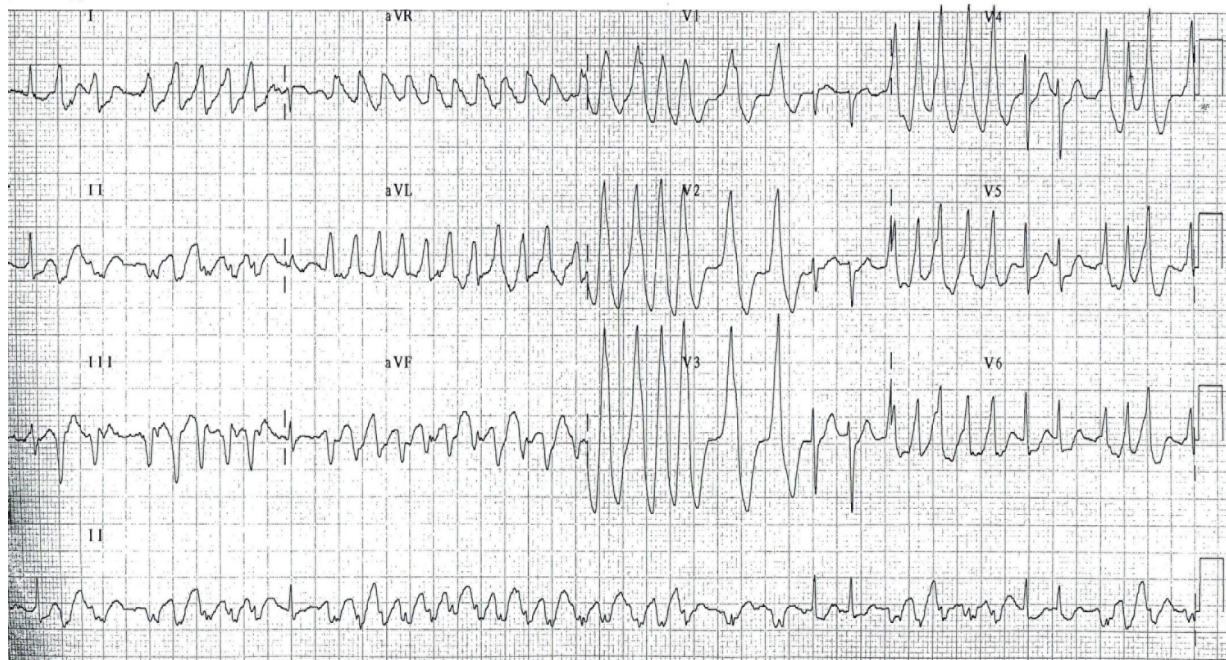














# Electrocardiographic and echocardiographic evaluation of a large cohort of peri-pubertal soccer players during pre-participation screening

Leonardo Calò<sup>1,2,3</sup>, Annamaria Martino<sup>1</sup>, Eliana Tranchita<sup>2</sup>, Fabio Sperandii<sup>4</sup>, Emanuele Guerra<sup>5</sup>, Federico Quaranta<sup>2</sup>, Attilio Parisi<sup>2</sup>, Antonia Nigro<sup>3</sup>, Luigi Sciarra<sup>1</sup>, Ermenegildo de Ruvo<sup>1</sup>, Maurizio Casasco<sup>6</sup> and Fabio Pigozzi<sup>1,2,3</sup>

European Journal of Preventive Cardiology  
2019, Vol. 26(13) 1444–1455  
© The European Society of Cardiology 2019  
Article reuse guidelines:  
sagepub.com/journals-permissions  
DOI: 10.1177/2047487319826312  
journals.sagepub.com/home/cpr  


**Table 1.** Electrocardiographic characteristics, sport-related adaptations and non-sport-related electrocardiographic abnormalities of the study population.

ECG characteristics	m ± SD
Mean HR (bpm)	68.7 ± 12.8
PR interval (ms)	137 ± 27.1
QRS axis (degrees)	61.2 ± 24.9
QRS duration (ms)	91.1 ± 10.4
QTc (ms)	395.9 ± 20.9
Sport-related physiological adaptations	n (%)
Sinus arrhythmia	40 (1.7)
Wandering pacemaker	13 (0.6)
Nodal rhythm	83 (3.7)
Sinus bradycardia	534 (23.6)
First degree atrio-ventricular block	10 (0.44)
Incomplete RBBB	355 (15.7)
Sokolow-Lyon QRS voltage criteria for LVH (S V1 + R V5 > 35 mm)	609 (26.93)
Romhilt QRS voltage criteria for LVH (S V2 + R V5–V6 > 45 mm) (n/%)	69 (3.05)
Early repolarization pattern	853 (37.72)
TWI in V1–V3 leads in athletes aged up to 13 years (n/%)	117 (5.17)

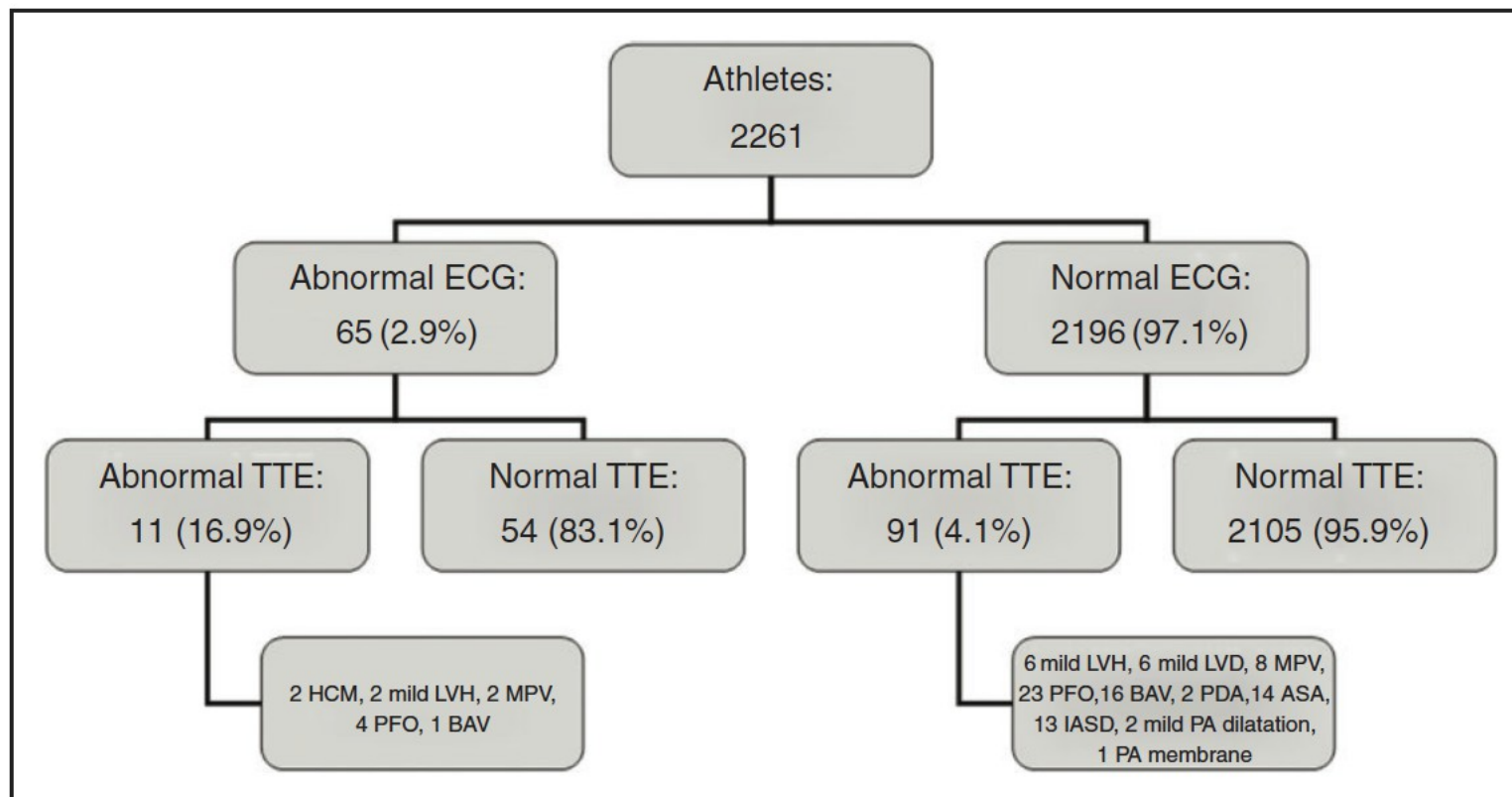
Non sport-related abnormalities	n (%)
TWI in V1–V3 leads in athletes aged > 13 years (n/%)	9 (0.4)
TWI in extended anterior, inferior and infero-lateral leads (n/%)	10 (0.44)
Ventricular pre-excitation (n/%)	3 (0.13)
Type II–III Brugada pattern (n/%)	2 (0.09)
Long QT interval (n/%)	1 (0.04)
Left axis deviation	20 (0.88)
Right axis deviation (n/%)	6 (0.26)
Left anterior hemiblock (n/%)	9 (0.39)
Complete RBBB (n/%)	4 (0.17)
Abnormal Q-waves (infero-lateral) (n/%)	1 (0.04)

HR: heart rate; LVH: left ventricular hypertrophy; m: mean; RBBB: right bundle branch block; SD: standard deviation; TWI: T wave inversion. Data are mean and SDs.

**Table 2.** Clinical profile of athletes with electrocardiogram (ECG) abnormalities.

ECG abnormality	Athletes <i>n</i>	Abnormal echocardiogram <i>n</i> (%)	Symptoms <i>n</i> (%)	Positive family history <i>n</i> (%)	Positive physical examination <i>n</i> (%)	Positive findings at further examinations <i>n</i> (%)
TWI VI–V3 (athletes older than 13 y)	9	MVP: 1 (11.1); PFO: 1 (11.1)	0	0	0	None
TWI VI–V4	2	0	0	Aortic disease: 1 (50)	Pectus excavatum: 1 (50)	None
TWI infero-lateral	8	HCM: 1 (12.5) LVH: 2 (25)	0	0	0	None
WPW	3	PFO: 1 (33.3)	0	0	0	Holter ECG, stress test: no arrhythmias
Brugada pattern	2	0	0	0	0	None
Long QTc	1	0	0	0	0	SCN5A gene s216L mutation; no arrhythmias
Q wave infero-lateral	1	HCM: 1 (100)	0	0	0	HCM at CMR
LAD	20	BAV: 1 (5)	0	0	5 (25)	None
LAH	9	MVP: 1 (11.1)	0	0	0	None
RAD	6	PFO: 1 (16.6)	0	0	0	Rare PVCs cc at Holter ECG:
RBBB	4	PFO: 1 (25)	Presyncope: 1 (25)	IVS defect: 1 (25)	0	None

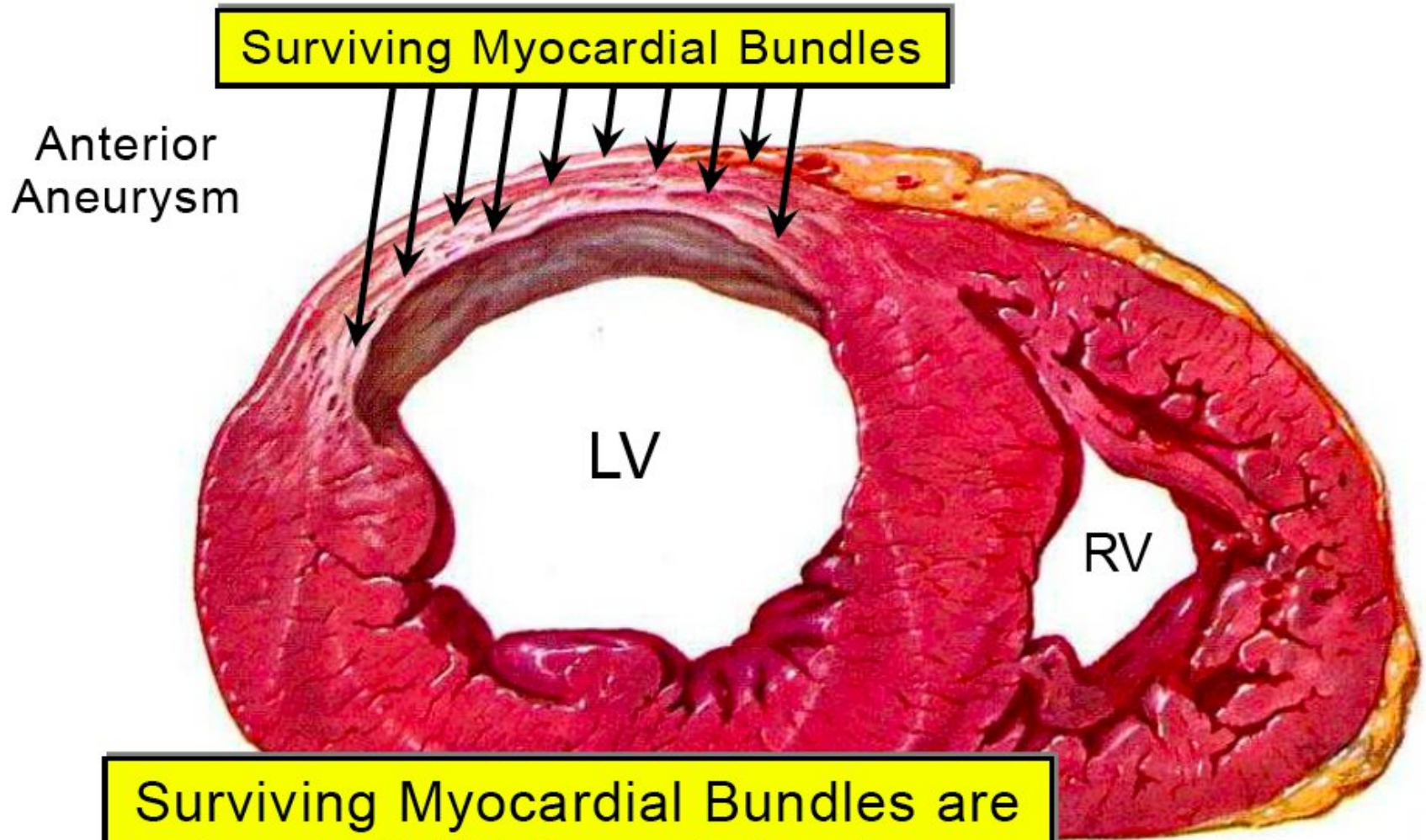
CMR: cardiac magnetic resonance; HCM: hypertrophic cardiomyopathy; IVS: inter-ventricular septal; LAD: left axis deviation; LAH: left anterior hemi-block; LVH: left ventricular hypertrophy; PFO: patent foramen ovale; PVCs: premature ventricular contractions; RAD: right axis deviation; RBBB: right bundle branch block; TWI: T wave inversion; WPW: Wolff-Parkinson-White. Data are absolute number (*n*) and percentage of the total (%).



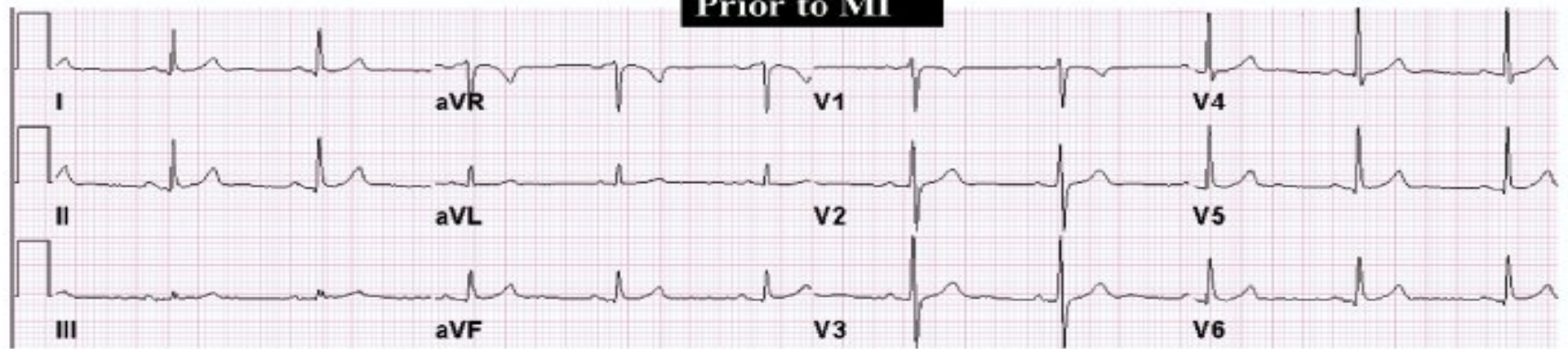


DEPOLARIZATION  
QRS

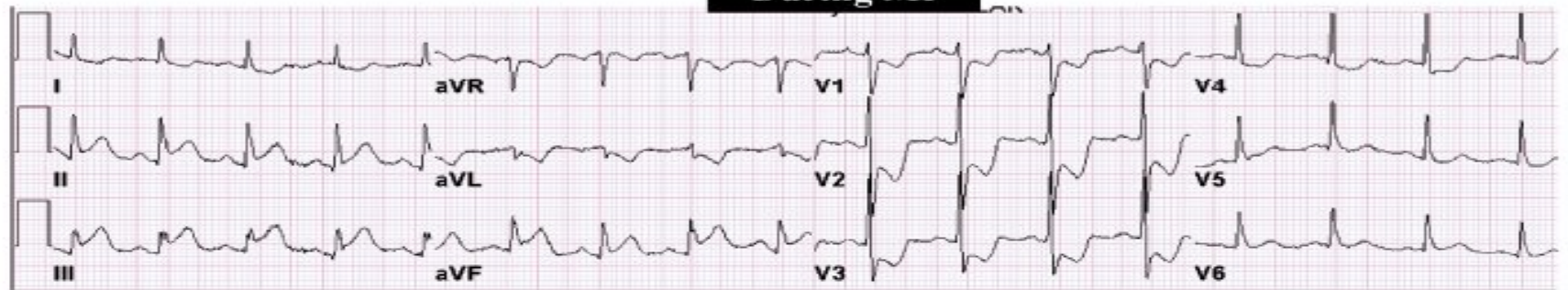
# Substrate for Ventricular Tachycardia



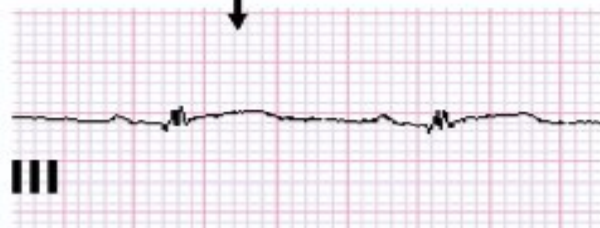
### Prior to MI



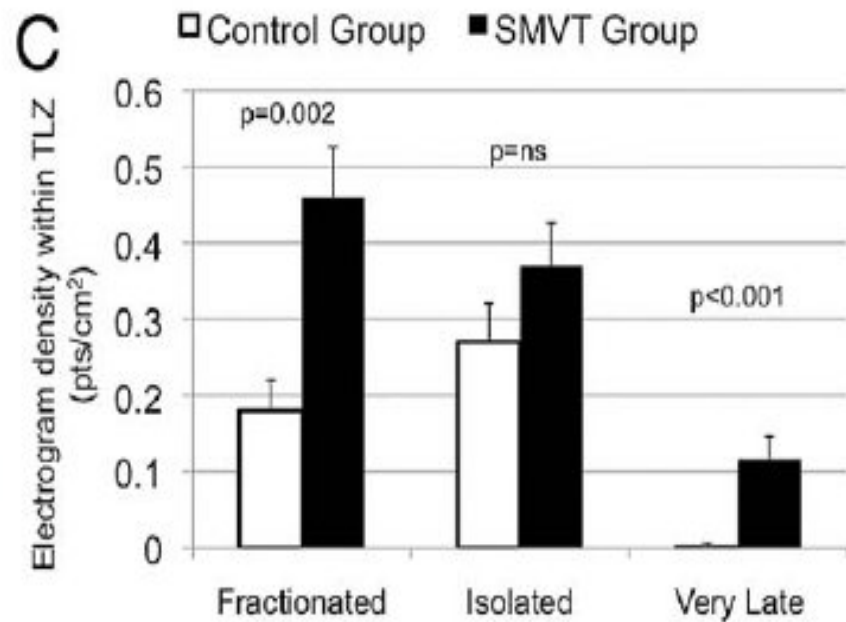
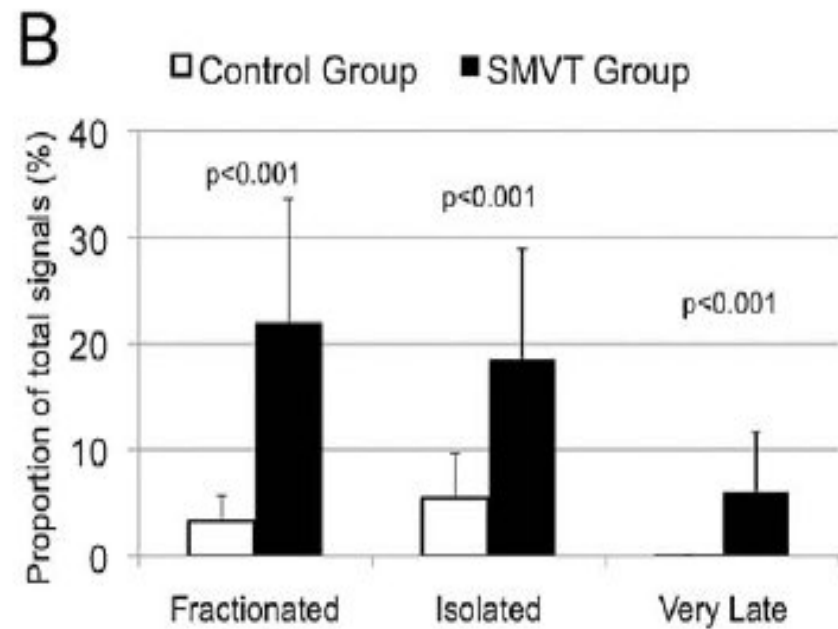
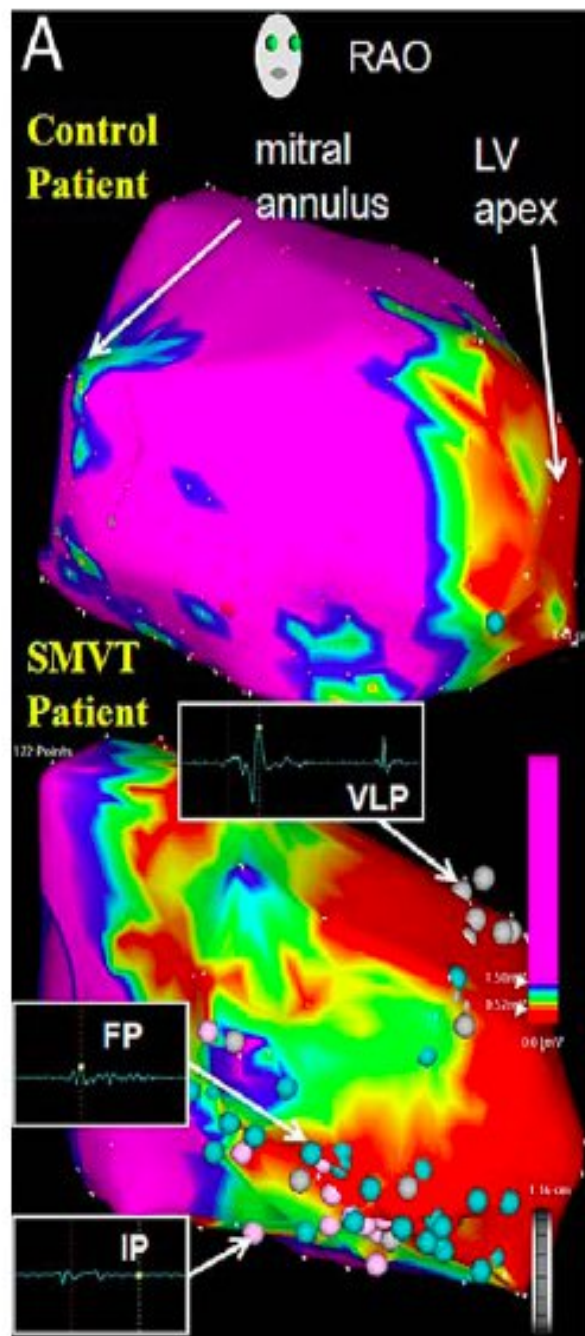
### During MI



### Three month post-MI





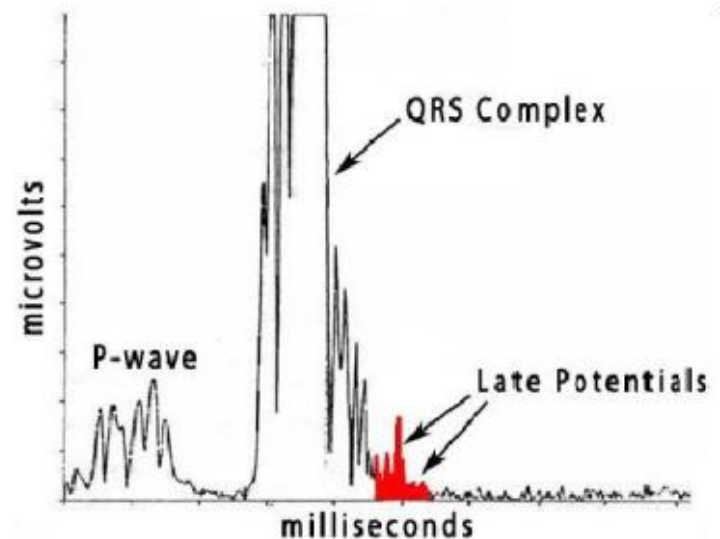


# Potenziali tardivi

1. Depolarizzazioni tardive di basso voltaggio
2. Espressione di aree a rallentata conduzione (tessuto disomogeneo)
3. Valutabili mediante metodica non invasiva (SAECG)

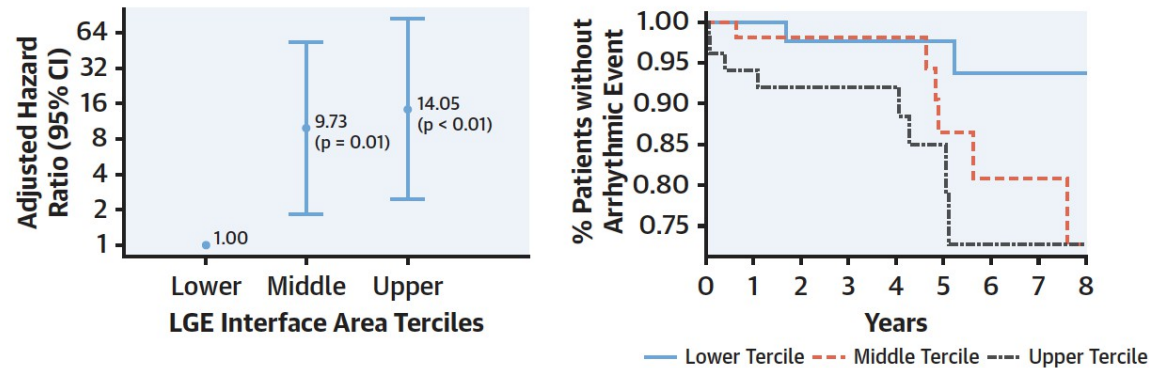
Criteri di positività:

- Durata del QRS filtrato > 114 msec
- Parte terminale QRSf < 40 mcV per più di 38 msec
- Segnale < 20 mcV negli ultimi 40 msec

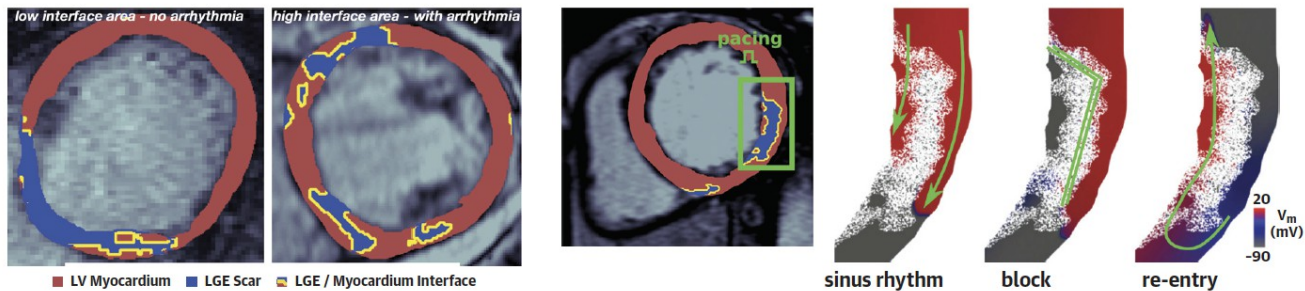


## CENTRAL ILLUSTRATION Interface Between Fibrosis and Healthy Myocardium Drives Arrhythmias in NIDCM

### Patients With Higher LGE-Myocardium Interface Area Show an Increased Risk of Arrhythmic Events



### Potential Mechanism of Arrhythmogenesis Driven by LGE-Myocardial Interface Elucidated by Detailed Computational Modeling

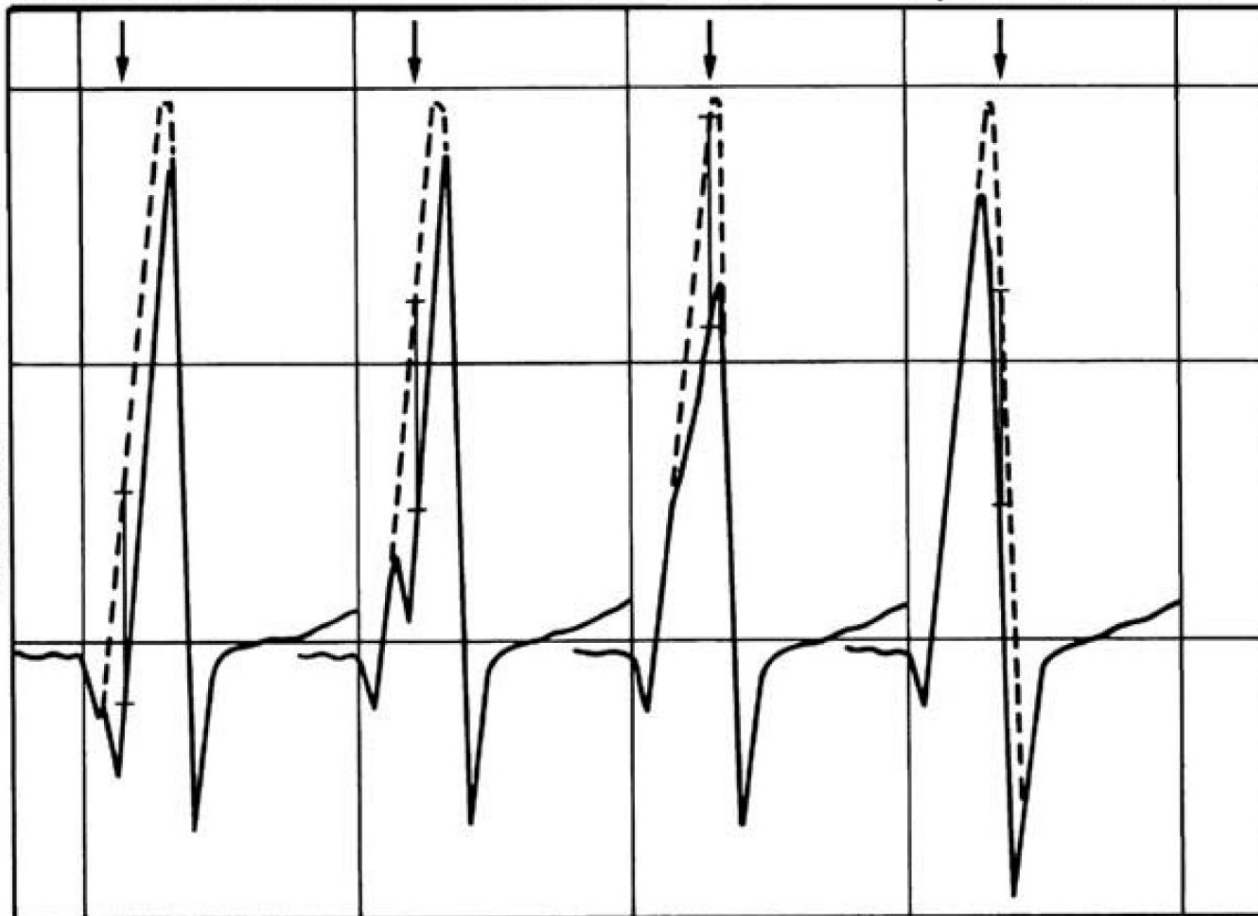


Balaban, G. et al. J Am Coll Cardiol EP. 2021;7(2):238-49.

Endocardial Infarct

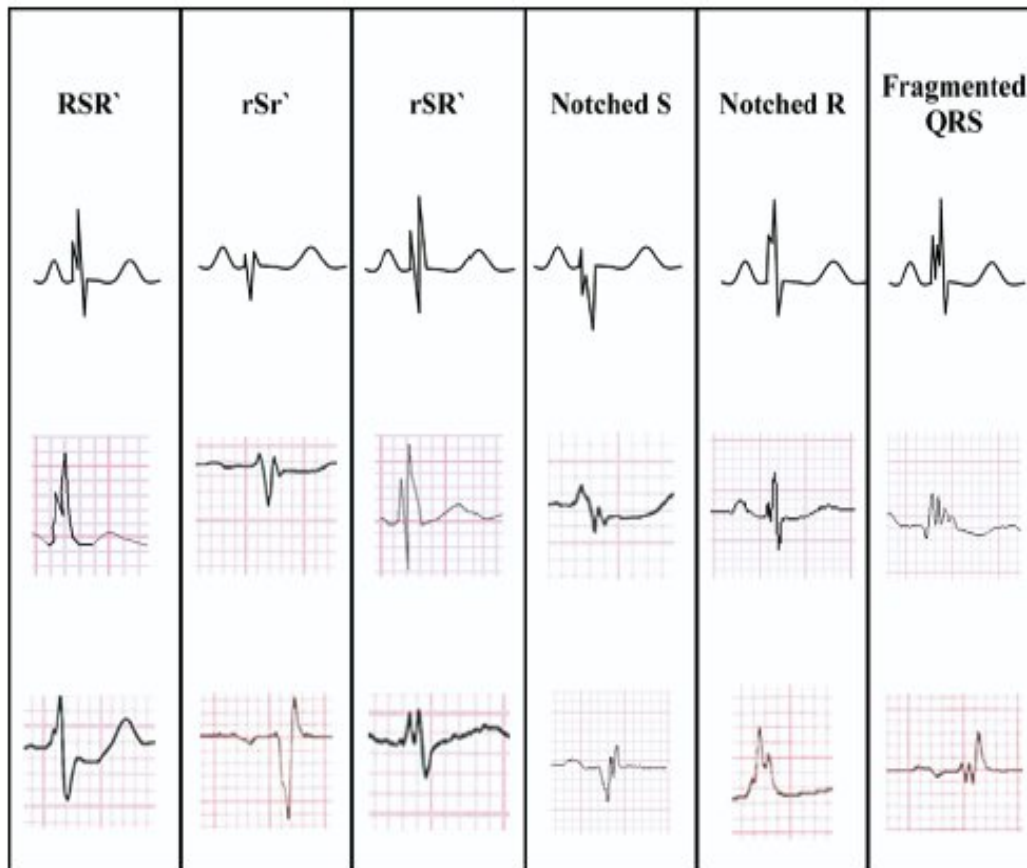
Midwall Infarct

Epicardial Infarct



# Fragmented QRS on a 12-lead ECG: A predictor of mortality and cardiac events in patients with coronary artery disease

Mithilesh Kumar Das, MD, MRCP, FACC,\* Chandan Saha, PhD,<sup>†</sup> Hicham El Masry, MD,\*  
Jonathan Peng, BS,\* Gopi Dandamudi, MD,\* Jo Mahenthiran, MD, MRCP, FACC,\* Paul McHenry, MD,\*  
Douglas P. Zipes, MD, FACC\*



## Different morphologies of fQRS

The fQRS included various RSR' patterns with or without the Q wave **and was defined by the presence of an additional R wave (R' prime), or notching in nadir of the S wave, notching of R wave, or the presence of more than one R prime (fragmentation) in two contiguous leads corresponding to a major coronary artery territory.**

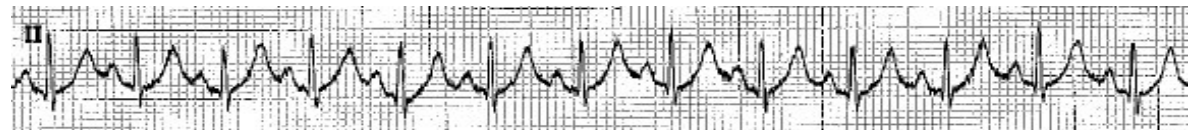
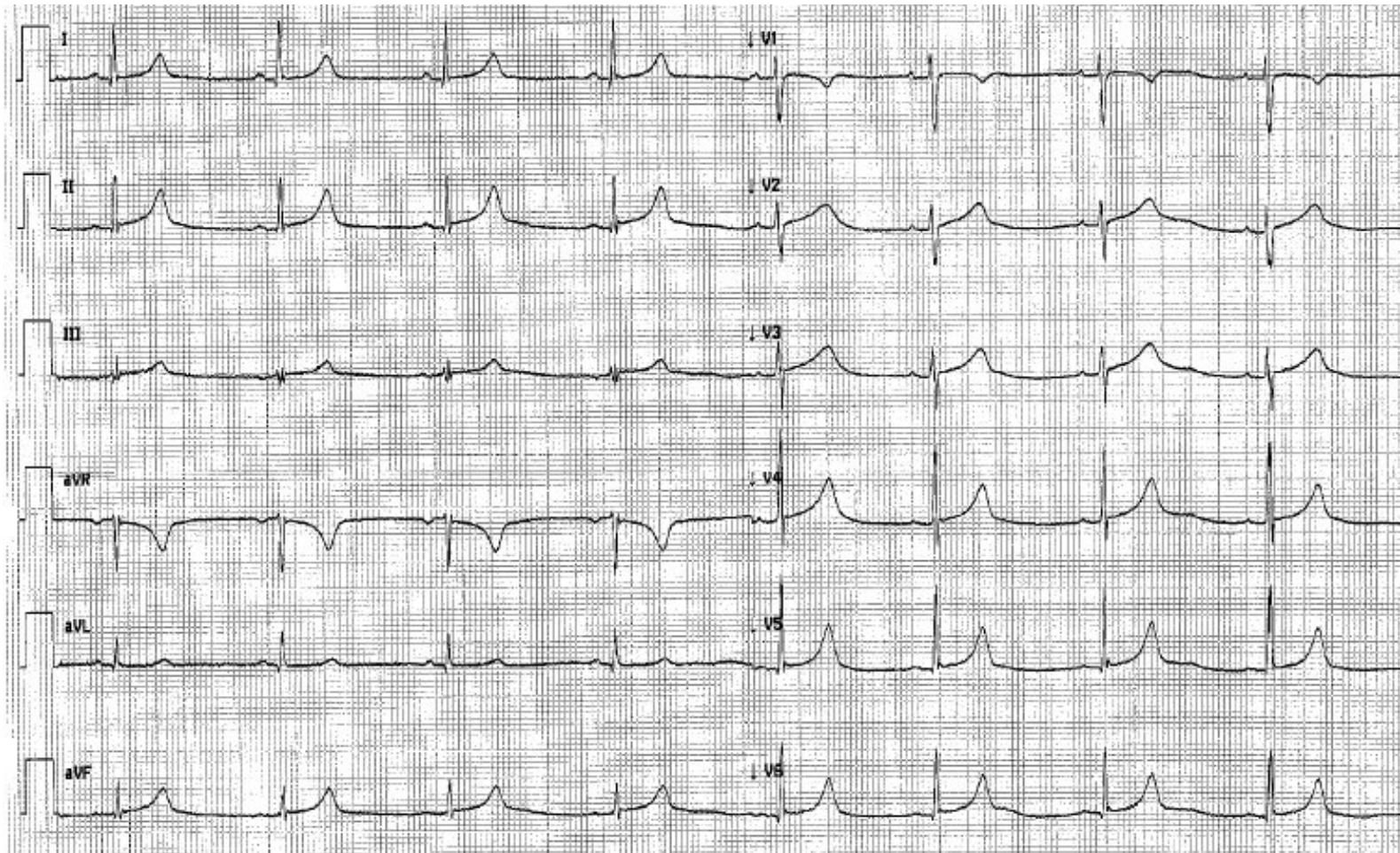


# RIPOLARIZATION QT

**Male 11 year-old**

**QTc 450/460ms**

**(Mutation S216L gene SCN5A dec 2010)**



## The diagnosis of LQTS is challenging

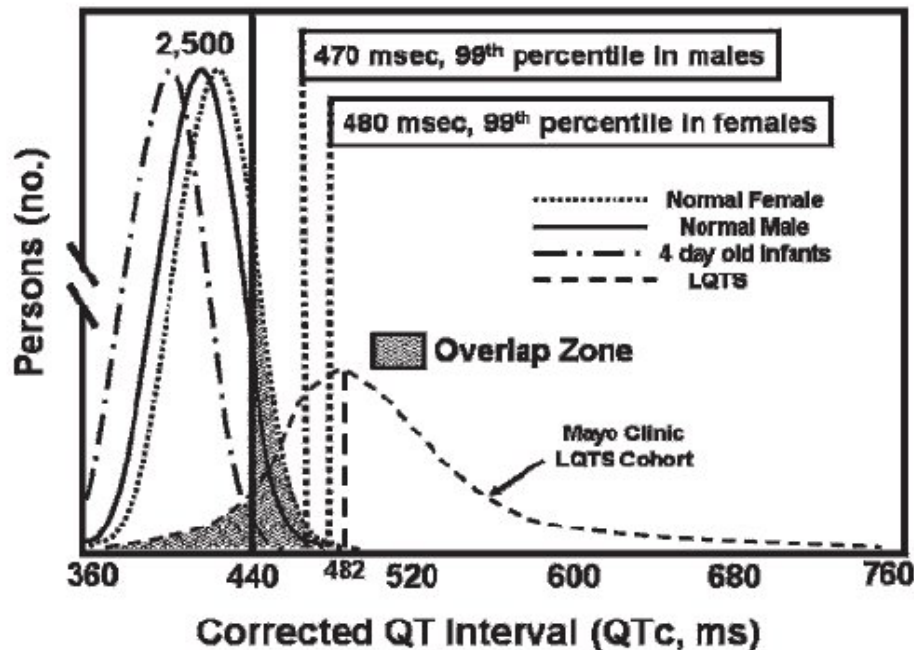


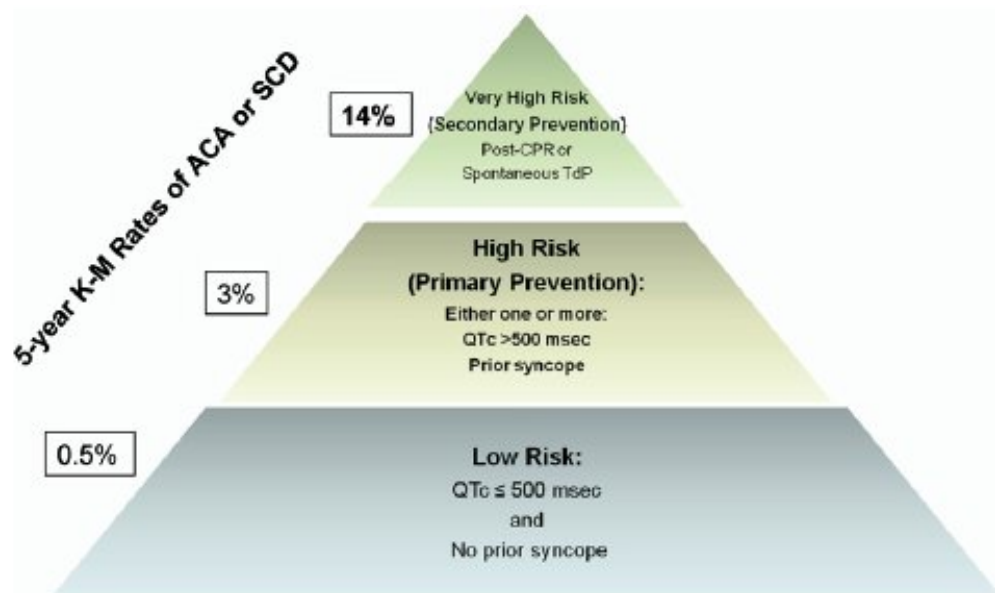
**Figure 1** Distribution of QTc values for patients with and without long QT syndrome (LQTS). The “borderline” QTc level of 440 ms is shown with a solid line. Note the significant overlap between “normal” and QTc values of mutation-positive patients from Mayo’s LQTS Clinic. Also note that the average QTc value in normal postpubertal females is on average 10 ms longer than that of normal postpubertal males. Modified from Taggart *et al*<sup>16</sup> with permission from the American Heart Association, copyright 2007.

Borderline QTc prolongation (440-470 ms):  
15% of the general population

LQTS-causing mutations carriers: 25% has  
QTc within normal range

Several recent reviews have proposed an “upper limit” of 460 ms in patients <15 years of age, 470 ms for adult females, and 450 ms for adult males.<sup>17–20</sup> In this algorithm, any QTc value within 20 ms of these designated upper limits is considered “borderline”.<sup>23</sup> Consequently, an adult male with a QTc of 431 ms is considered by these criteria to exhibit “borderline” QT prolongation. Others have proposed that any patient with a QTc between 440 and 470 ms be labelled “borderline”.<sup>18</sup> A 2005 European protocol proposed the use of a QTc value greater than 440 ms in males and 460 ms in females as a definition of a “prolonged” QTc.<sup>30–45</sup> Even the latest 2009 AHA/ACCF/HRS Recommendations for the Standardization and Interpretation of the Electrocardiogram states that a QTc  $\geq 450$  ms (males) and  $\geq 460$  ms (females) “be considered a prolonged QT interval”.<sup>46</sup>





Europace (2010) 12, 1156–1175  
doi:10.1093/europace/euq261

#### POSITION PAPER

### Heart Rhythm UK position statement on clinical indications for implantable cardioverter defibrillators in adult patients with familial sudden cardiac death syndromes

Clifford J. Garratt (co-chair)<sup>1\*</sup>, Perry Elliott (co-chair)<sup>2</sup>, Elijah Behr<sup>3</sup>, A. John Camm<sup>3</sup>, Campbell Cowan<sup>4</sup>, Stephanie Cruickshank<sup>5,†</sup>, Andrew Grace<sup>6</sup>, Michael J. Griffith<sup>7</sup>, Anne Jolly<sup>8,†</sup>, Pier Lambiase<sup>2</sup>, Pascal McKeown<sup>9</sup>, Peter O'Callaghan<sup>10</sup>, Graham Stuart<sup>11</sup>, and Hugh Watkins<sup>12</sup> (the Heart Rhythm UK Familial Sudden Cardiac Death Syndromes Statement Development Group)

**Class I.** Implantation of an ICD along with the use of beta-blockers is recommended for LQTS patients with previous cardiac arrest (level of evidence: A).

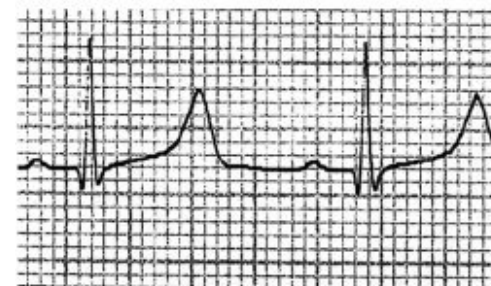
**Class IIa.** Implantation of an ICD with continued use of beta-blockers can be effective to reduce SCD in LQTS patients experiencing syncope and/or VT while receiving beta-blockers (level of evidence: B).



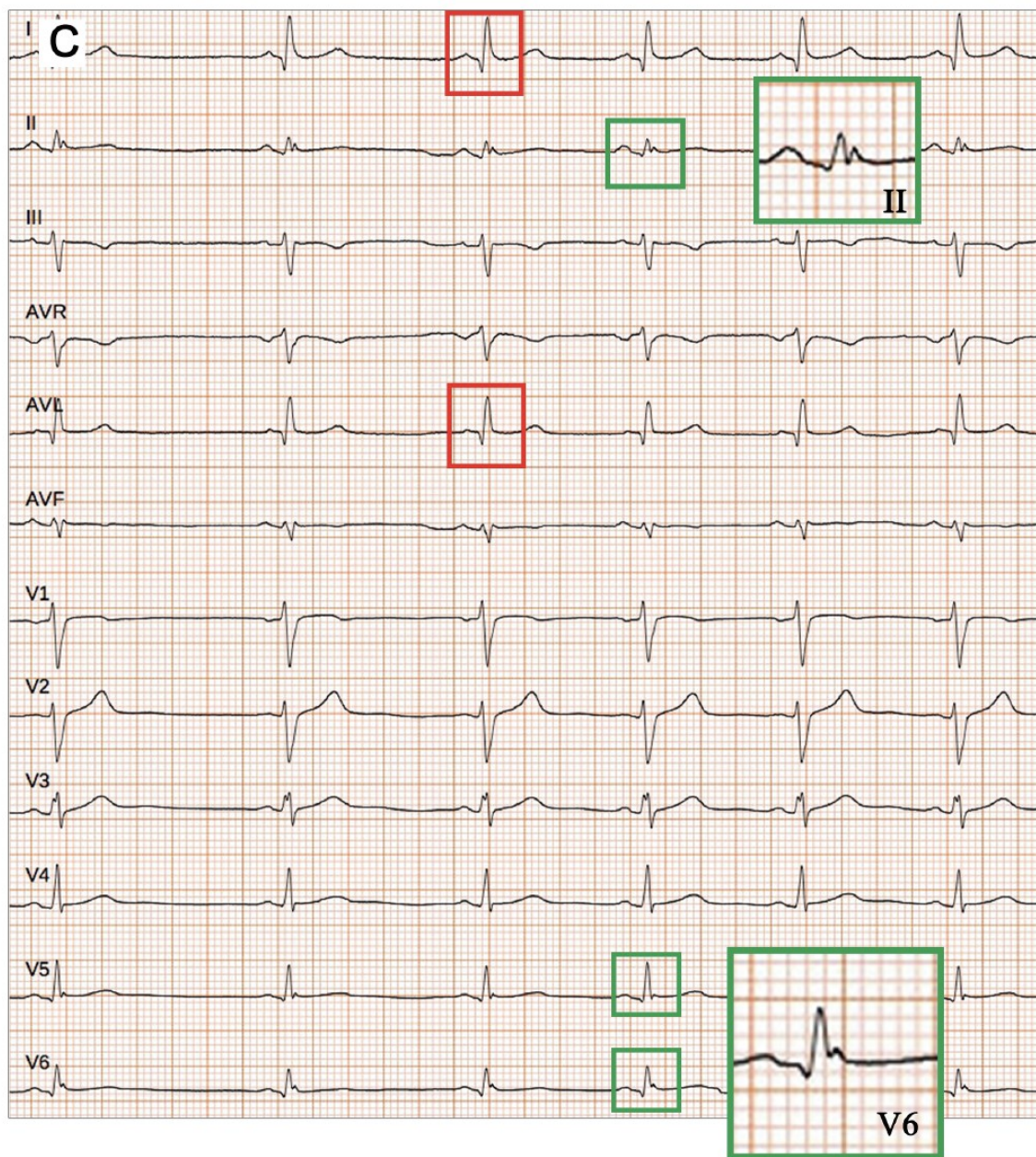
LQTS 1



LQTS 2



LQTS 3





# J-Point Elevation in Survivors of Primary Ventricular Fibrillation and Matched Control Subjects

## Incidence and Clinical Significance

Raphael Rosso, MD,\* Evgeni Kogan, MD,\* Bernard Belhassen, MD,\* Uri Rozovski, MD,\*  
Melvin M. Scheinman, MD,§ David Zeltser, MD,\* Amir Halkin, MD,\* Arie Steinvil, MD,\*  
Karin Heller, MD,\* Michael Glikson, MD,† Amos Katz, MD,‡ Sami Viskin, MD\*

*Tel Aviv and Beer-Sheva, Israel; and San Francisco, California*

### Objectives

The purpose of this study was to determine whether J-point elevation is a marker of arrhythmic risk.

### Background

J-point elevation has been considered an innocent finding among healthy young individuals (the "early repolarization" pattern). However, this electrocardiogram (ECG) finding is increasingly being associated with idiopathic ventricular fibrillation (VF).

### Methods

In a case-control study, the ECG of 45 patients with idiopathic VF were compared with those of 124 age- and gender-matched control subjects and with those of 121 young athletes. We measured the height of J-point and ST-segment elevation and counted the presence of slurring in the terminal portion of the R-wave.

### Results

J-point elevation was more common among patients with idiopathic VF than among matched control subjects (42% vs. 13%,  $p = 0.001$ ). This was true for J-point elevation in the inferior leads (27% vs. 8%,  $p = 0.006$ ) and for J-point elevation in leads I to aVL (13% vs. 1%,  $p = 0.009$ ). J-point elevation in  $V_4$  to  $V_6$  occurred with equal frequency among patients and matched control subjects (6.7% vs. 7.3%,  $p = 0.86$ ). Male subjects had J-point elevation more often than female subjects and young athletes had J-point elevation more often than healthy adults but less often than patients with idiopathic VF. The presence of ST-segment elevation or QRS slurring did not add diagnostic value to the presence of J-point elevation.

### Conclusions

J-point elevation is found more frequently among patients with idiopathic VF than among healthy control subjects. The frequency of J-point elevation among young athletes is intermediate (higher than among healthy adults but lower than among patients with idiopathic VF). (J Am Coll Cardiol 2008;52:1231-8) © 2008 by the American College of Cardiology Foundation

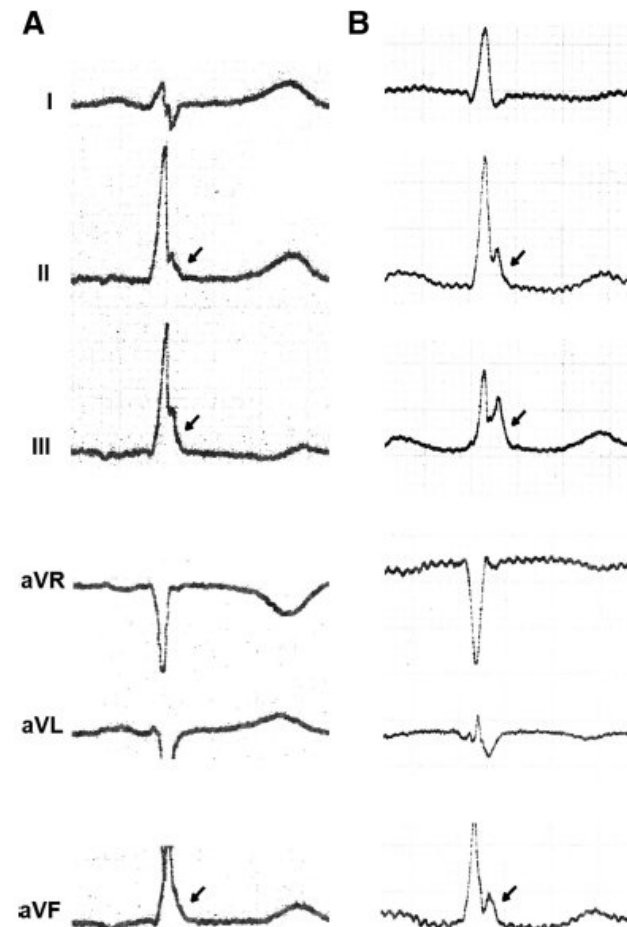
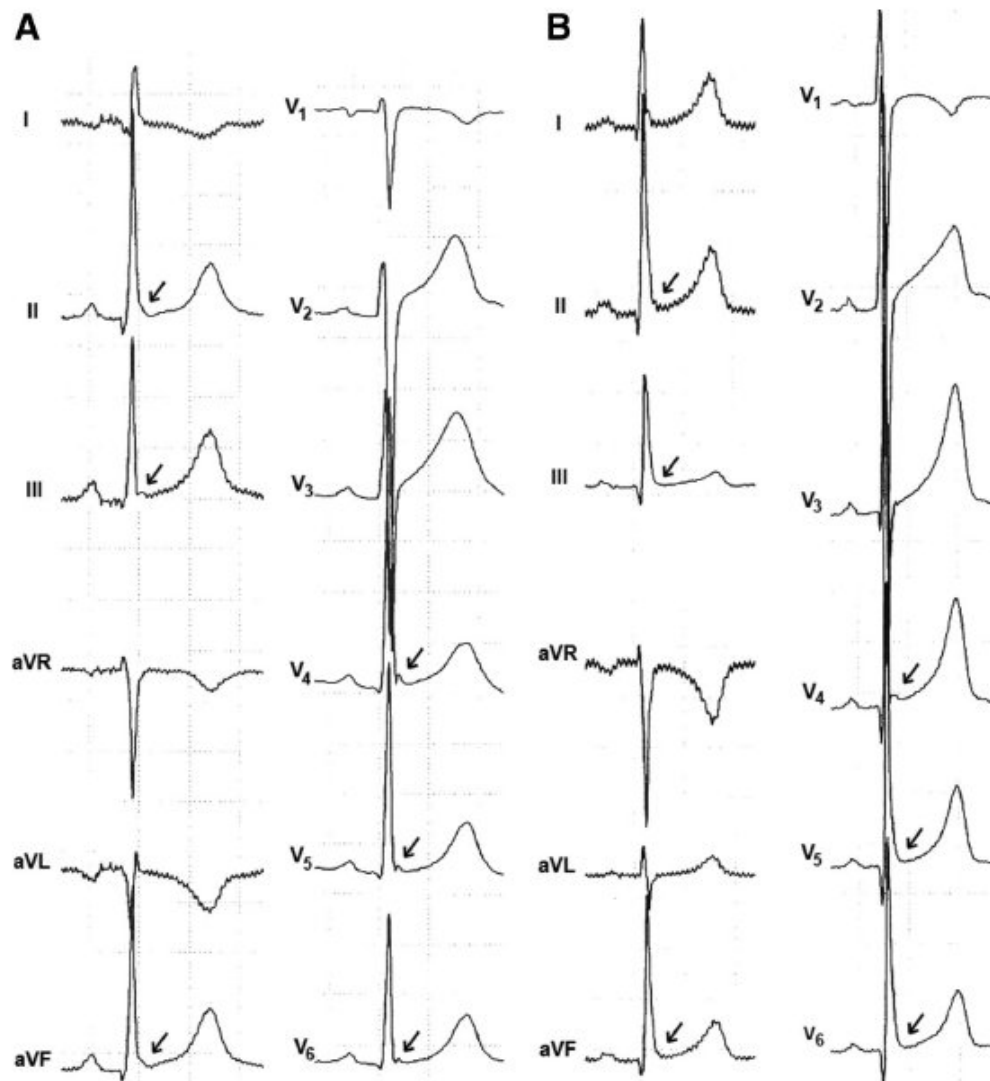
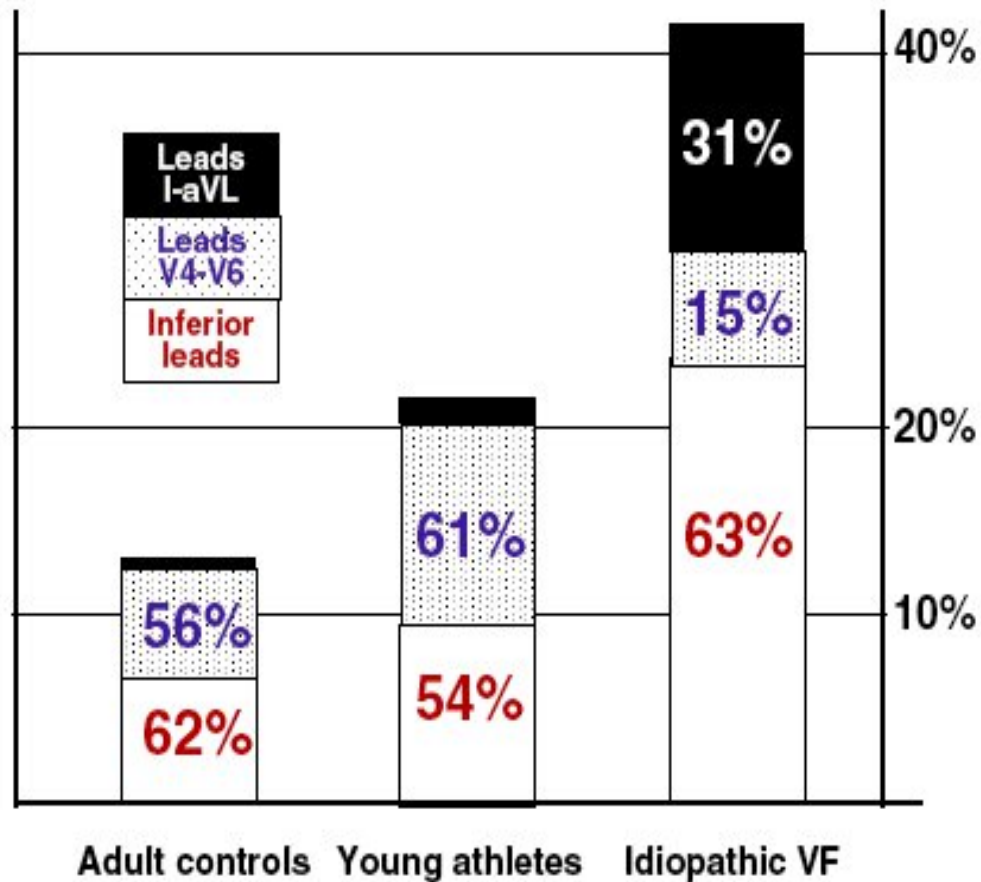


**Figure 3.** Horizontal/descending ST-segment patterns from 2 subjects in the general population. Subject **A** presented horizontal/descending ER (dominant horizontal ST segment in leads II and aVF and descending ST segment in lead III). Subject **B** presented ER with horizontal/descending ST segments (dominant horizontal ST segment in leads II, III, and aVF). In the middle-aged general population, only ER with horizontal/descending ST segment predicted arrhythmic death. Black arrows indicate terminal QRS notching or slurring.



Distribution of J Waves Among Patients With Idiopathic VF, Matched Control Subjects, and Healthy Athletes



## The J wave and fragmented QRS complexes in inferior leads associated with sudden cardiac death in patients with chronic heart failure

Juanhui Pei<sup>1</sup>, Ning Li<sup>1</sup>, Yonghong Gao<sup>2</sup>, Zengwu Wang<sup>1</sup>, Xian Li<sup>1</sup>, Yinhui Zhang<sup>1</sup>, Jingzhou Chen<sup>1</sup>, Ping Zhang<sup>3†</sup>, Kejiang Cao<sup>4†</sup>, and Jielin Pu<sup>1\*</sup>

<sup>1</sup>State Key Laboratory of Translational Cardiovascular Medicine, Fuwai Hospital & Cardiovascular Institute, Chinese Academy of Medical Sciences and Peking Union Medical College, 167 Bei-Li-Shi Road, Xi-Cheng District, Beijing 100037, China; <sup>2</sup>Beijing Aerospace Hospitals, Beijing, China; <sup>3</sup>People's Hospital, Peking University, Beijing, China; and <sup>4</sup>First People's Hospital of Jiangsu Province, Nanjing, China

Received 9 October 2011; accepted after revision 29 December 2011; online publish-ahead-of-print 2 February 2012

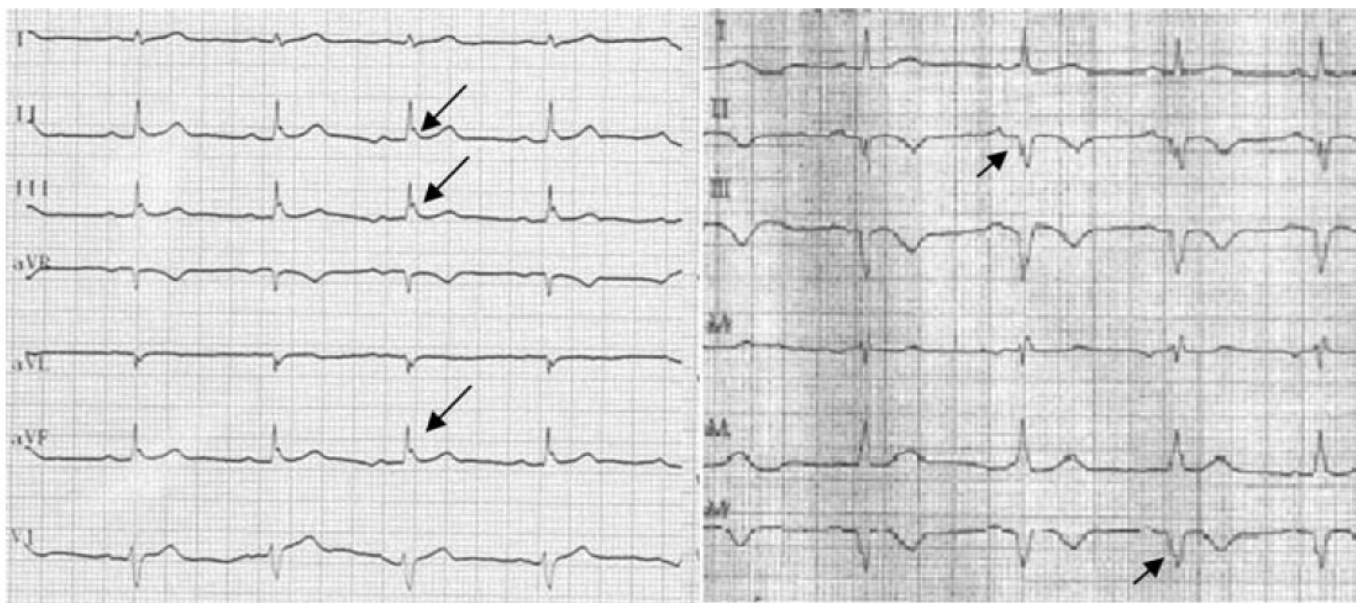
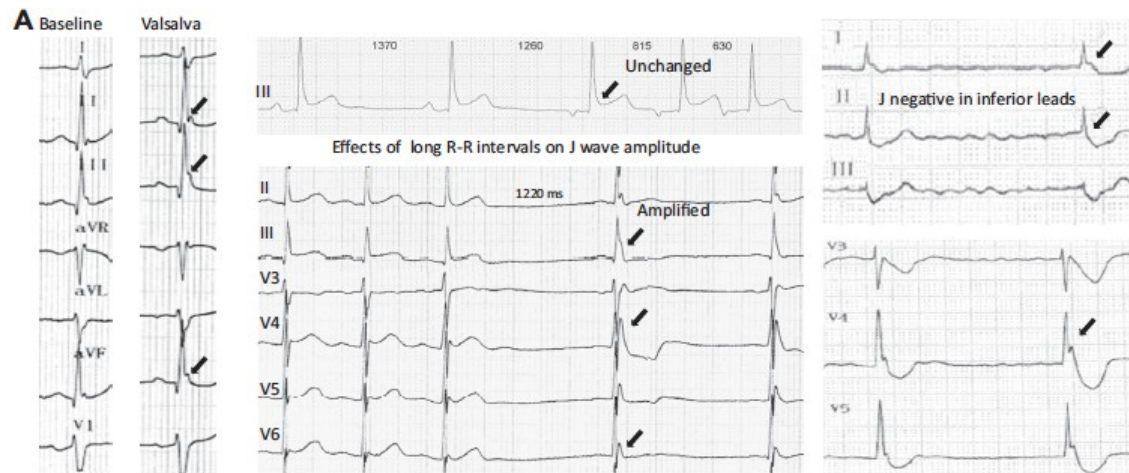



**Figure 1** Patient with prominent J waves in inferior leads (left arrow) and fragmented QRS complex in inferior leads (right arrow).

# Depolarization versus repolarization abnormality underlying inferolateral J-wave syndromes: New concepts in sudden cardiac death with apparently normal hearts

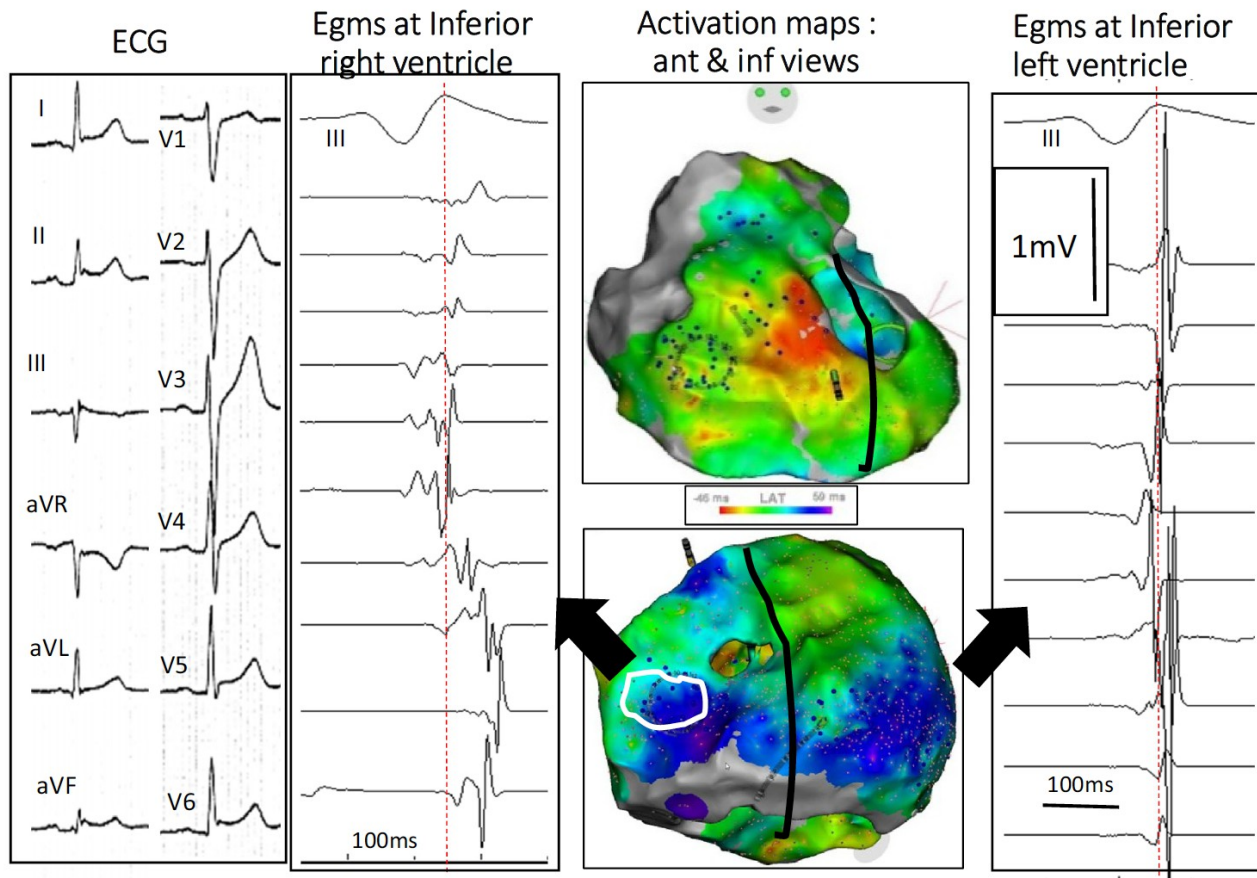
Michel Haïssaguerre, MD,<sup>\*†‡1</sup> Koonlawee Nademanee, MD,<sup>§1</sup> Méléze Hocini, MD,<sup>\*†‡</sup> Ghassen Cheniti, MD,<sup>\*†‡</sup> Josselin Duchateau, MD,<sup>\*†‡</sup> Antonio Frontera, MD,<sup>\*</sup> Frédéric Sacher, MD,<sup>\*†‡</sup> Nicolas Derval, MD,<sup>\*†‡</sup> Arnaud Denis, MD,<sup>\*†‡</sup> Thomas Pambrun, MD,<sup>\*†‡</sup> Rémi Dubois, PhD,<sup>†‡</sup> Pierre Jaïs, MD,<sup>\*†‡</sup> David Benoist, PhD,<sup>†‡</sup> Richard D. Walton, PhD,<sup>†‡</sup> Akihiko Nogami, MD,<sup>||</sup> Ruben Coronel, MD, PhD,<sup>†</sup> Mark Potse, PhD,<sup>†</sup> Olivier Bernus, PhD<sup>†‡</sup>



**B**

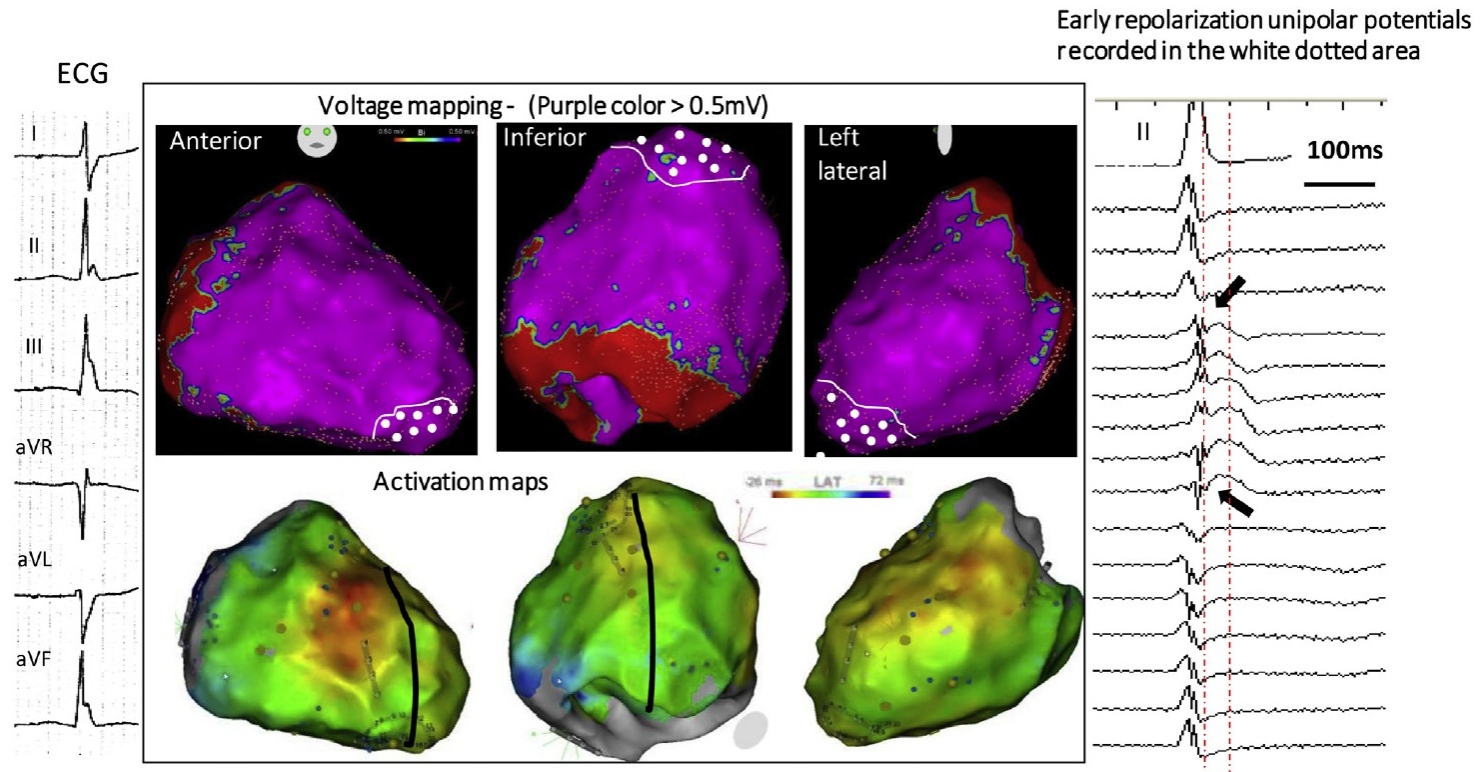
Clinical		Electrocardiographic
Cardiac arrest	 <b>Increased Risk of Arrhythmia</b>	Short coupled VPBs
Syncopes with severe criteria: agonal breathing, apnea, injury, convulsions, urine loss.		Dynamic J wave changes
		Widespread J wave
Family history of SCD		Associated pathology : Brugada, SHD, Fragmented QRS–LQT, ...
		Amplitude > 2mm of J point
		Horizontal/descending ST segment

## Inferolateral J-wave syndrome due to abnormal depolarization

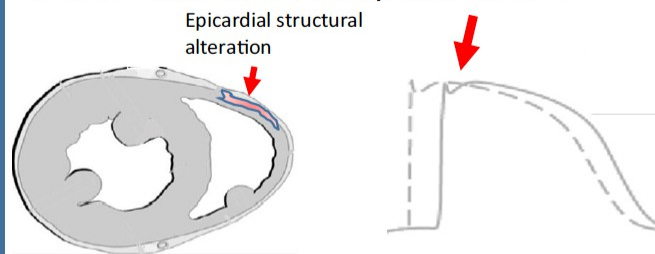




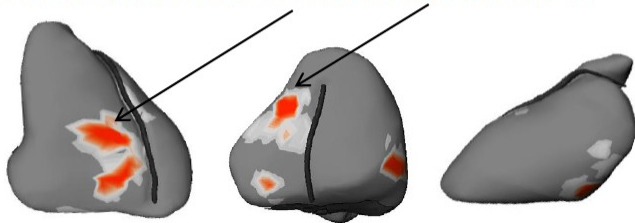
## Inferolateral J-wave syndrome due to early repolarization



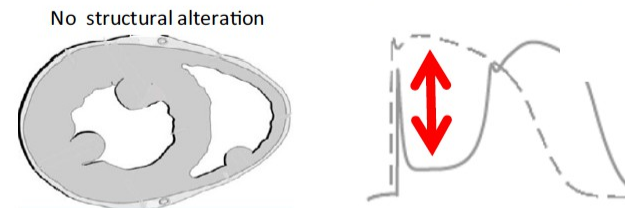
### J wave due to late depolarisation



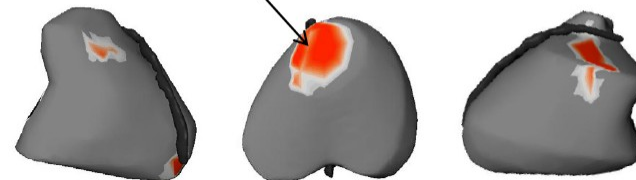
VF drivers dominant in anterior and inferior RV

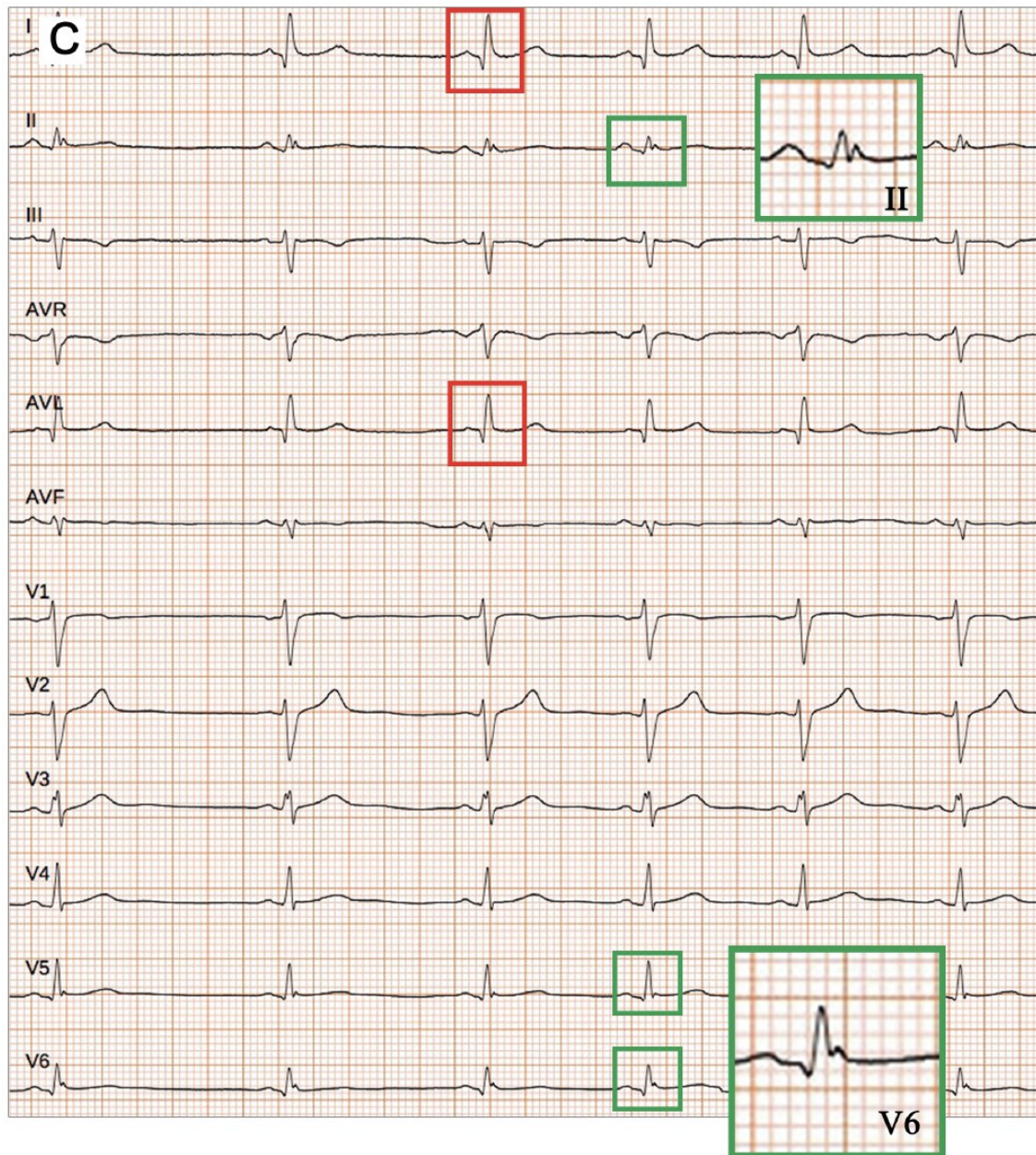


### J wave due to early repolarisation gradient



VF drivers dominant in inferior septum





Patient #8, 20-year-old man, pathogenic variant in desmoplakin (c.5851 C>T, p.Arg1951Ter)





# A New Electrocardiographic Marker of Sudden Death in Brugada Syndrome



## The S-Wave in Lead I

Leonardo Calò, MD,<sup>a</sup> Carla Giustetto, MD,<sup>b</sup> Annamaria Martino, MD,<sup>a</sup> Luigi Sciarra, MD,<sup>a</sup> Natascia Cerrato, MD,<sup>b</sup> Marta Marziali, MD,<sup>a</sup> Jessica Rauzino, MD,<sup>c</sup> Giulia Carlino, MD,<sup>d</sup> Ermenegildo de Ruvo, MD,<sup>a</sup> Federico Guerra, MD,<sup>e</sup> Marco Rebecchi, MD,<sup>a</sup> Chiara Lanzillo, MD, PhD,<sup>a</sup> Matteo Anselmino, MD,<sup>b</sup> Antonio Castro, MD,<sup>f</sup> Federico Turreni, MD,<sup>f</sup> Maria Penco, MD,<sup>d</sup> Massimo Volpe, MD,<sup>c</sup> Alessandro Capucci, MD,<sup>e</sup> Fiorenzo Gaita, MD<sup>b</sup>

### ABSTRACT

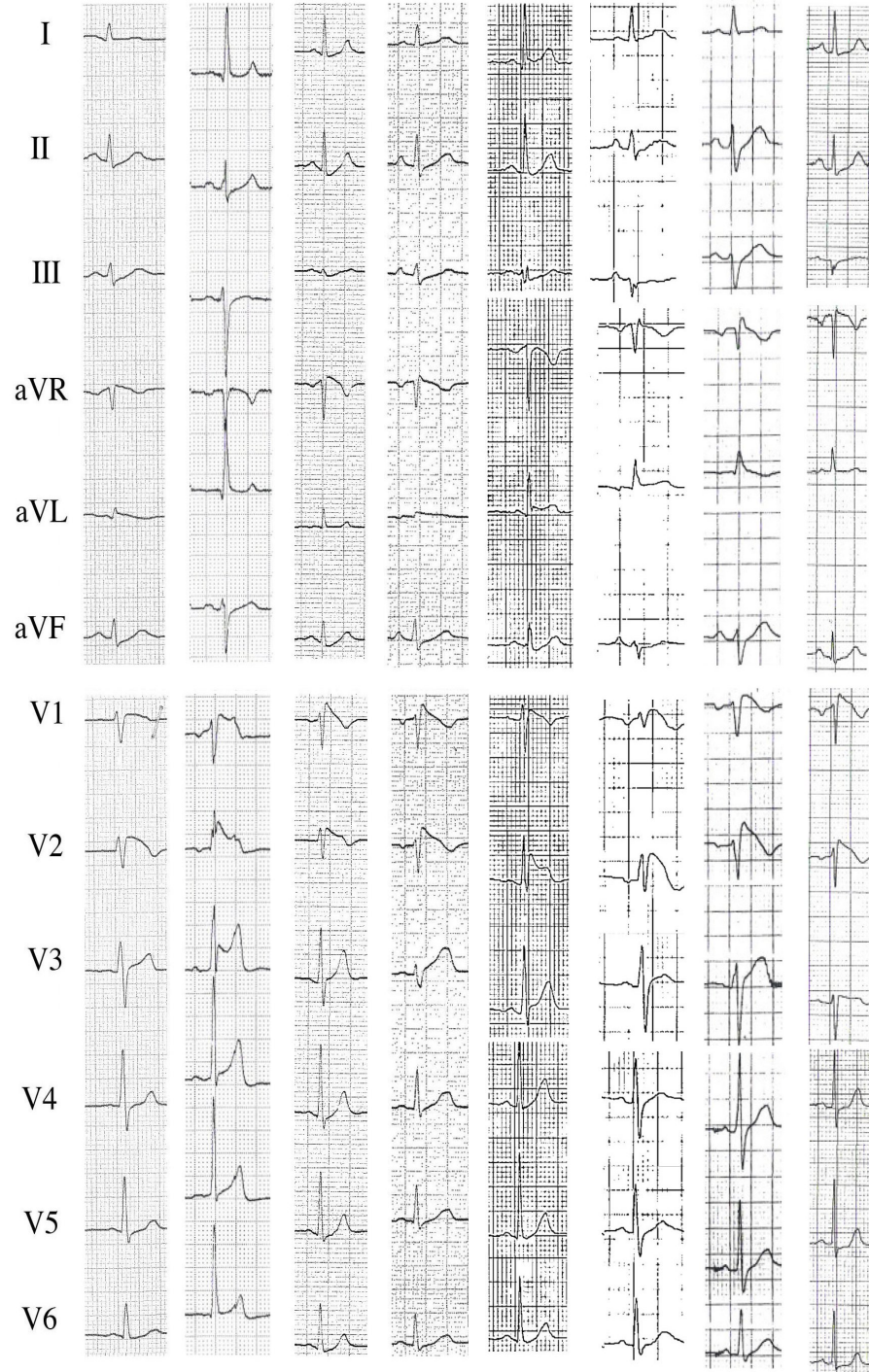
**BACKGROUND** Risk stratification in asymptomatic patients remains by far the most important yet unresolved clinical problem in the Brugada syndrome (BrS).

**OBJECTIVES** This study sought to analyze the usefulness of electrocardiographic parameters as markers of sudden cardiac death (SCD) in BrS.

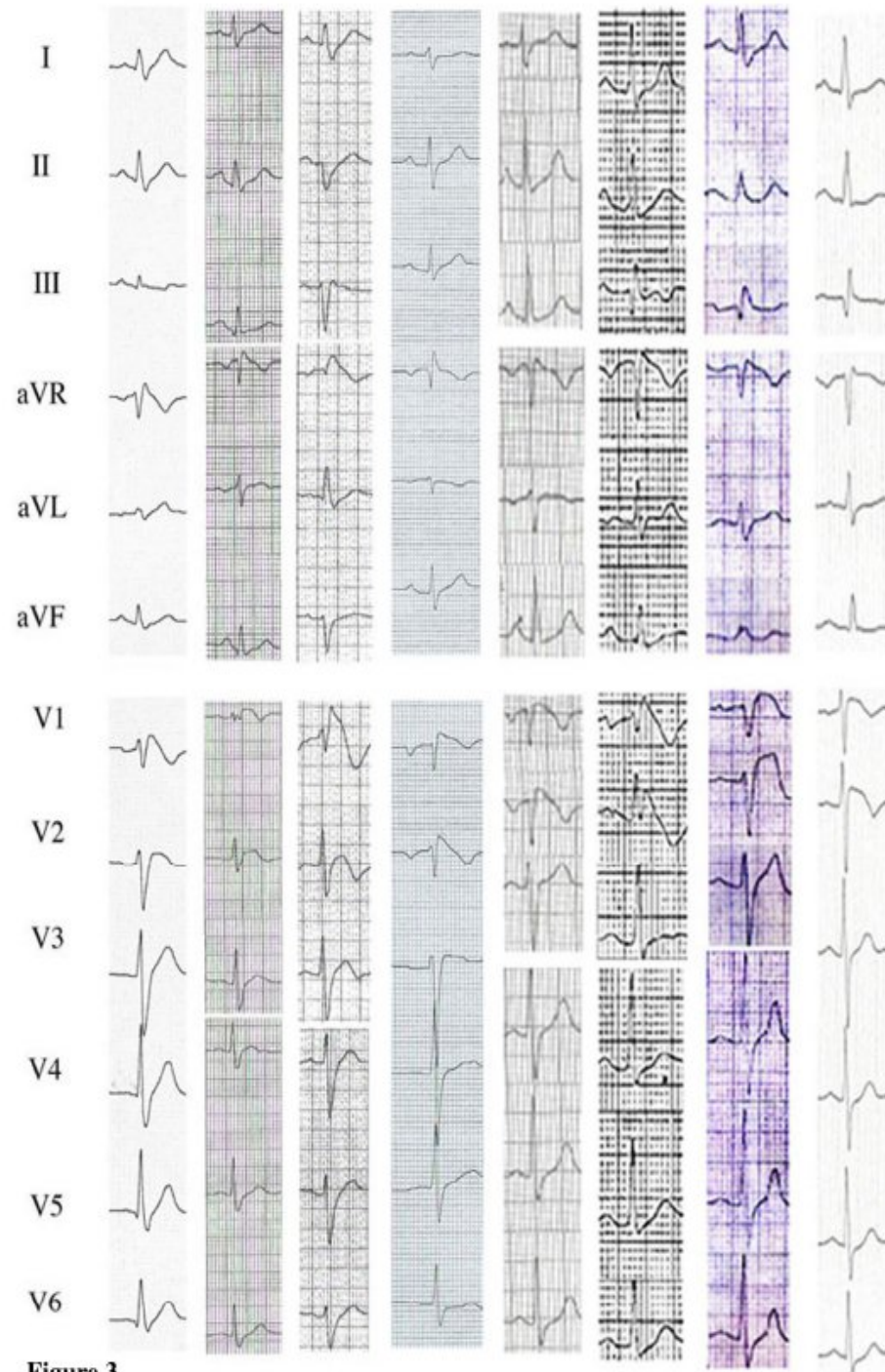
**METHODS** This study analyzed data from 347 consecutive patients (78.4% male; mean age  $45 \pm 13.1$  years) with spontaneous type 1 BrS by ECG parameters but with no history of cardiac arrest (including 91.1% asymptomatic at presentation, 5.2% with a history of atrial fibrillation [AF], and 4% with a history of arrhythmic syncope). Electrocardiographic characteristics at the first clinic visit were analyzed to predict ventricular fibrillation (VF)/SCD during follow-up.

**RESULTS** During the follow-up ( $48 \pm 38$  months), 276 (79.5%) patients remained asymptomatic, 39 (11.2%) developed syncope, and 32 (9.2%) developed VF/SCD. Patients who developed VF/SCD had a lower prevalence of *SCN5A* gene mutations ( $p = 0.009$ ) and a higher prevalence of positive electrophysiological study results ( $p < 0.0001$ ), a family history of SCD ( $p = 0.03$ ), and AF ( $p < 0.0001$ ). The most powerful marker for VF/SCD was a significant S-wave ( $\geq 0.1$  mV and/or  $\geq 40$  ms) in lead I. In the multivariate analysis, the duration of S-wave in lead I  $\geq 40$  ms (hazard ratio: 39.1) and AF (hazard ratio: 3.7) were independent predictors of VF/SCD during follow-up. Electroanatomic mapping in 12 patients showed an endocardial activation time significantly longer in patients with an S-wave in lead I, mostly because of a significant delay in the anterolateral right ventricular outflow tract.

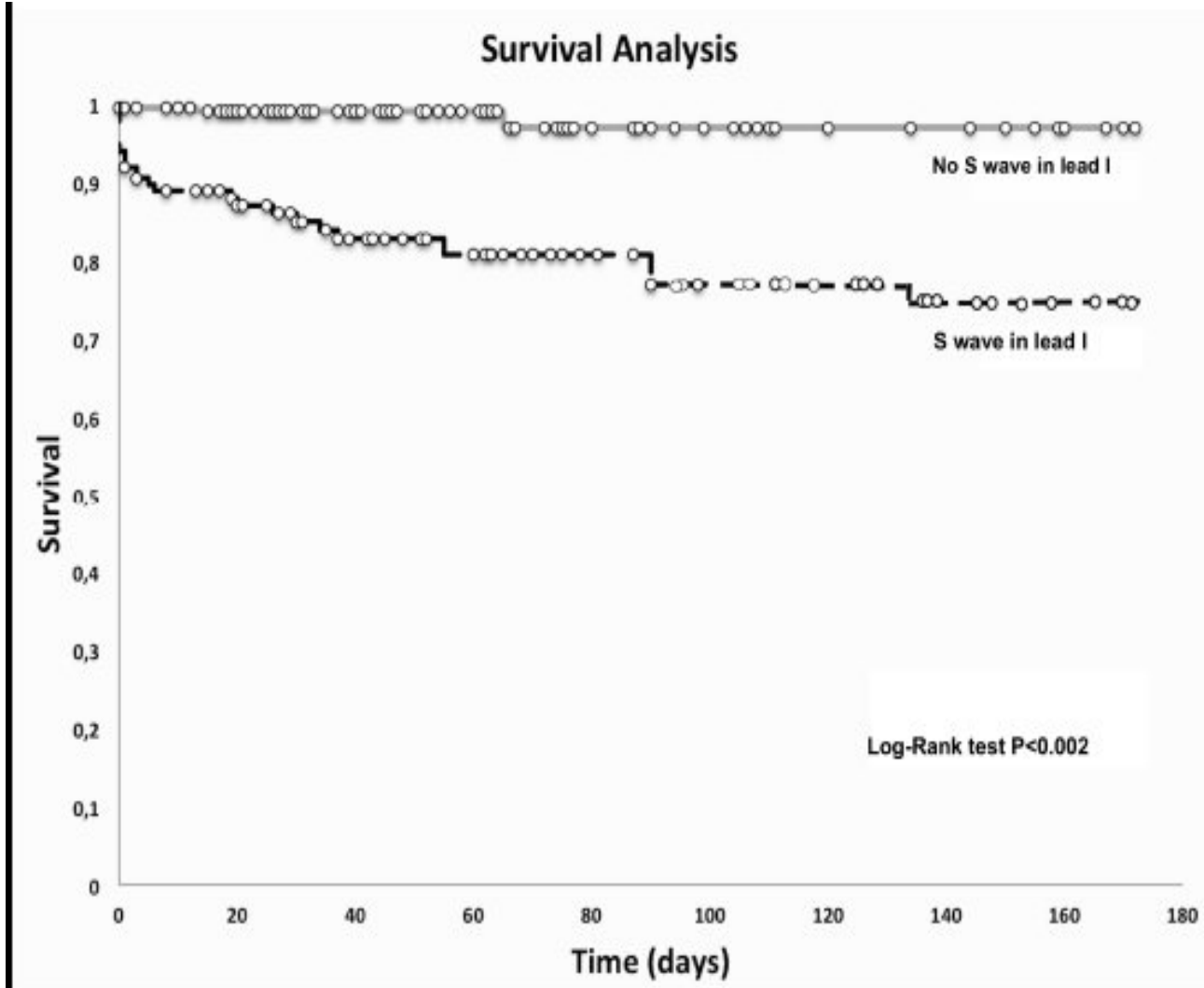
**CONCLUSIONS** The presence of a wide and/or large S-wave in lead I was a powerful predictor of life-threatening ventricular arrhythmias in patients with BrS and no history of cardiac arrest at presentation. However, the prognostic value of a significant S-wave in lead I should be confirmed by larger studies and by an independent confirmation cohort of healthy subjects. (J Am Coll Cardiol 2016;67:1427–40) © 2016 by the American College of Cardiology Foundation.

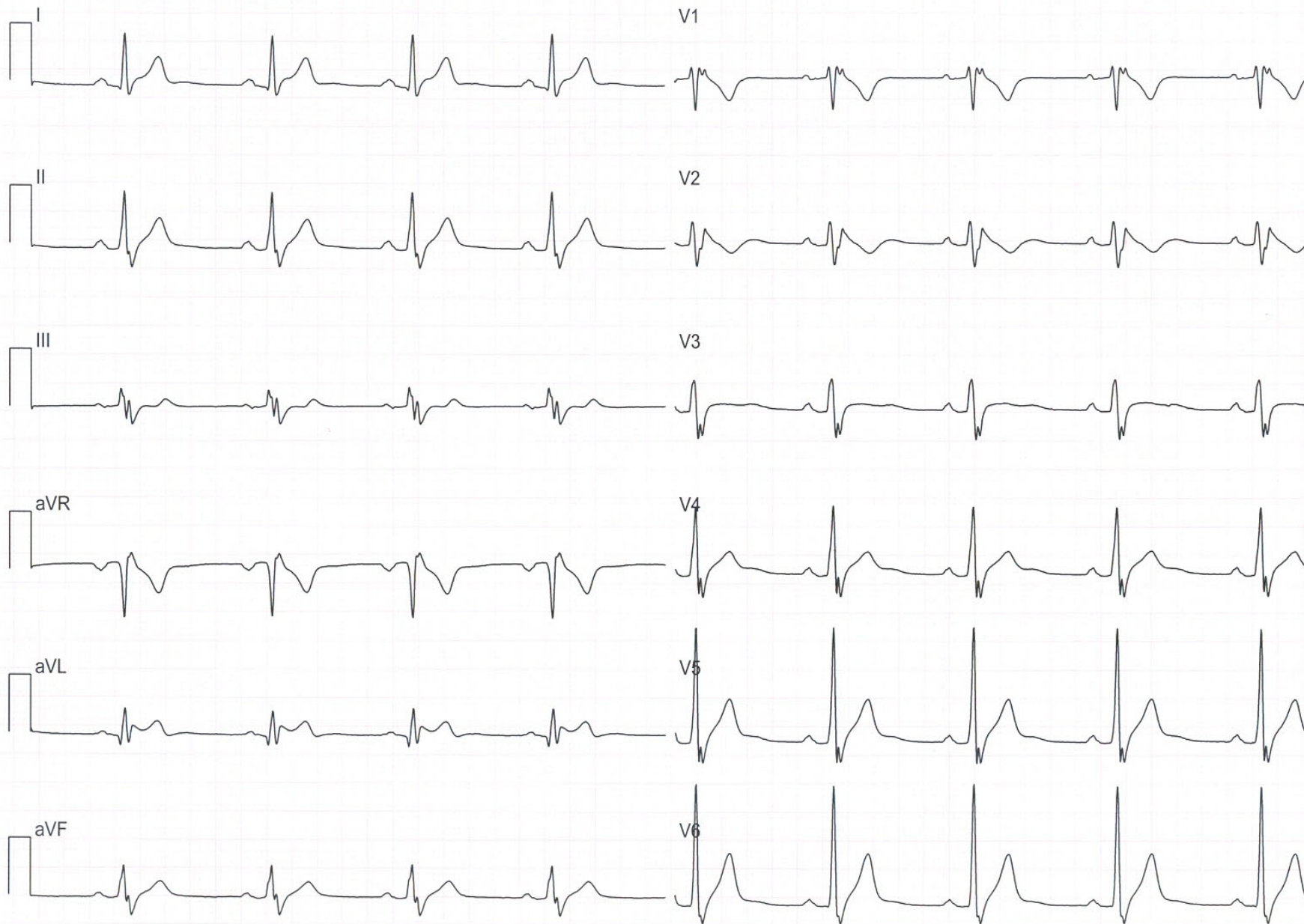






**Figure 3**







# Fibrosis, Connexin-43, and Conduction Abnormalities in the Brugada Syndrome



Koonlawee Nademanee, MD,\* Hariharan Raju, PhD,† Sofia V. de Noronha, PhD,† Michael Papadakis, MD,† Laurence Robinson, MBBS,† Stephen Rothery, BSc,† Naomasa Makita, MD,§ Shinya Kowase, MD,|| Nakorn Boonmee, MD,¶ Vorapot Vitayakritsirikul, MD,¶ Samreng Ratanarapee, MD,# Sanjay Sharma, MD,† Allard C. van der Wal, MD,\*\* Michael Christiansen, MD,†† Hanno L. Tan, MD,\*\* Arthur A. Wilde, MD,\*\*†† Akihiko Nogami, MD,§§ Mary N. Sheppard, MD,† Gumpanart Veerakul, MD,¶ Elijah R. Behr, MD†

## ABSTRACT

**BACKGROUND** The right ventricular outflow tract (RVOT) is acknowledged to be responsible for arrhythmogenesis in Brugada syndrome (BrS), but the pathophysiology remains controversial.

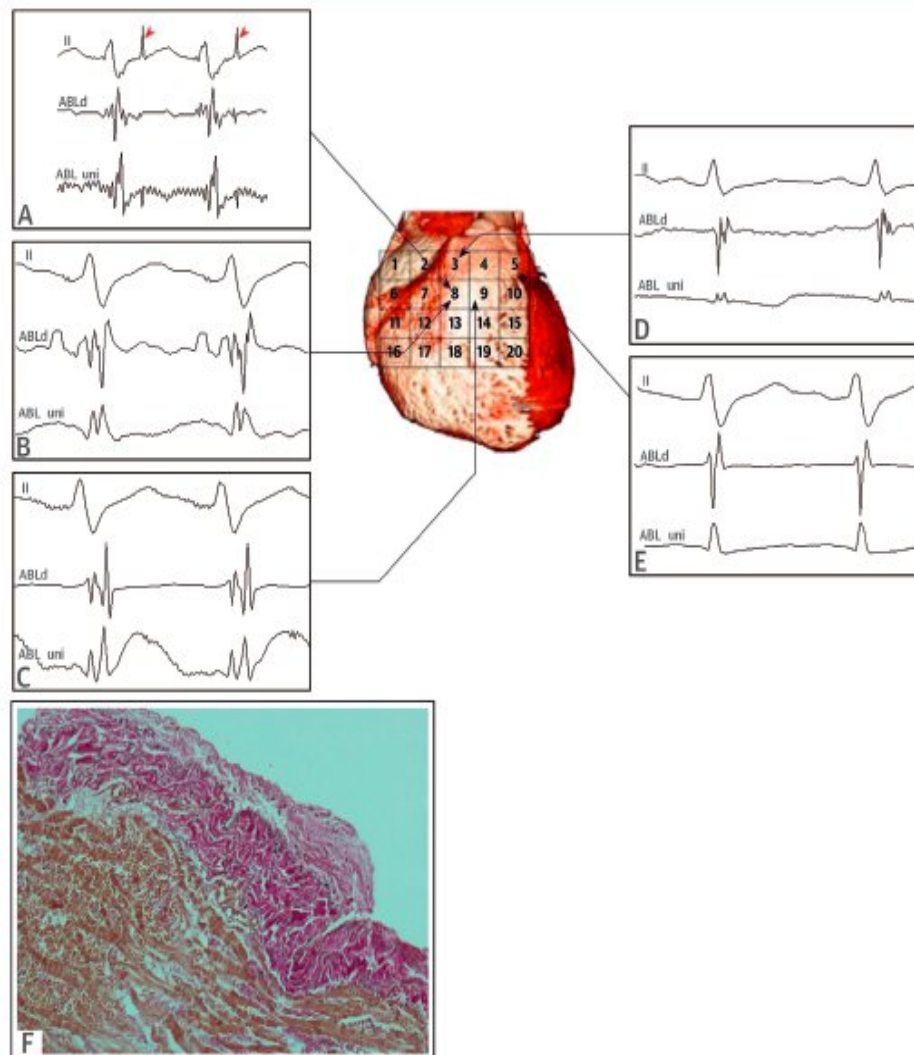
**OBJECTIVES** This study assessed the substrate underlying BrS at post-mortem and in vivo, and the role for open thoracotomy ablation.

**METHODS** Six whole hearts from male post-mortem cases of unexplained sudden death (mean age 23.2 years) with negative specialist cardiac autopsy and familial BrS were used and matched to 6 homograft control hearts by sex and age (within 3 years) by random risk set sampling. Cardiac autopsy sections from cases and control hearts were stained with picrosirius red for collagen. The RVOT was evaluated in detail, including immunofluorescent stain for connexin-43 (Cx43). Collagen and Cx43 were quantified digitally and compared. An in vivo study was undertaken on 6 consecutive BrS patients (mean age 39.8 years, all men) during epicardial RVOT ablation for arrhythmia via thoracotomy. Abnormal late and fractionated potentials indicative of slowed conduction were identified, and biopsies were taken before ablation.

**RESULTS** Collagen was increased in BrS autopsy cases compared with control hearts (odds ratio [OR]: 1.42;  $p = 0.026$ ). Fibrosis was greatest in the RVOT (OR: 1.98;  $p = 0.003$ ) and the epicardium (OR: 2.00;  $p = 0.001$ ). The Cx43 signal was reduced in BrS RVOT (OR: 0.59;  $p = 0.001$ ). Autopsy and in vivo RVOT samples identified epicardial and interstitial fibrosis. This was collocated with abnormal potentials in vivo that, when ablated, abolished the type 1 Brugada electrocardiogram without ventricular arrhythmia over  $24.6 \pm 9.7$  months.

**CONCLUSIONS** BrS is associated with epicardial surface and interstitial fibrosis and reduced gap junction expression in the RVOT. This collocates to abnormal potentials, and their ablation abolishes the BrS phenotype and life-threatening arrhythmias. BrS is also associated with increased collagen throughout the heart. Abnormal myocardial structure and conduction are therefore responsible for BrS. (J Am Coll Cardiol 2015;66:1976-86) © 2015 by the American College of Cardiology Foundation.

**FIGURE 2** Computed Tomography Scan, Epicardial Electrograms, and Histology of RVOT of In Vivo BrS Patient



Computed tomography scan of the heart (**center**) of in vivo BrS patient V2 showing an anatomical grid over the anterior RVOT. ECG Lead II and a distal bipolar (0.4 mV/cm voltage scale at 30- to 300-Hz filter settings) and unipolar (5 mV/cm voltage scale at 0.05- to 300-Hz filter settings) electrograms at labeled sites are given in surrounding panels, with pacing stimuli indicated by **red arrowheads**. Abnormal fractionated electrograms are on the (**A to C**) left and normal electrograms on the (**D to E**) right. (**F**) Epicardial biopsy and histology (PSR) at the site of the abnormal electrogram shows epicardial fibrosis with focal finger-like projections of collagen into myocardium. ABL d = distal bipolar ablation catheter electrogram; ABL uni = unipolar ablation catheter electrogram; BrS = Brugada syndrome; RVOT = right ventricular outflow tract; other abbreviations as in [Figure 1](#).

BLOCCO DI BRANCA  
DESTRA



A

CONTROL

F 6 J 4 K 3  
I 6 B 5 M 3  
L 6 E 5  
E 7 K 5  
H 7 M 5  
K 7 B 7  
M 7 B 9  
J 8 F 12  
E 9  
H 9  
K 9  
D 11  
F 11  
H 11

DOG 743

10  
MSEC

CUT  
FALSE  
TENDON

M 7 M 5 K 3 E 5  
K 9 L 6 H 7 F 6  
B 7 K 7 I 6  
B 9 J 8 E 7  
D 11 E 9  
H 11 H 9  
F 12 F 11

B

CONTROL

K 9 J 4 K 3 B 5  
H 5 M 3 B 7  
K 5 E 5 B 9  
H 7 N 5  
K 7 E 7  
M 7 D 11  
E 9 F 13  
H 9  
F 11  
H 11

10  
MSEC

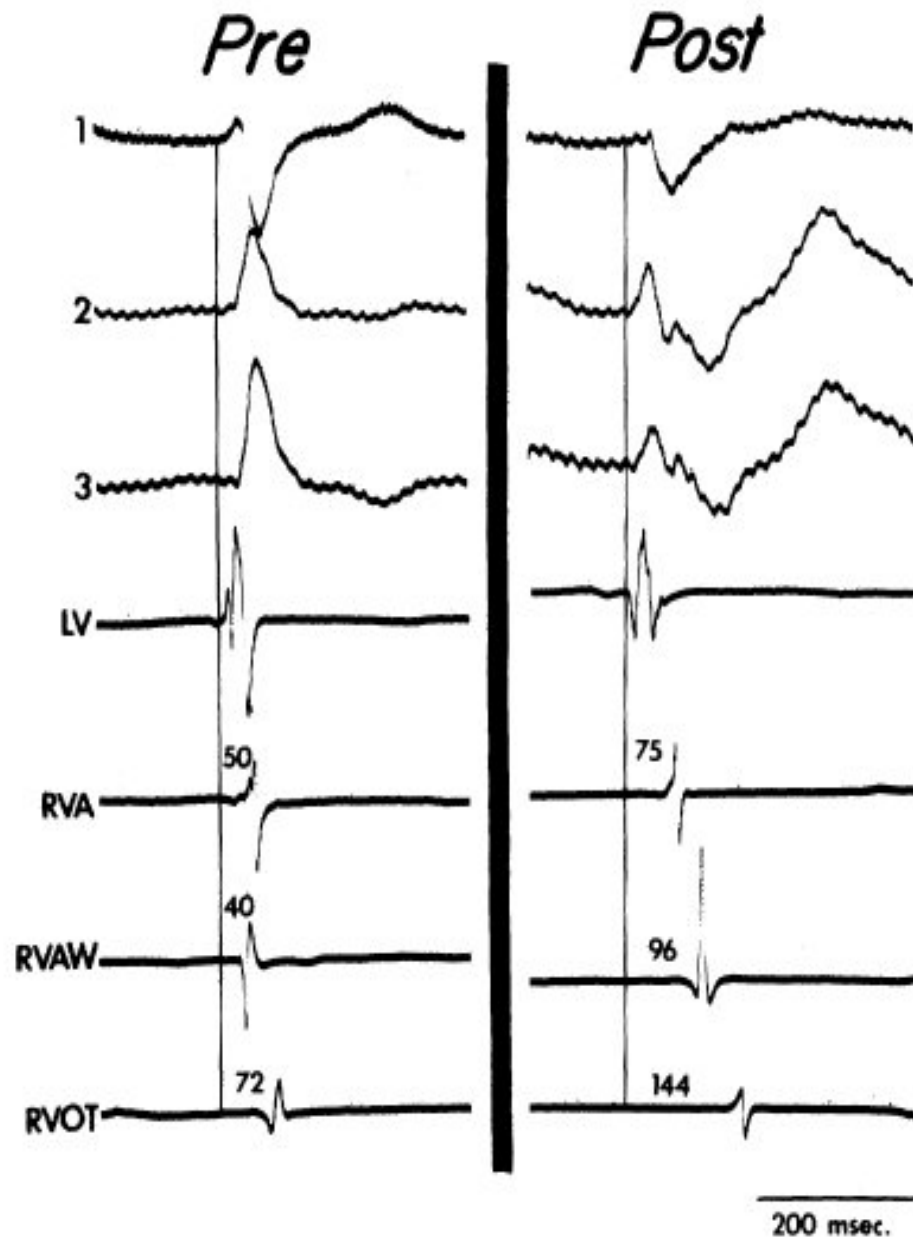
CUT RIGHT  
BUNDLE BRANCH

B 5 B 9 E 5 M 3 K 3  
B 7 H 5 N 5 J 4  
E 9 E 7 K 5  
K 9 H 7 K 7  
D 11 M 7 H 9  
H 11 F 11  
F 13

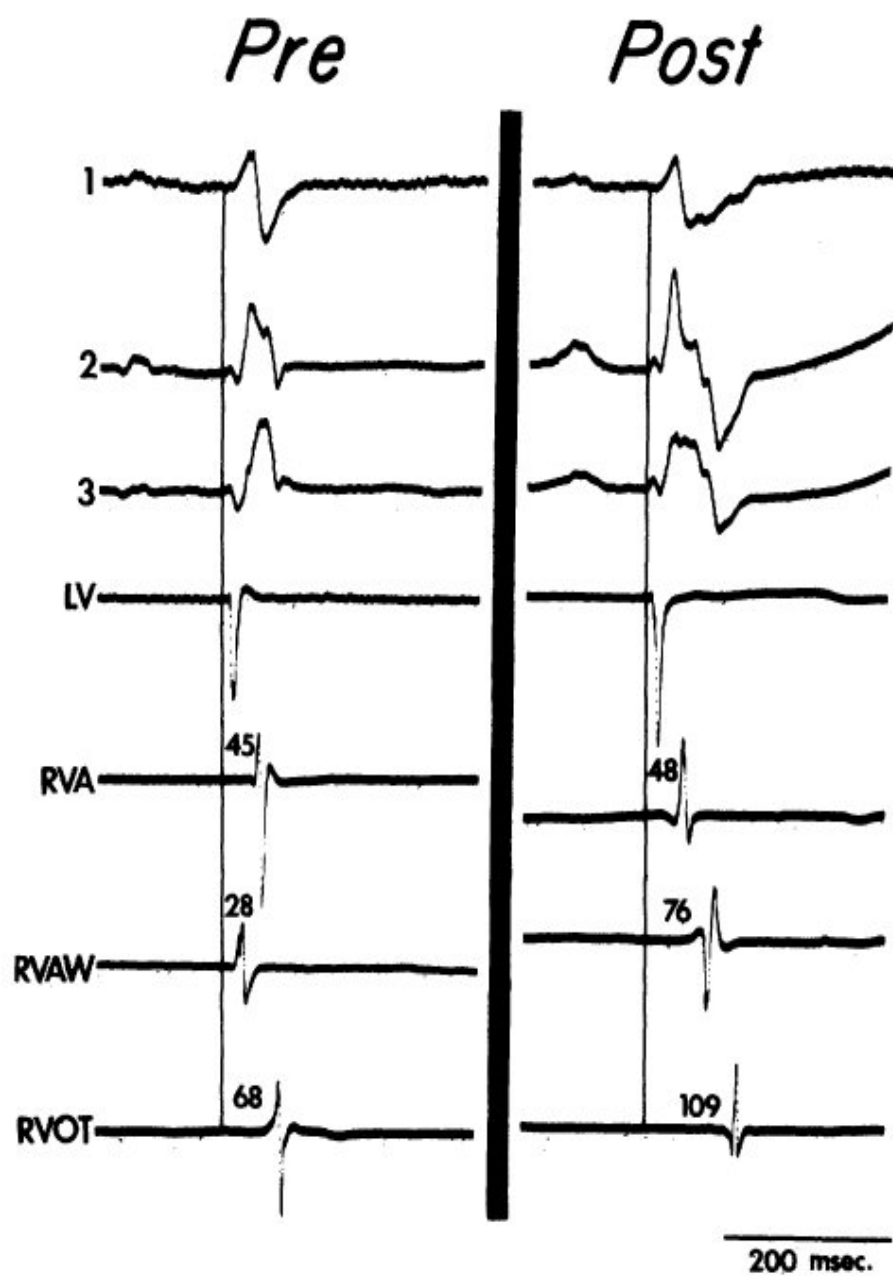
# **Postoperative Right Bundle Branch Block: Identification of Three Levels of Block**

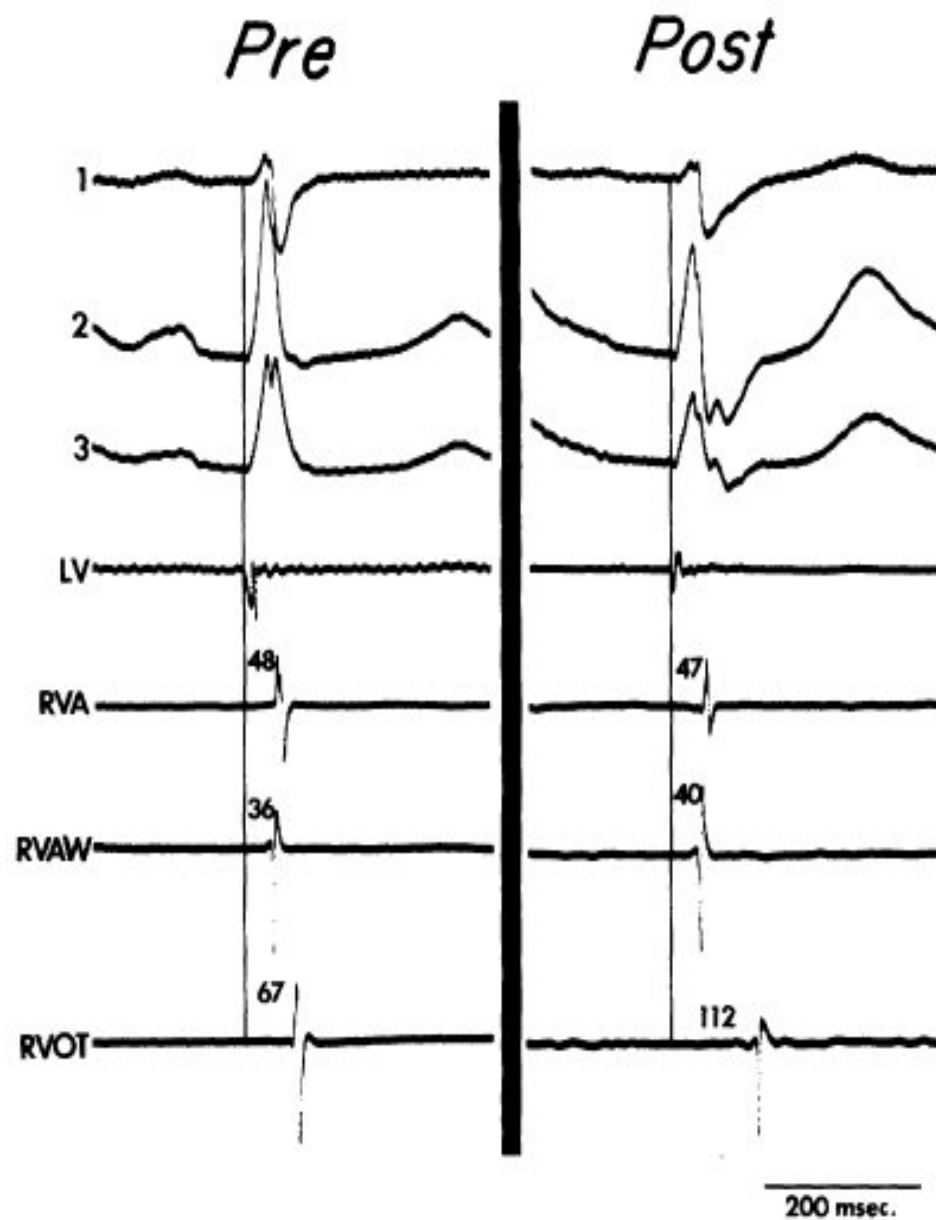
LEONARD N. HOROWITZ, M.D., JAMES A. ALEXANDER, M.D.,  
AND L. HENRY EDMUNDS, JR., M.D.

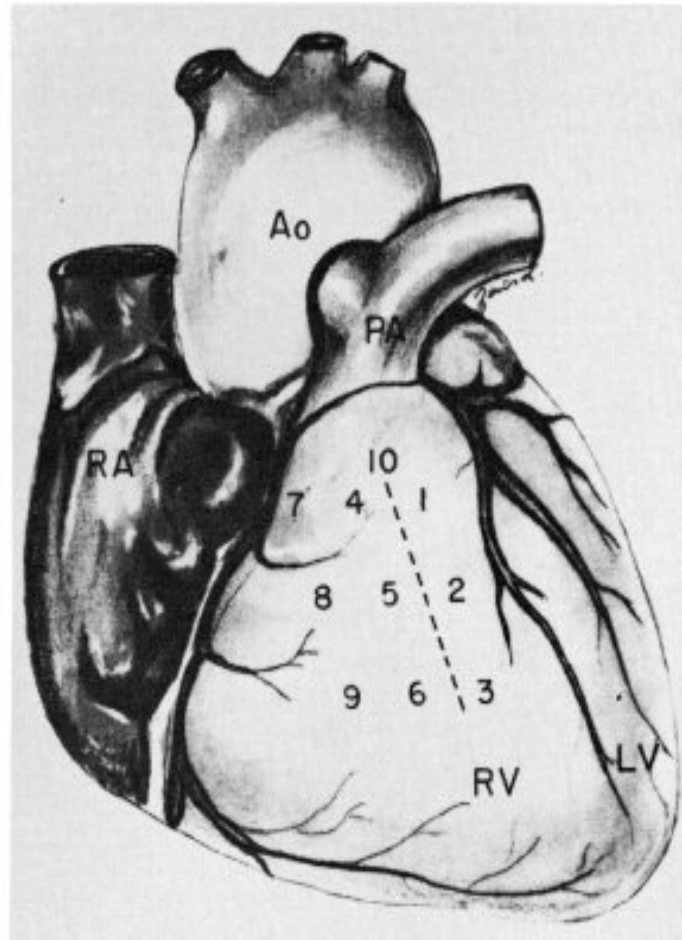
**SUMMARY** It has been postulated that postoperative right bundle branch block (RBBB) may be produced by conduction block at any of several sites. In this study the site of block and resultant pattern of ventricular activation were documented in 20 patients in whom RBBB developed during repair of congenital cardiac defects. Intraoperative epicardial and endocardial mapping and recording from the right ventricular specialized conduction system were performed before and after repair in each patient. In eight patients right bundle branch (RBB) conduction was interrupted proximally in the area of the ventricular septal defect. Right ventricular (RV) activation in these patients was delayed at all sites. In five patients RBB conduction was interrupted distally in the area of the moderator band. RV activation in these patients was delayed at most sites; however, the apical septal sites were activated normally. In seven patients, RBB conduction was interrupted terminally in the area of the terminal fascicular network. In these patients RV activation was delayed only in basilar areas. We conclude that at least three distinct types of postoperative RBBB exist and can be identified by differences in RV activation.





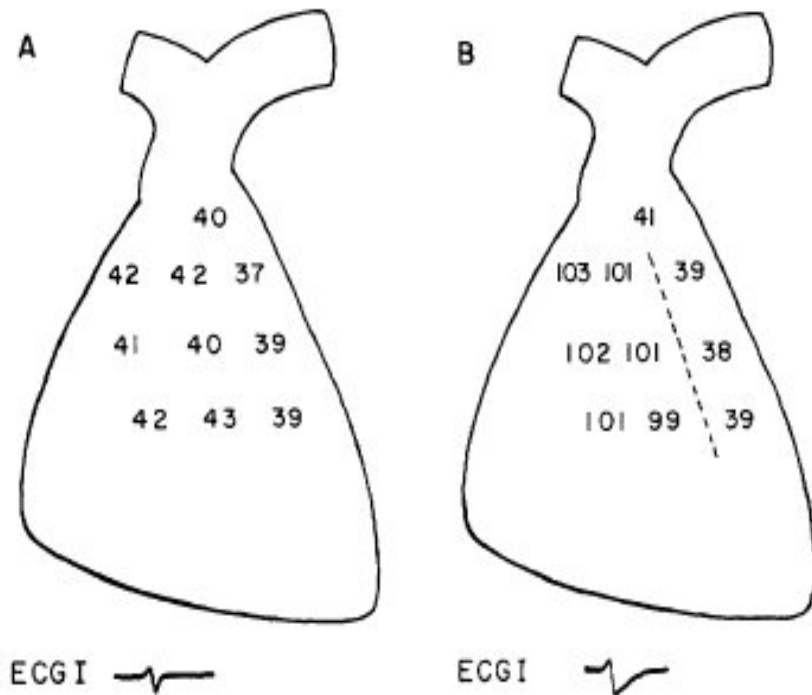




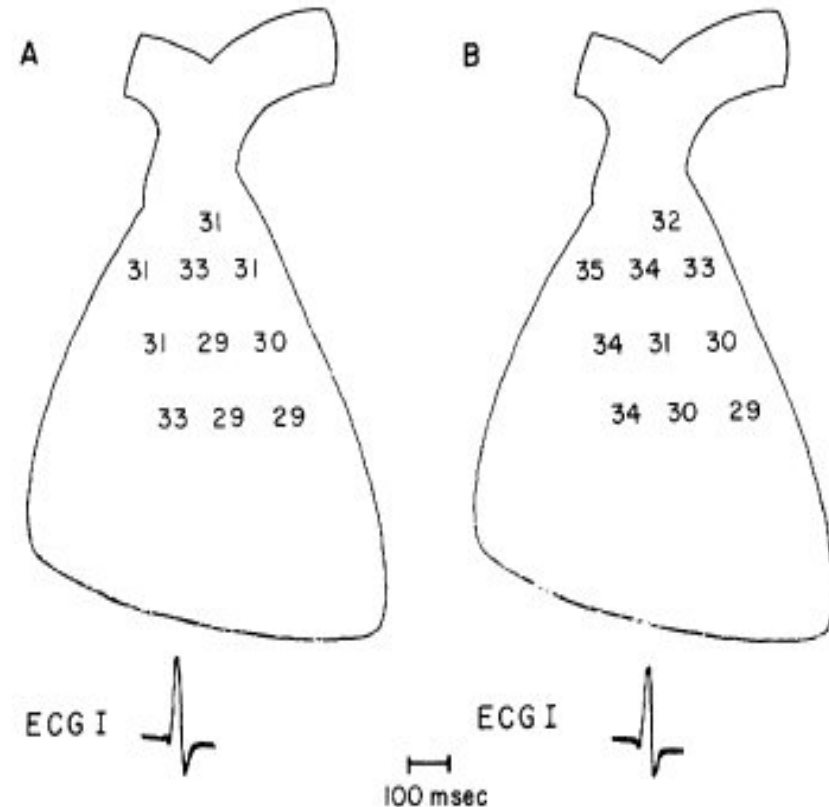


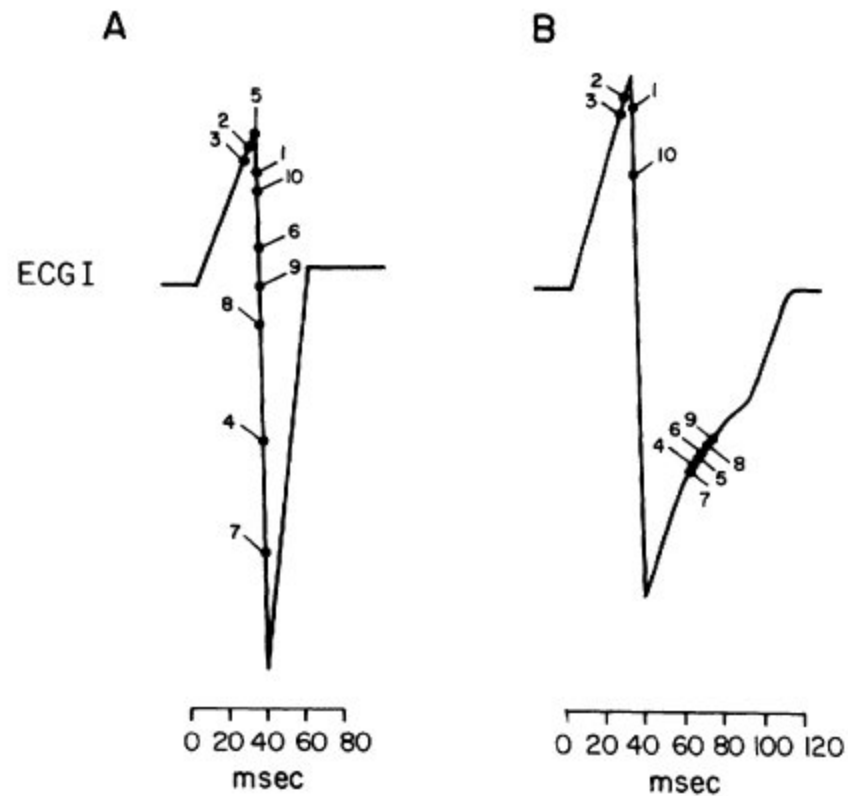


Effect of a vertical  
ventriculotomy on the  
activation  
times to the right ventricular  
epicardial recording sites  
in a representative patient



Right ventricular epicardial  
activation times after repair  
of VSD via the right atrium

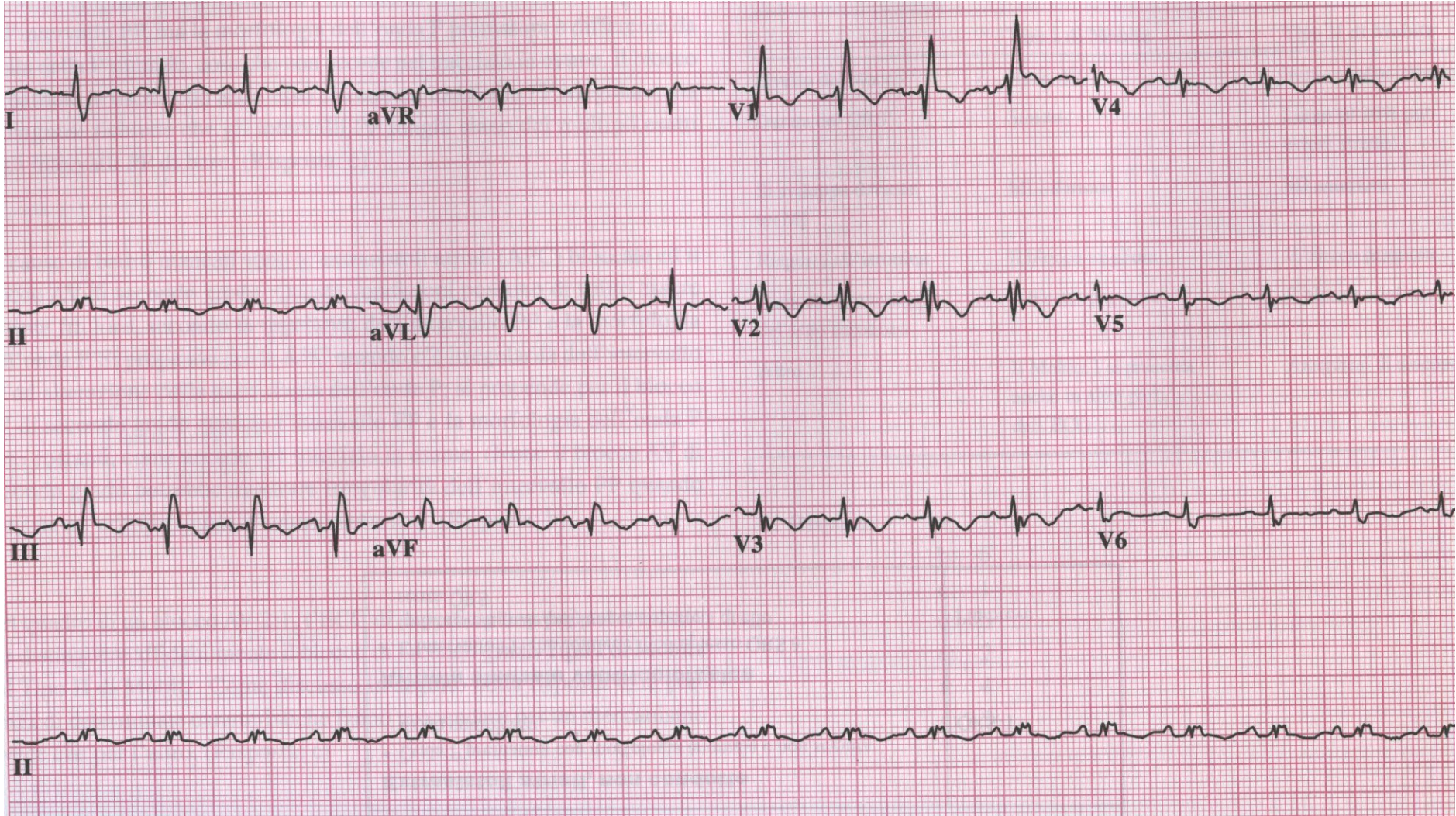




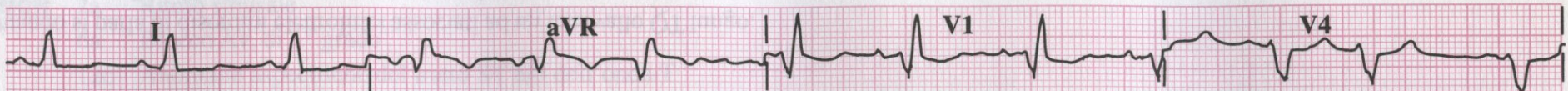
**Temporal relation of the time of activation of the 10 epicardial sites plotted on an electrocardiographic lead-1 QRS complex before (A), and immediately after (B), ventriculotomy in patient 9.**



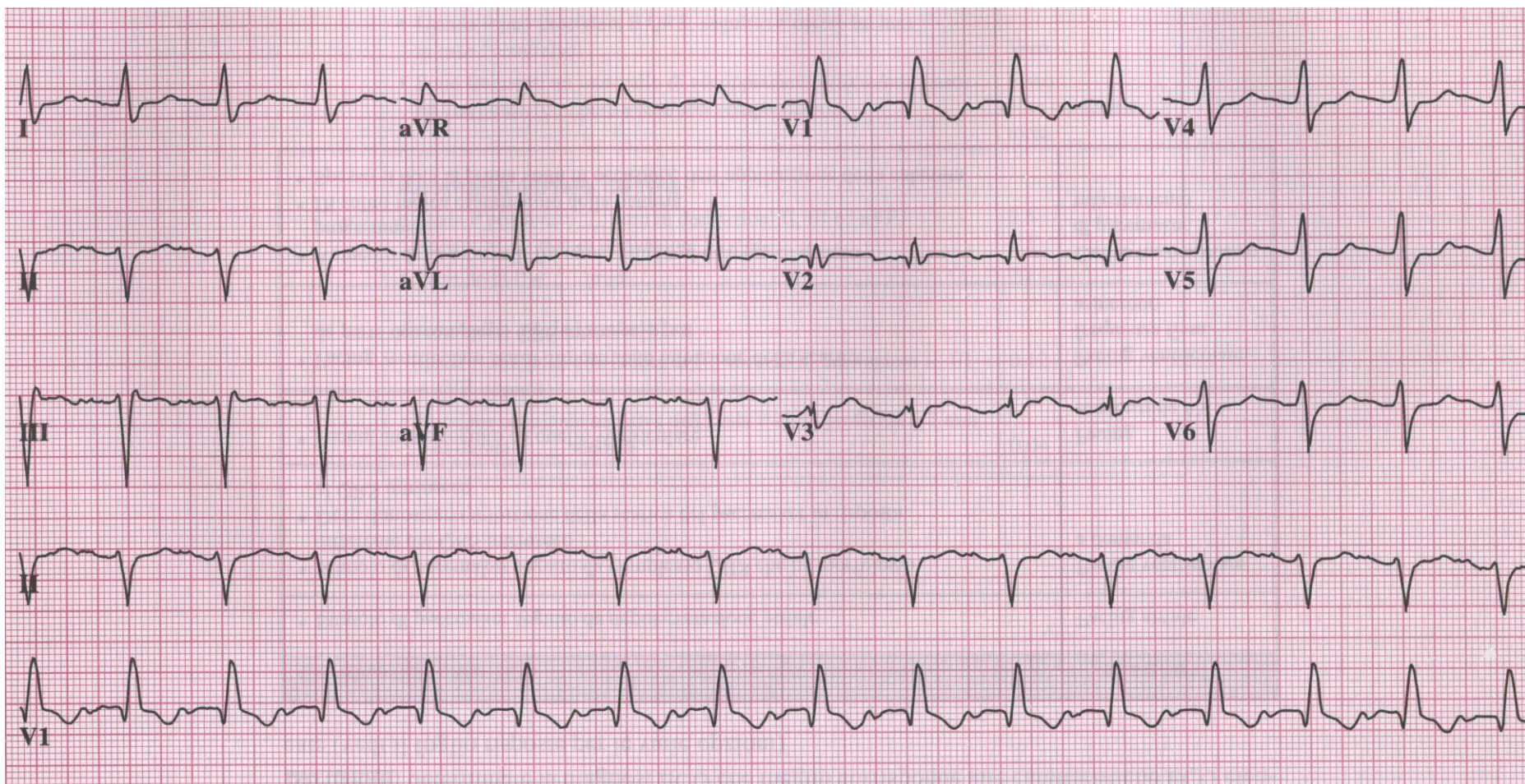














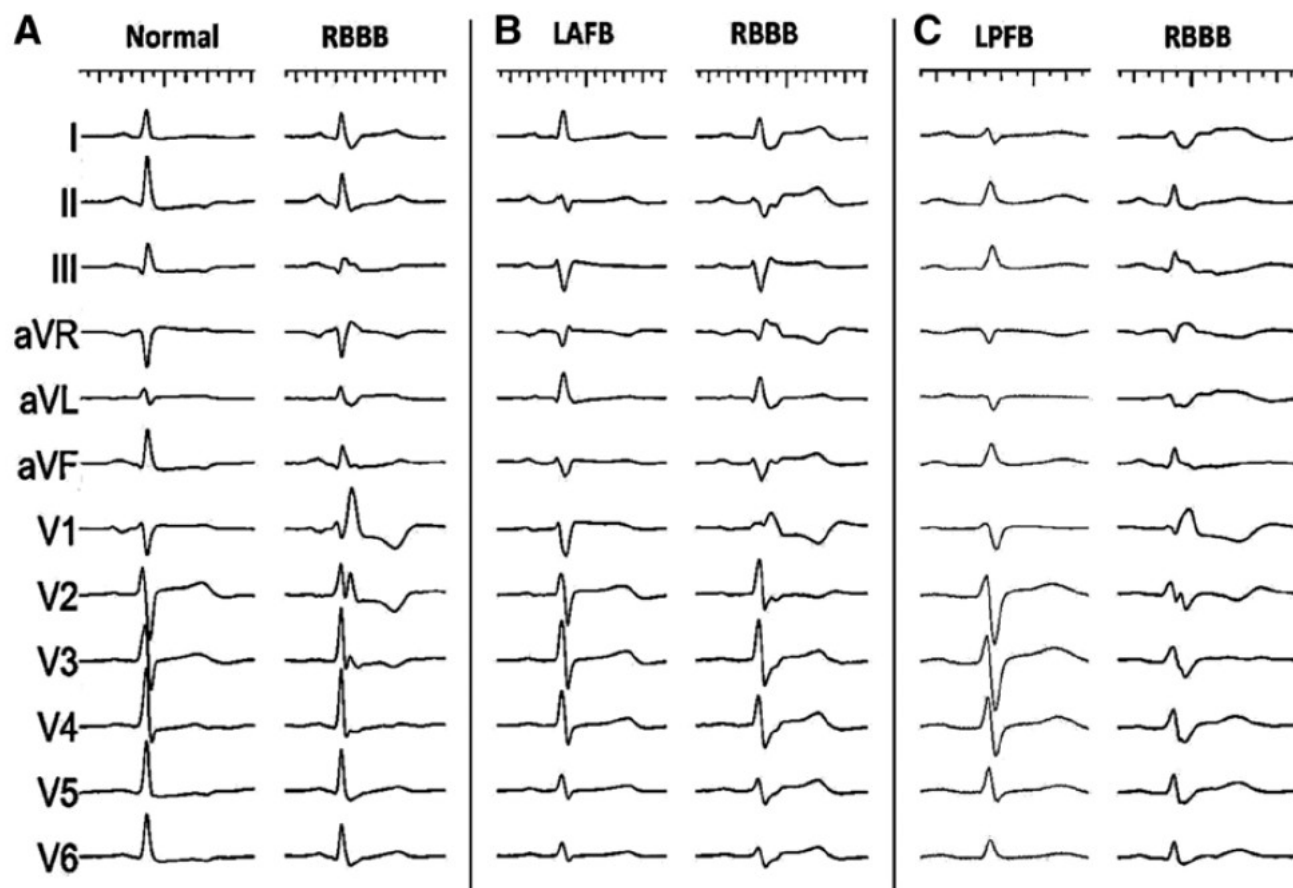
# Electrocardiographic Features and Prevalence of Bilateral Bundle-Branch Delay

Leonidas Tzogias, MD; Leonard A. Steinberg, MD; Andrew J. Williams, MD;  
Kent E. Morris, MD; William J. Mahlow, MD; Richard I. Fogel, MD; Jeff A. Olson, DO;  
Eric N. Prystowsky, MD; Benzy J. Padanilam, MD

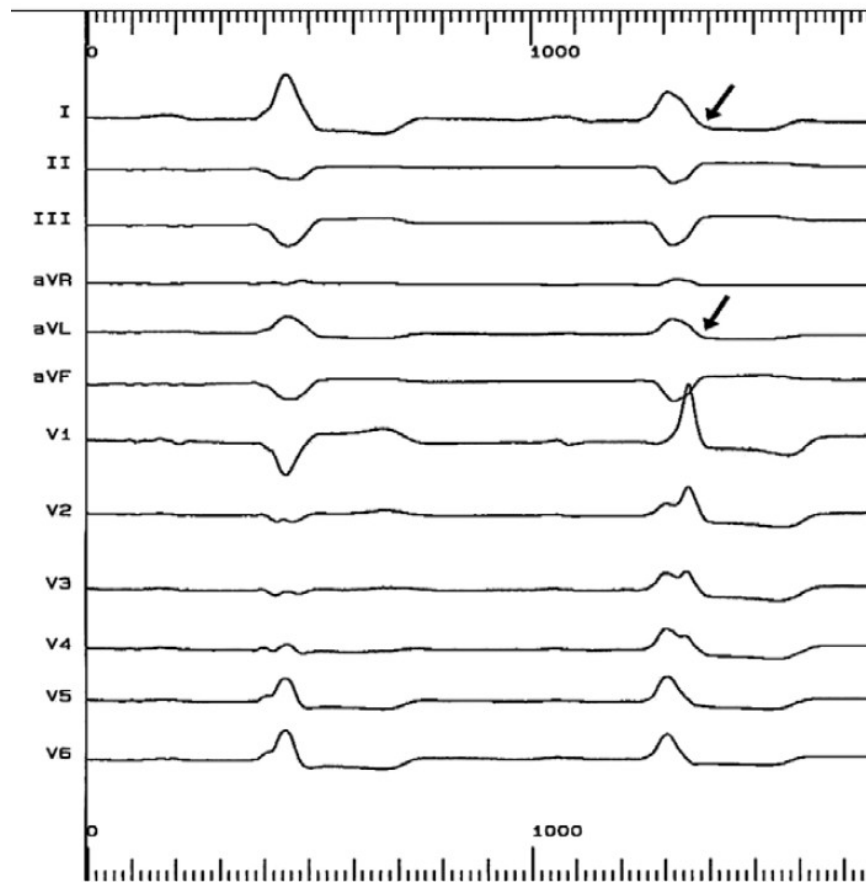
**Background**—Definitive diagnosis of bilateral bundle-branch delay/block may be made when catheter-induced right bundle-branch block (RBBB) develops in patients with baseline left bundle-branch (LBB) block. We hypothesized that a RBBB pattern with absent S waves in leads I and aVL will identify bilateral bundle-branch delay/block.

**Methods and Results**—Fifty patients developing transient RBBB pattern in lead V1 during right heart catheterization were studied. Patients were grouped according to whether the baseline ECG demonstrated a normal QRS, left fascicular blocks, or LBB block pattern. The RBBB morphologies in each group were compared. The prevalence of bilateral bundle-branch delay/block pattern was examined in our hospital ECG database. All patients with baseline normal QRS complexes (n=30) or left fascicular blocks (4 anterior, 5 posterior) developed a typical RBBB pattern. Among the 11 patients with a baseline LBB block pattern, 7 developed an atypical RBBB pattern with absent S waves in leads I and aVL and the remaining 4 demonstrated a typical RBBB. The absence of S waves in leads I and aVL during RBBB was 100% specific and 64% sensitive for the presence of pre-existing LBB block. Among the consecutive 2253 hospitalized patients with RBBB, 34 (1.5%) had the bilateral bundle-branch delay/block pattern.

**Conclusions**—An ECG pattern of RBBB in lead V1 with absent S wave in leads I and aVL indicates concomitant LBB delay. Pure RBBB and bifascicular blocks are associated with S waves in leads I and aVL. (*Circ Arrhythm Electrophysiol.* 2014;7:640-644.)



Catheter trauma induced right bundle-branch block (RBBB) in patients with baseline (A) normal; (B) left anterior fascicular block (LAFB); and (C) left posterior fascicular block (LPFB). Note the presence of S waves in leads I and aVL during RBBB morphology



Catheter trauma induced right bundle-branch block (RBBB) in a patient with baseline left bundle-branch block (LBBB). The QRS morphology changes from LBBB to RBBB from the first to the second complex. Note the absence of S waves (arrows) in leads I and aVL during RBBB morphology



Atypical RBBB is defined by the absence of the characteristic S wave in leads I and aVL (S duration < R duration and < 40 ms).

This absence of the S wave in lateral ECG leads with RBBB pattern is suggestive of a concomitant delayed activation of LV free wall and commonly presents with left-axis deviation.

Patients with atypical RBBB as compared with typical RBBB have a longer Q-LV (>110 ms) and accordingly favorably respond to CRT (71 versus 19%) [1].

**[1] Pastore G et al. Patients with right bundle branch block and concomitant delayed left ventricular activation respond to cardiac resynchronization therapy. Europace. 2018;20:e171**

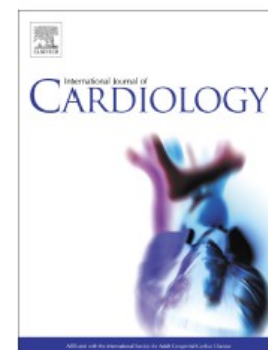


## Diagnosis of arrhythmogenic cardiomyopathy: The Padua criteria

Domenico Corrado, Martina Perazzolo Marra, Alessandro Zorzi, Giorgia Beffagna, Alberto Cipriani, Manuel De Lazzari, Federico Migliore, Kalliopi Pilichou, Alessandra Rampazzo, Ilaria Rigato, Stefania Rizzo, Gaetano Thiene, Aris Anastasakis, Angeliki Asimaki, Chiara Bucciarelli-Ducci, Kristine H. Haugaa, Francis E. Marchlinski, Andrea Mazzanti, William J. McKenna, Antonis Pantazis, Antonio Pelliccia, Christian Schmied, Sanjay Sharma, Thomas Wichter, Barbara Bauce, Cristina Basso

PII: S0167-5273(20)33293-9

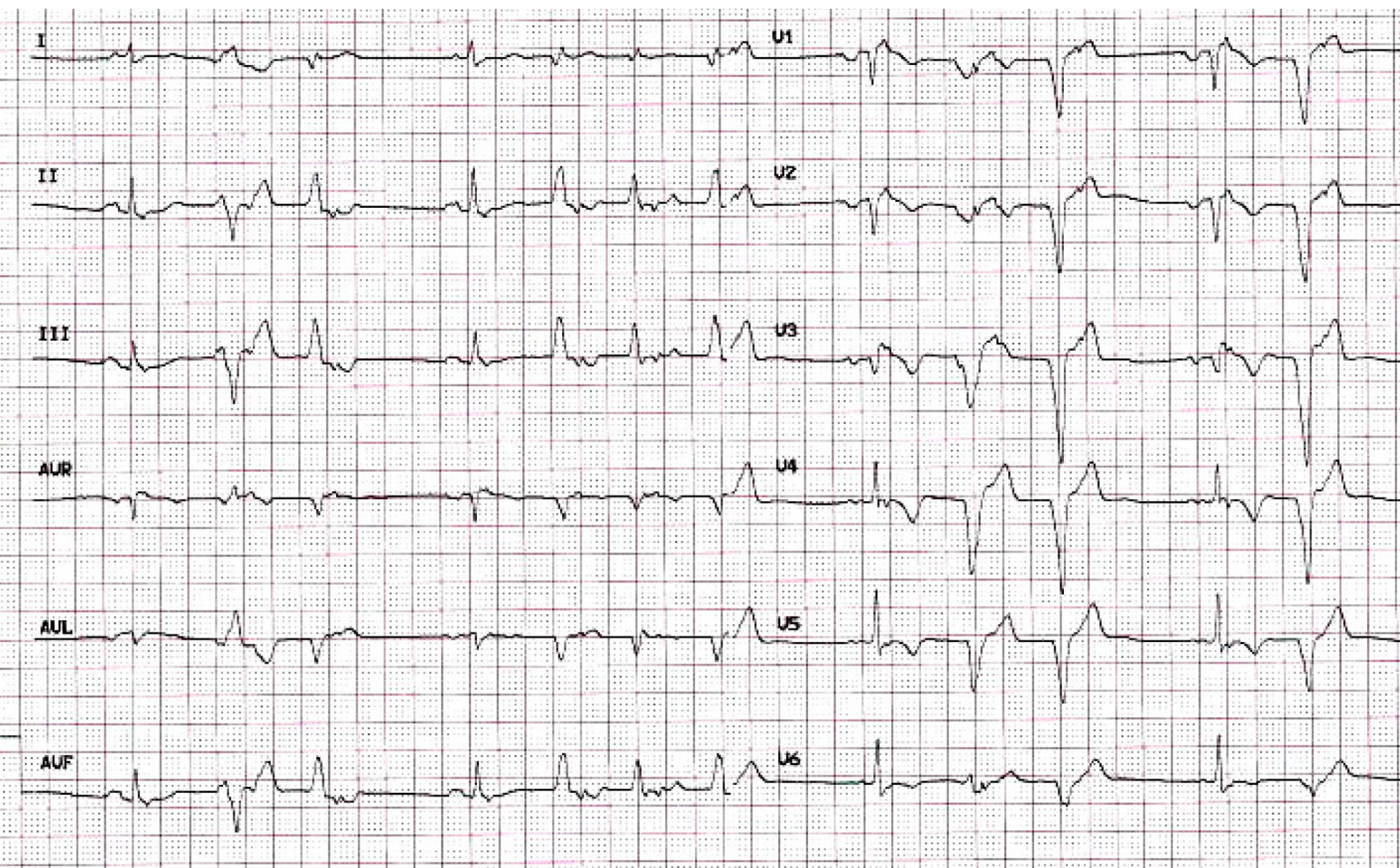
DOI: <https://doi.org/10.1016/j.ijcard.2020.06.005>



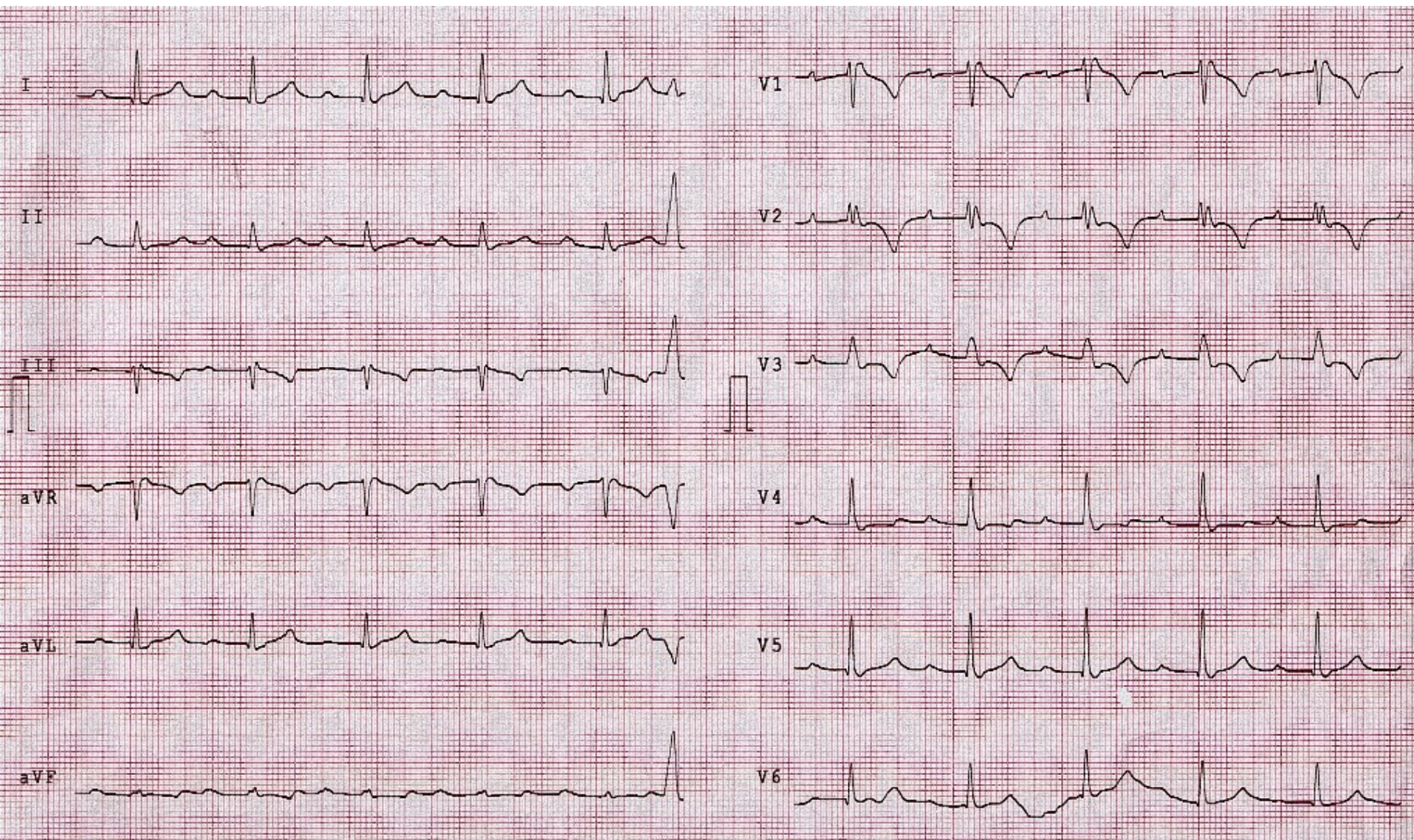


Category	Right ventricle (upgraded 2010 ITF diagnostic criteria)	Left ventricle (new diagnostic criteria)
<b>III. Repolarization abnormalities</b>	<p><i>Major</i></p> <ul style="list-style-type: none"> <li>Inverted T waves in right precordial leads (V<sub>1</sub>, V<sub>2</sub>, and V<sub>3</sub>) or beyond in individuals with complete pubertal development (in the absence of complete RBBB)</li> </ul>	<p><i>Minor</i></p> <ul style="list-style-type: none"> <li>Inverted T waves in left precordial leads (V<sub>4</sub>-V<sub>6</sub>) (in the absence of complete LBBB)</li> </ul>
	<p><i>Minor</i></p> <ul style="list-style-type: none"> <li>Inverted T waves in leads V1 and V2 in individuals with completed pubertal development (in the absence of complete RBBB)</li> <li>Inverted T waves in V1, V2, V3 and V4 in individuals with completed pubertal development in the presence of complete RBBB.</li> </ul>	
<b>IV. Depolarization abnormalities</b>	<p><i>Minor</i></p> <ul style="list-style-type: none"> <li>Epsilon wave (reproducible low-amplitude signals between end of QRS complex to onset of the T wave) in the right precordial leads (V1 to V3)</li> <li>Terminal activation duration of QRS <math>\geq 55</math> ms measured from the nadir of the S wave to the end of the QRS, including R', in V1, V2, or V3 (in the absence of complete RBBB)</li> </ul>	<p><i>Minor</i></p> <ul style="list-style-type: none"> <li>Low QRS voltages (<math>&lt;0.5</math> mV peak to peak) in limb leads (in the absence of obesity, emphysema, or pericardial effusion)</li> </ul>











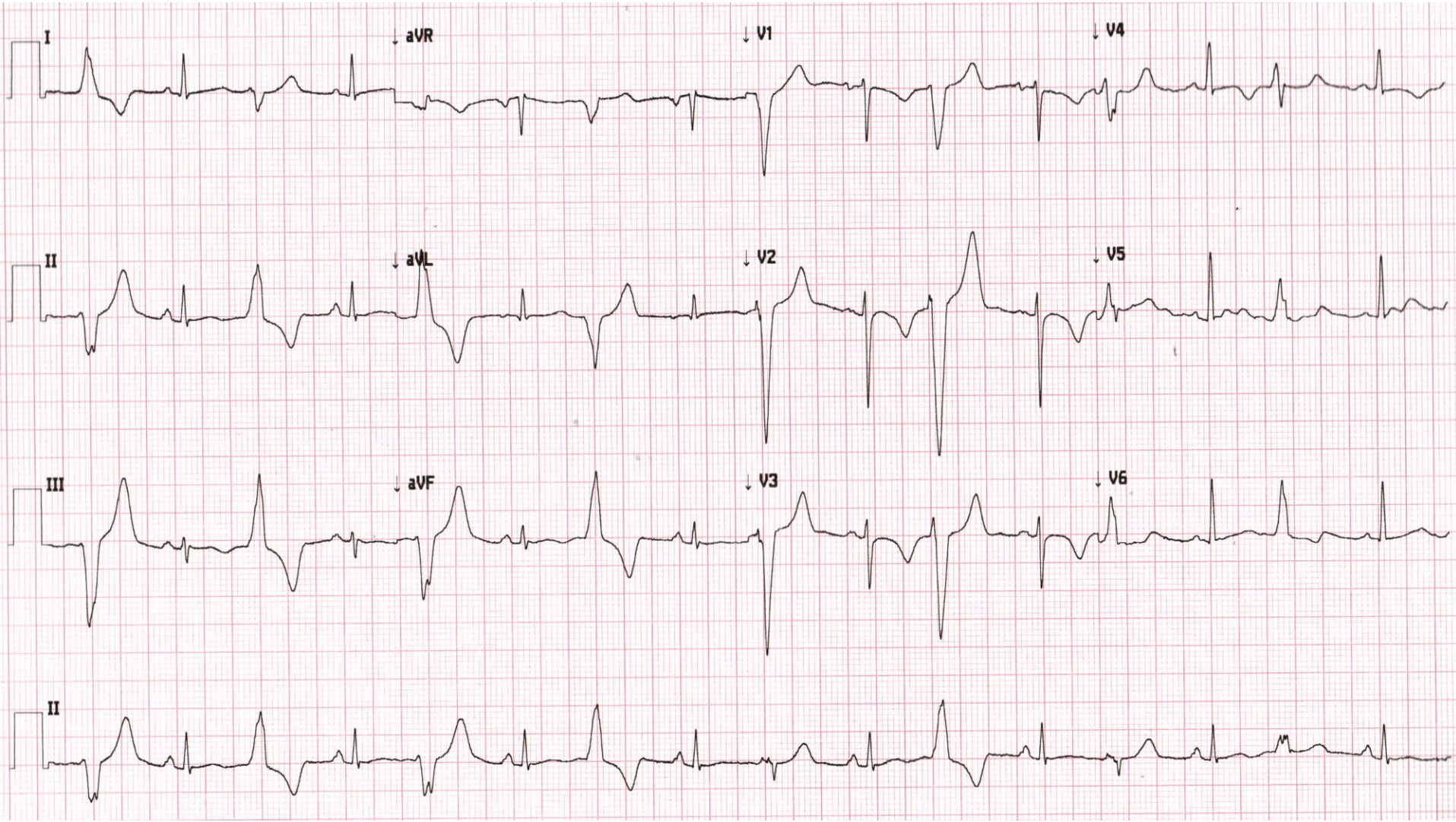
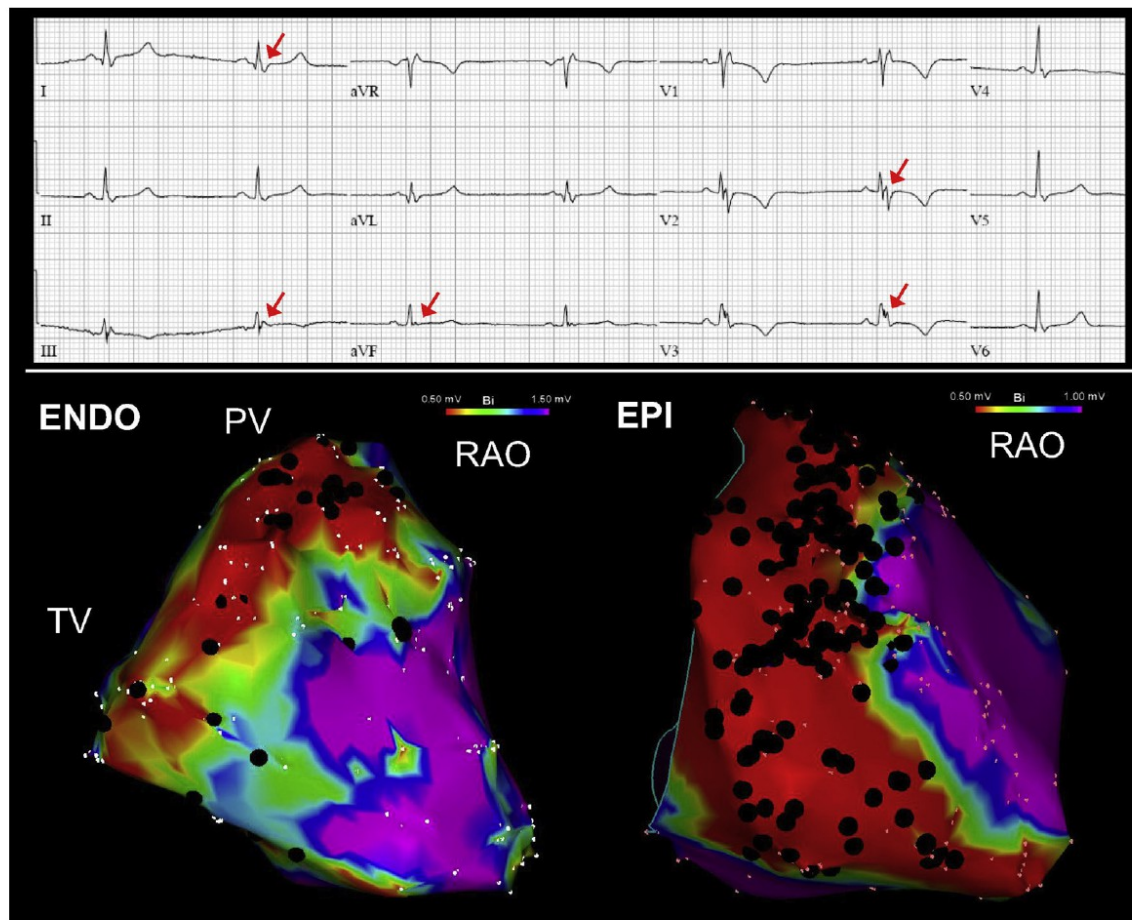
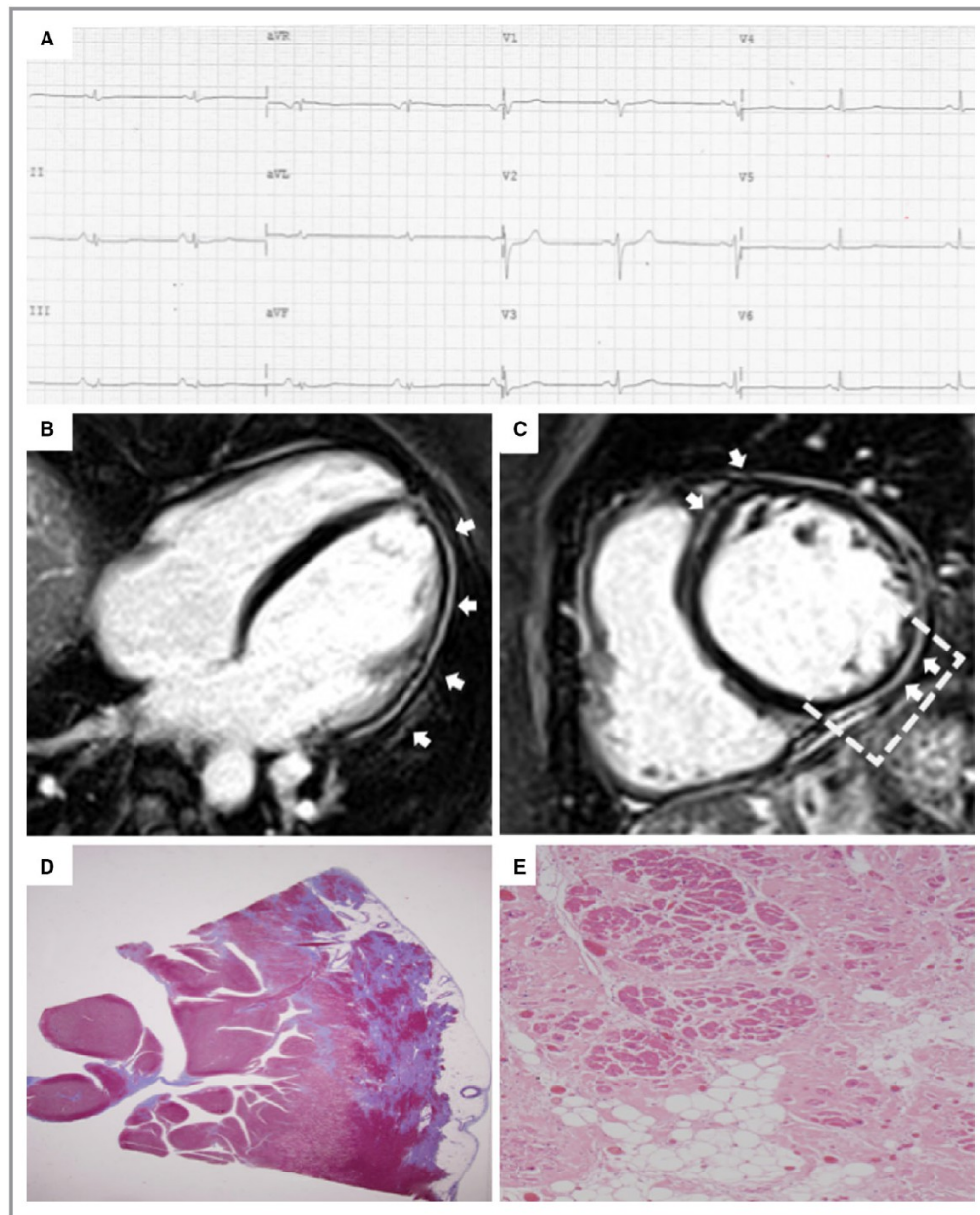


**FIGURE 7** Anterior, Inferior, and Superior ECG Depolarization Abnormalities and RV Electroanatomic Substrate



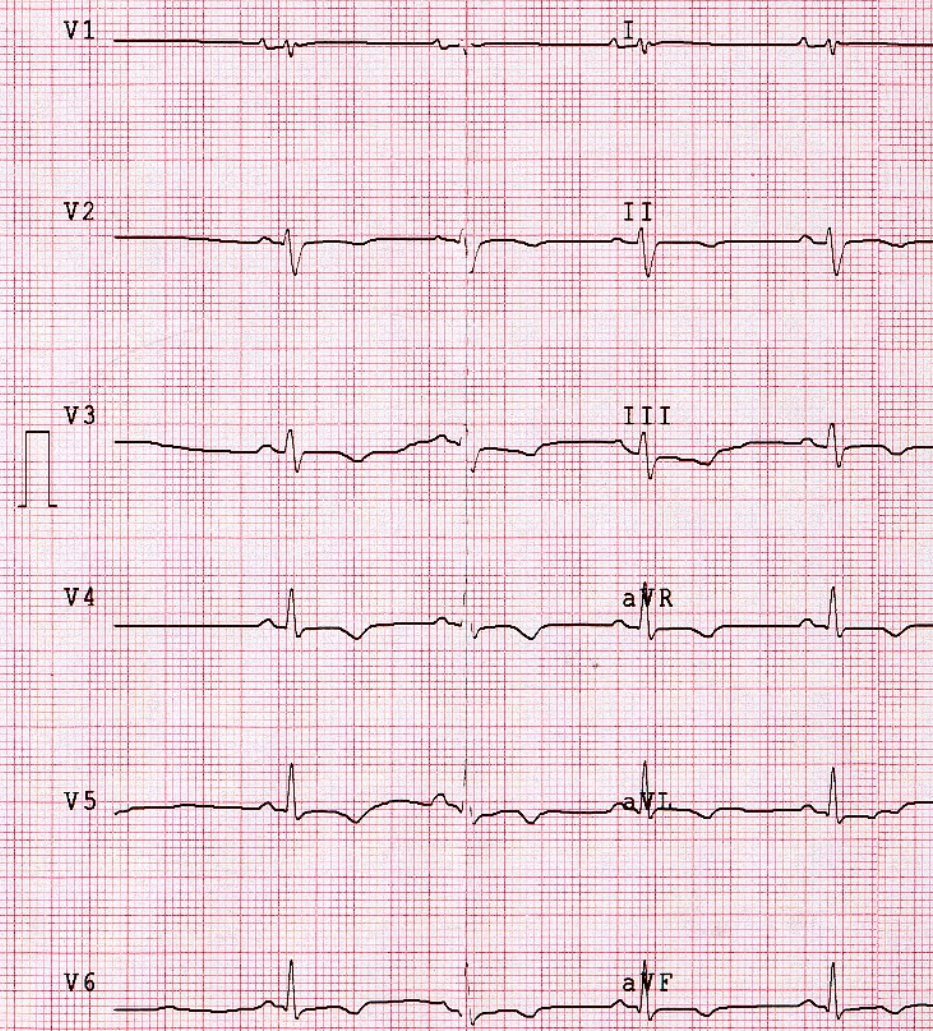
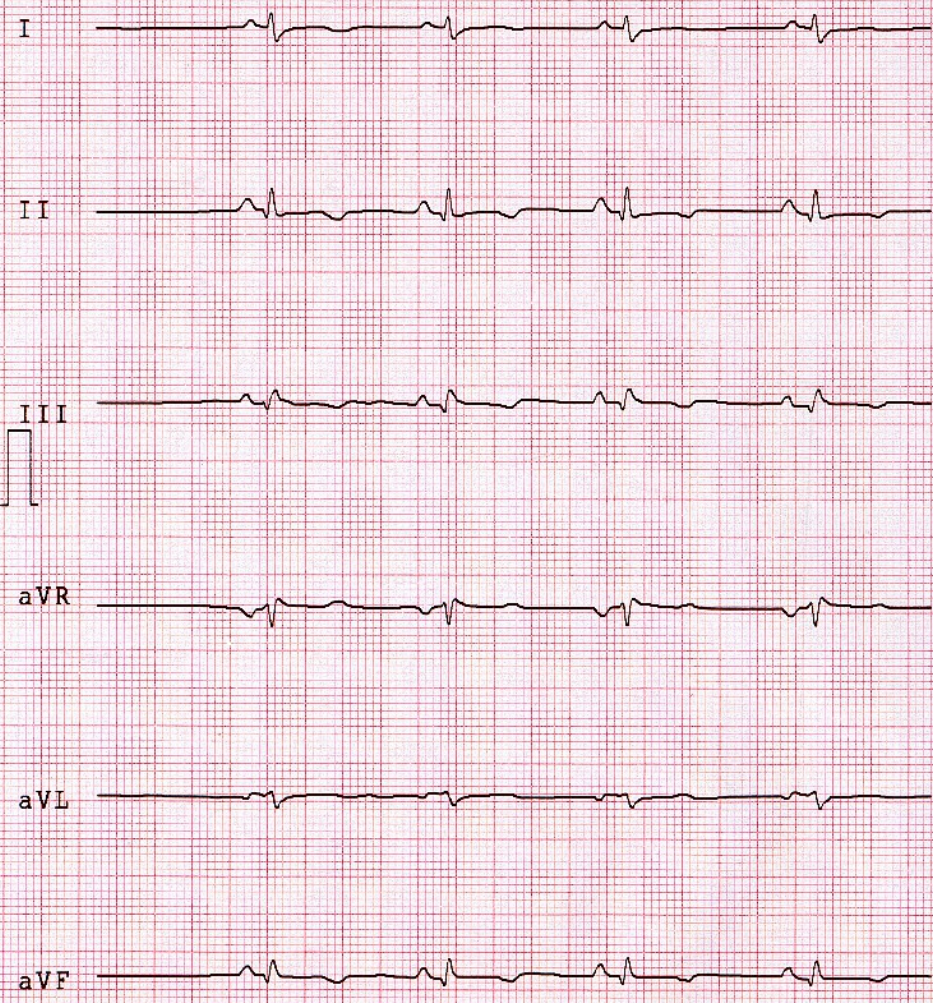
**(Top)** Baseline 12-lead ECG with anterior, inferior, and superior depolarization abnormalities (**red arrows**). **(Bottom)** RV ENDO (0.5 to 1.5 mV) and EPI (0.5 to 1.0 mV) voltage maps in the RAO projection in the same patient. There are extensive ENDO and EPI signal abnormalities including low voltage and late potentials (**black tags**) in the inferior free wall, mid-free wall, and RVOT anatomic locations consistent with ECG regional abnormalities. Abbreviations as in [Figures 1, 2, and 5](#).





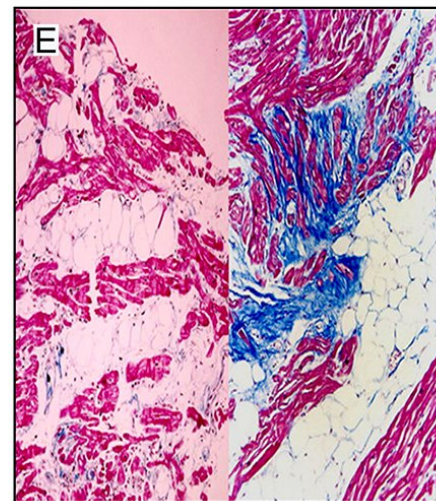
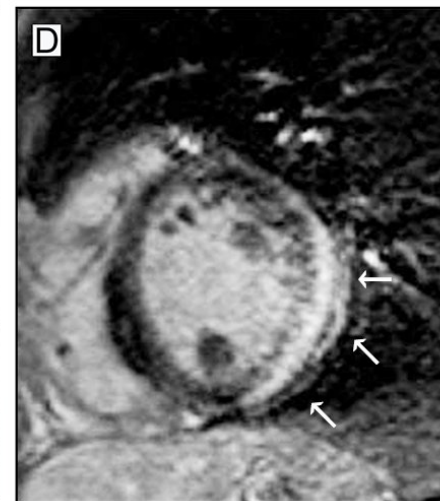
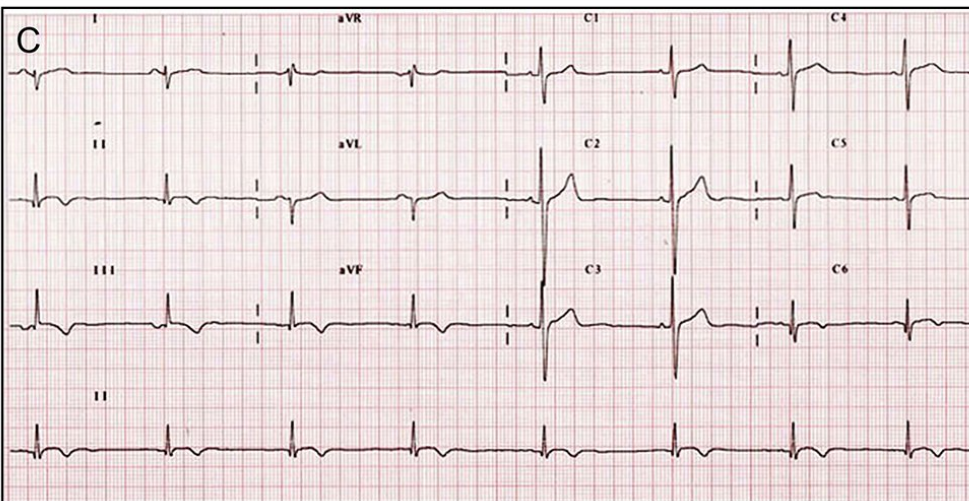
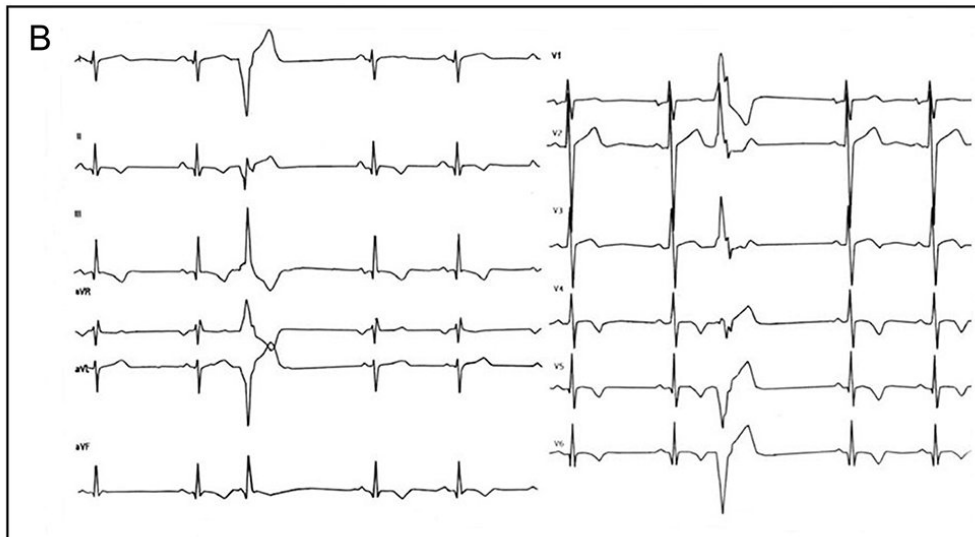
**Figure 5.** Electrocardiographic, CMR imaging, and histological features of a representative patient with ARVC undergoing cardiac transplantation. Basal ECG showing low voltages in limb leads and flattened T-waves in the inferolateral leads (A). Post-contrast CMR images in long-axis (B) and short-axis (C) views



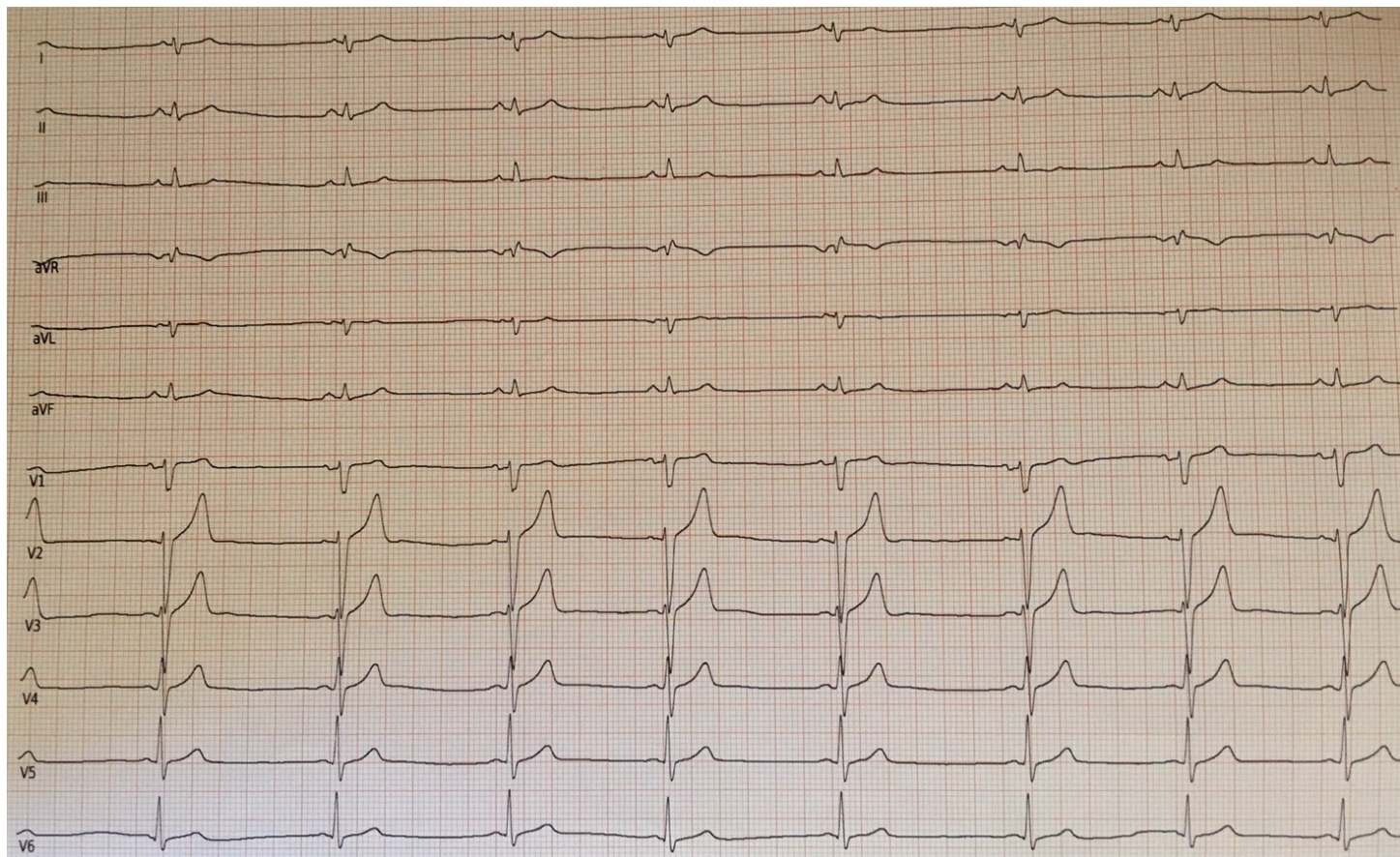








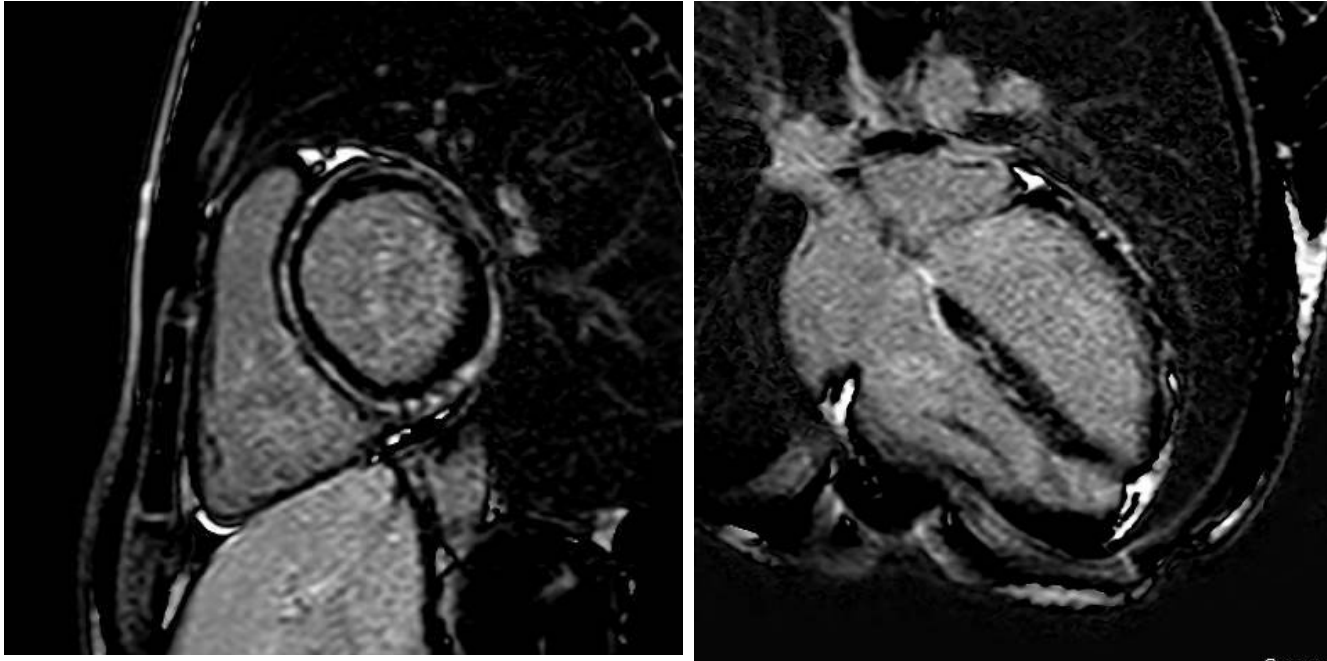




# ECG Holter monitoring

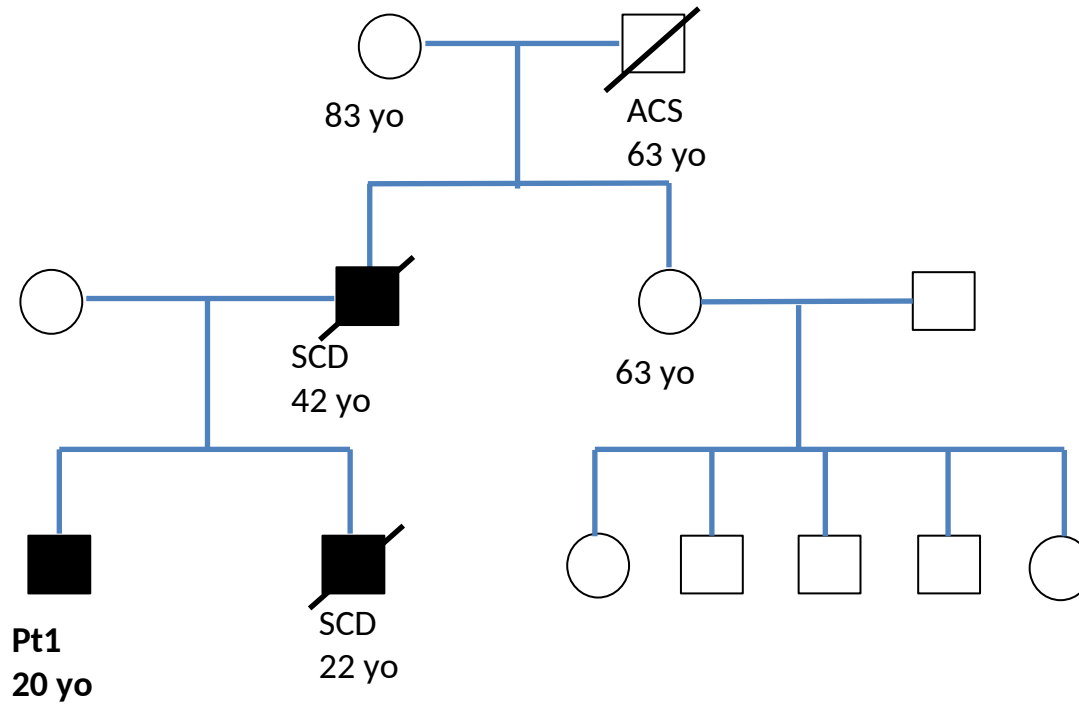


# Cardiac Magnetic Resonance

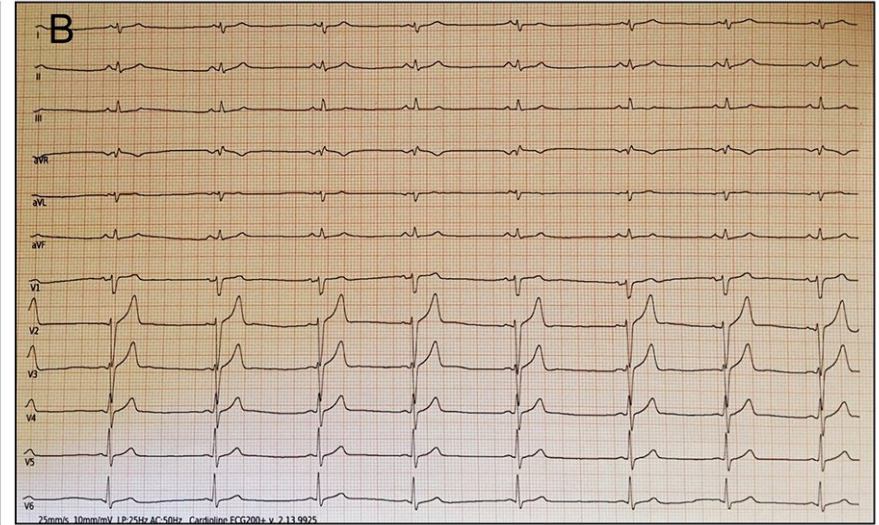
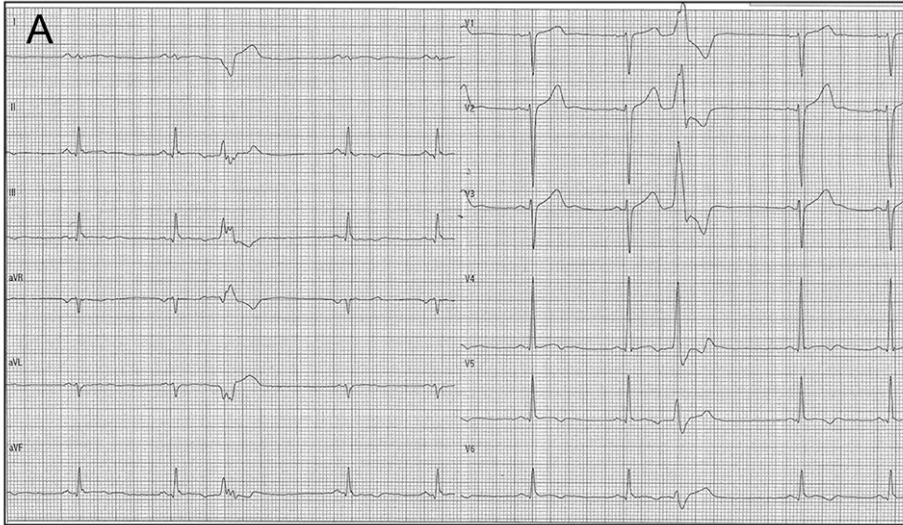




# Family history



# Two brothers in comparison

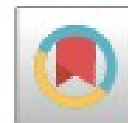


- Pt 9 CMR reveals **subepicardial/intramycardial circumferential LGE**.
- The autopsy of his brother shows the same **LV circumferential scar**, mostly located in the subepicardium, with gross features of fibroadipose myocardial replacement.





# Left Posterior Fascicular Block and Increased Risk of Sudden Cardiac Death in Young People



We retrospectively compared the clinical data for 109 consecutive individuals age  $\leq 40$  years who had ACA or SCD (86 men;  $32.3 \pm 5.9$  years [range: 17 to 40 years]) and who had at least 1 ECG in the 3 years preceding the ACA or SCD to data for 8,892 healthy individuals age  $\leq 40$  years (6,265 men;  $30.5 \pm 8.6$  years [range: 17 to 40 years]) consecutively referred to our institution for screening. LPFB was defined by the presence of all of the following: frontal axis  $100^\circ$  to  $180^\circ$ ; rS pattern in leads I and aVL; qR pattern in III and aVF; QRS duration  $< 110$  ms; and no QS pattern in I and aVL. The association of LPFB with ACA/SCD was analyzed by nominal logistic regression and was estimated with unadjusted odds ratios (ORs) and 95% confidence intervals (CIs). The study (CARITMO) was approved by our Institutional Review Board.

\*Leonardo Calò, MD

Roberta Della Bona, MD, PhD

Annamaria Martino, MD, PhD

Cinzia Crescenzi, MD

Germana Panattoni, MD, PhD

Giulia d'Amati, MD, PhD

Fiorenzo Gaita, MD

Ruggiero Mango, MD, PhD

Luigi Sciarra, MD

Mikael Laredo, MD, MSc

\*Division of Cardiology

Policlinico Casilino Rome

Via Casilina 1049

00169 Rome

Italy

E-mail: [leonardocalo.doc@gmail.com](mailto:leonardocalo.doc@gmail.com)

Twitter: [@cinzi1988](https://twitter.com/cinzi1988), [@LaredoMikael](https://twitter.com/LaredoMikael)

<https://doi.org/10.1016/j.jacc.2020.12.033>

© 2021 by the American College of Cardiology Foundation. Published by Elsevier.

JACC VOL. 77, NO. 8, 2021

MARCH 2, 2021:1141-8

# LPFB as a Sign for Cardiomyopathy and Increased Risk of SCD in Young People

**109** young consecutive patients with **ACA/SCD**

**Pre-ACA/SCD ECG analysis**

**LPFB in 10 (9%) patients**

**CMR in 6 patients**

**Abnormal CMR in 6 (100%)**

- **LV LGE in 6 (100%)**
  - Inferolateral LGE in 3
  - Inferior LGE in 1
  - Inferoseptal in 1
  - Diffuse in 1
- **LV systolic dysfunction in 4 (80%)**

**Autopsy in 3 patients; EMB in 1 patients**

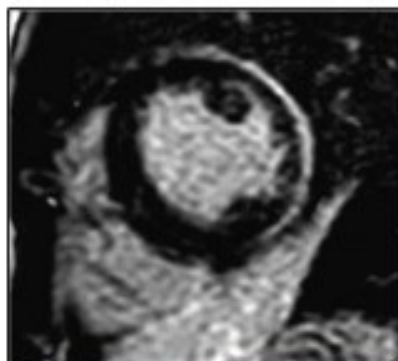
- **Abnormal histopathological findings in 4 (100%)**
  - **LV fibrosis in 4 (100%)**

**Genetic analysis in 5 patients**

- **Pathogenic variants in 2 (40%): DSG2, TTN**
  - **VUS in 1 (20%): TTN**



LPFB Odds Ratio for SCD/ACA  
**112.2** (95% CI 43.3-290.2)



**8892** young **healthy** individuals

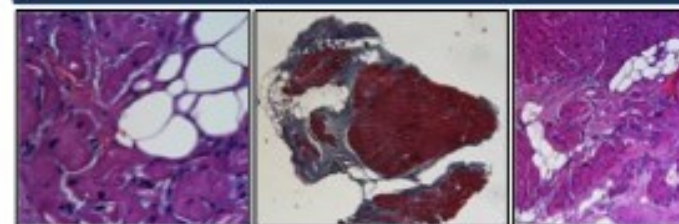
**ECG analysis**

**LPFB in 8 (0.09%) patients**

**CMR in 6 healthy subjects**

**Abnormal CMR in 4 (67%)**

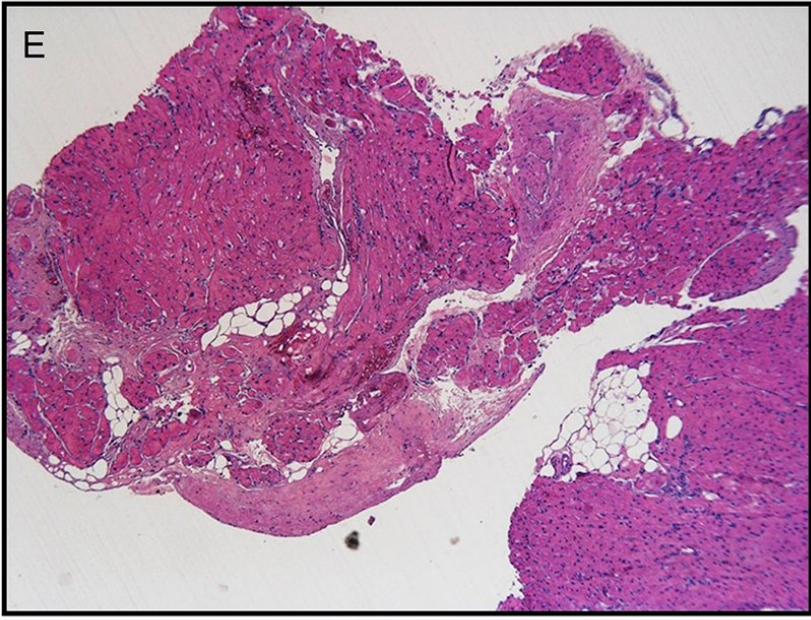
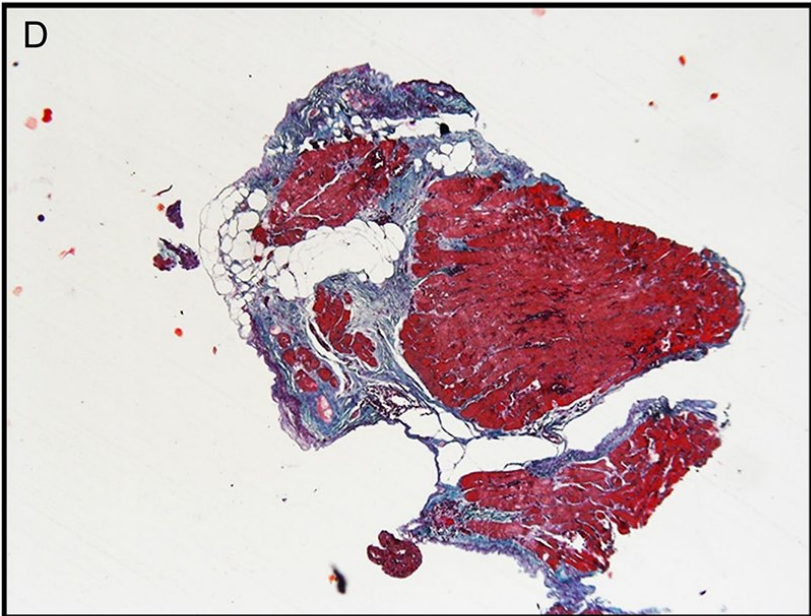
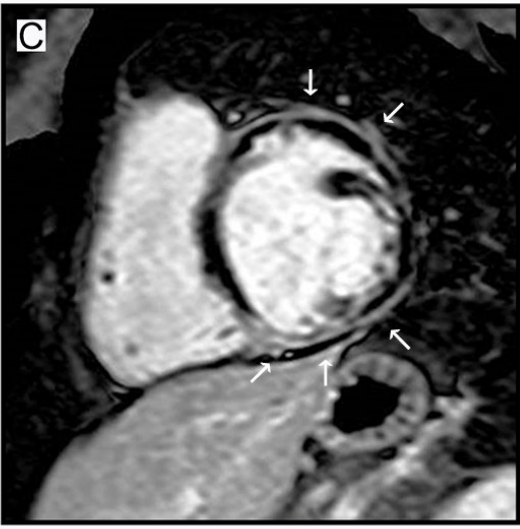
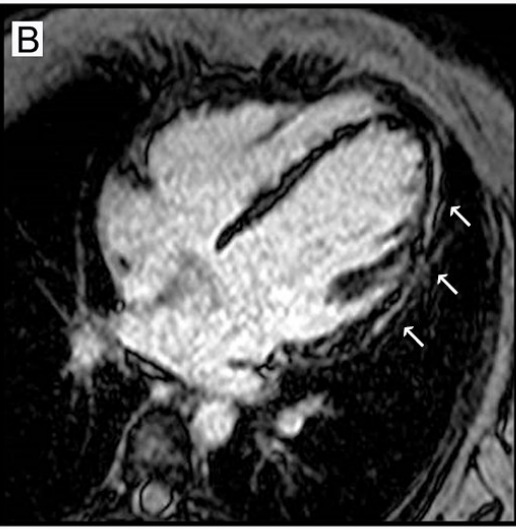
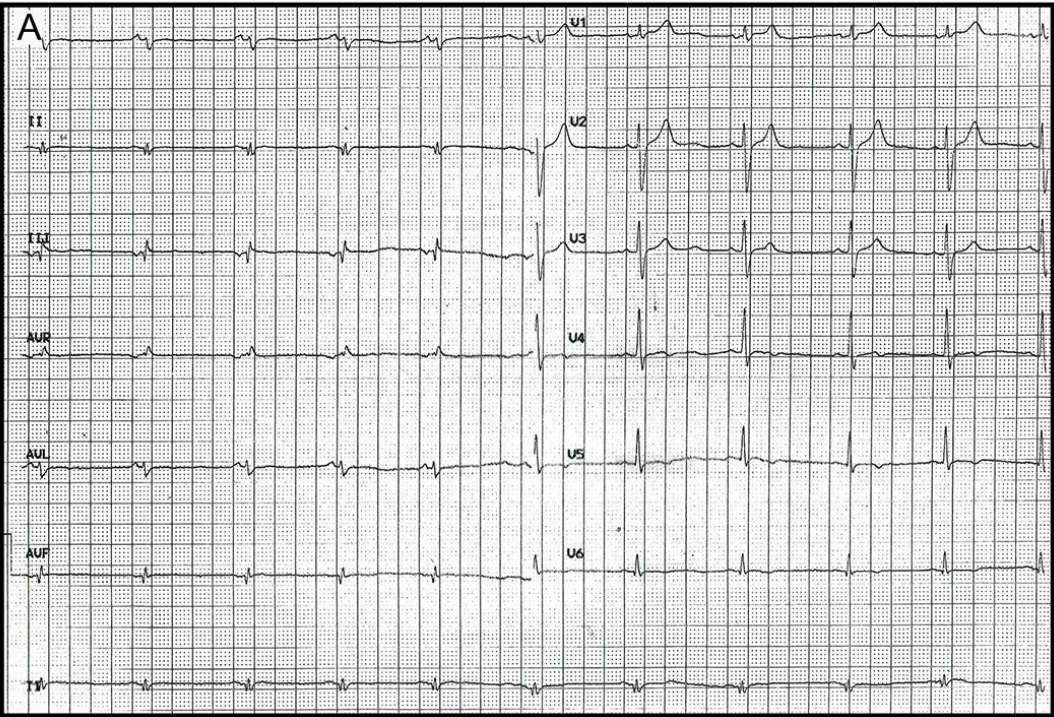
- **LV LGE in 2 (33%)**
- **LV systolic dysfunction in 1 (17%)**
- **LV hypertrophy in 1 (17%)**



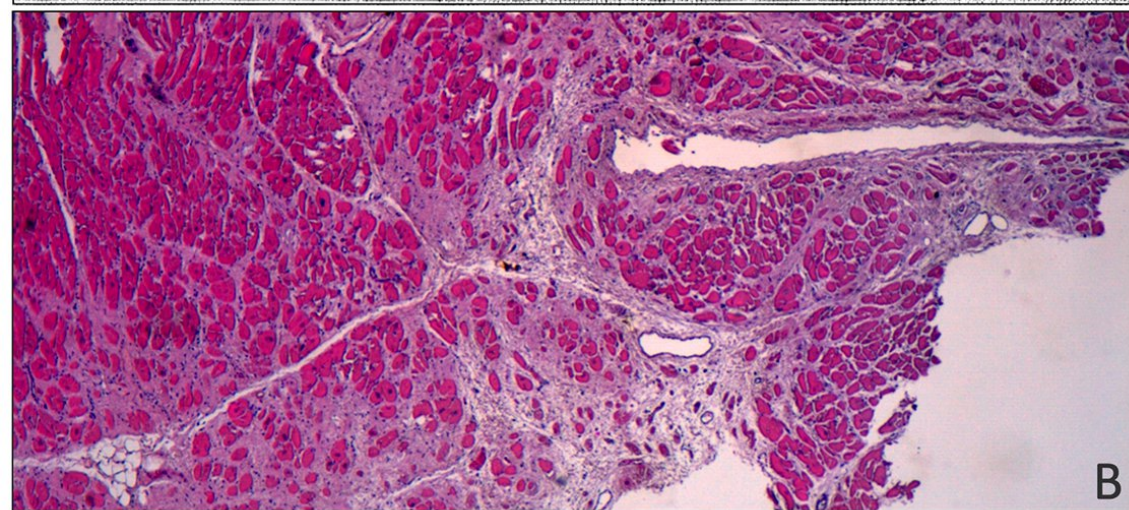
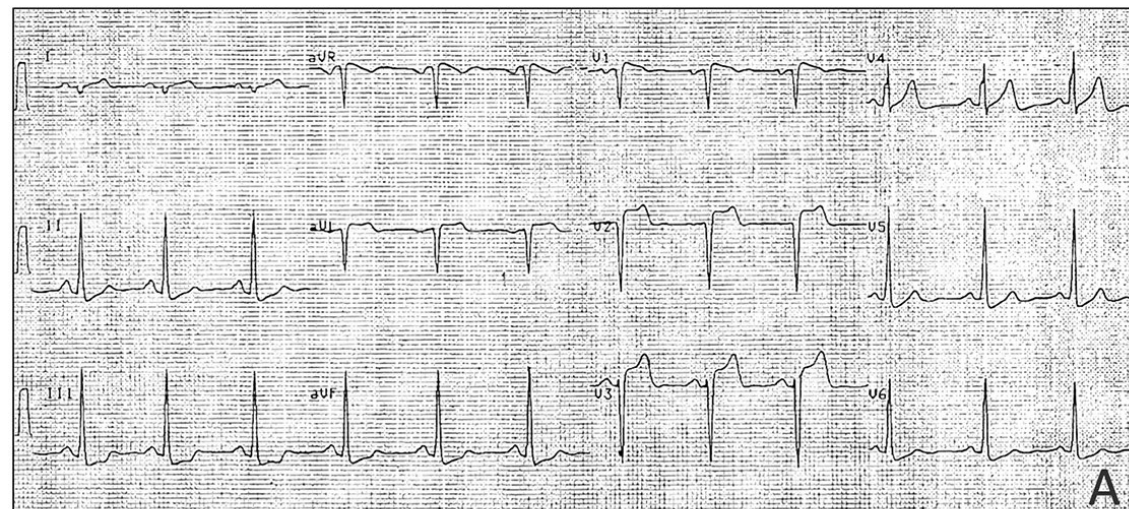
**Genetic analysis in 3 subjects**

- **Pathogenic variant in 1 (33%): DSP**

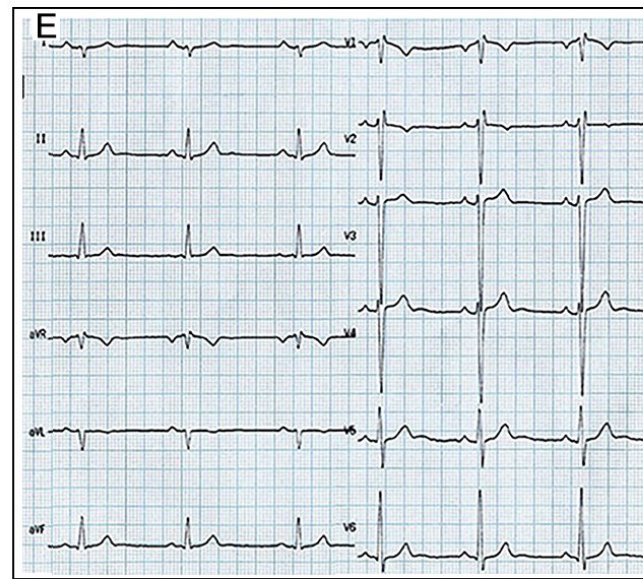
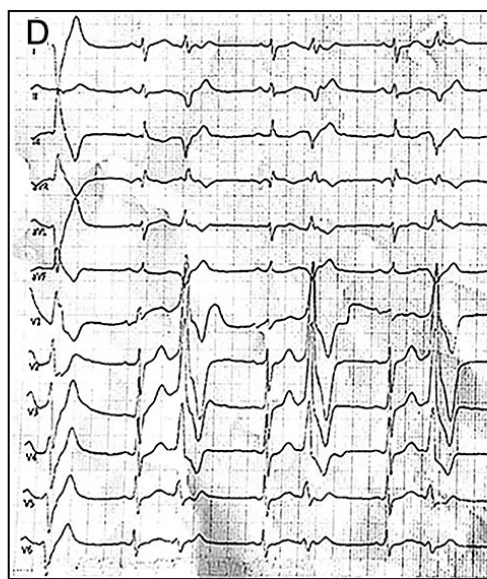
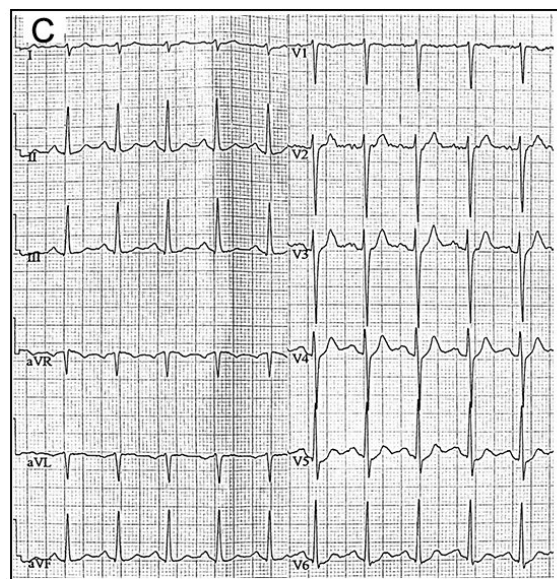
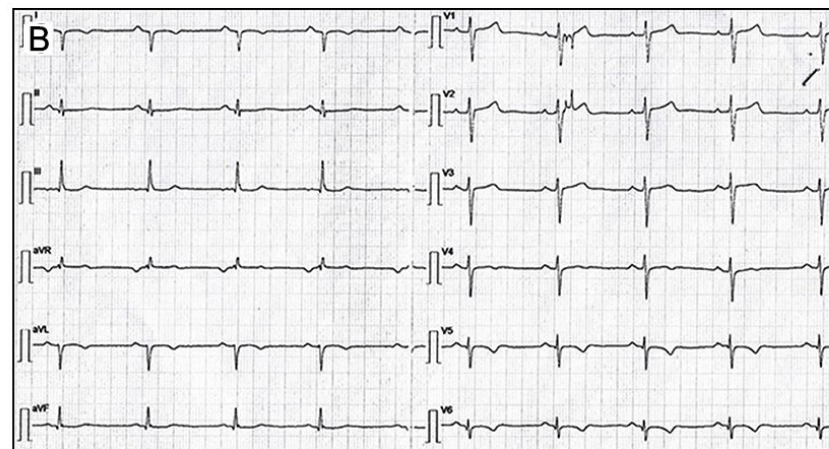
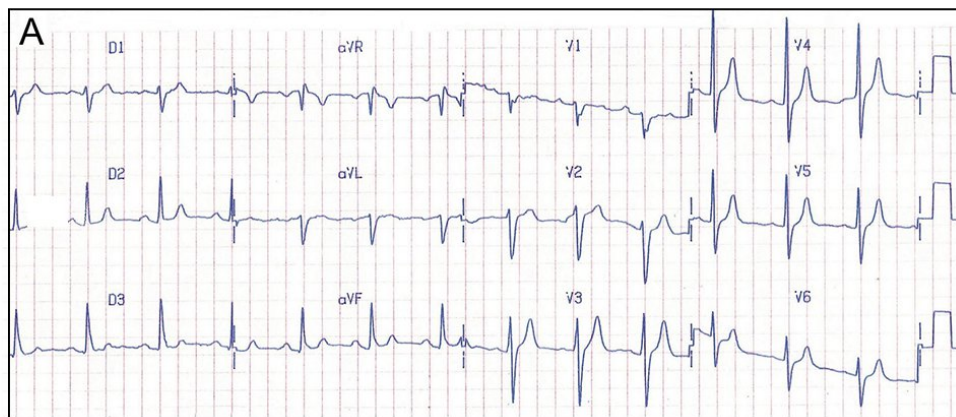




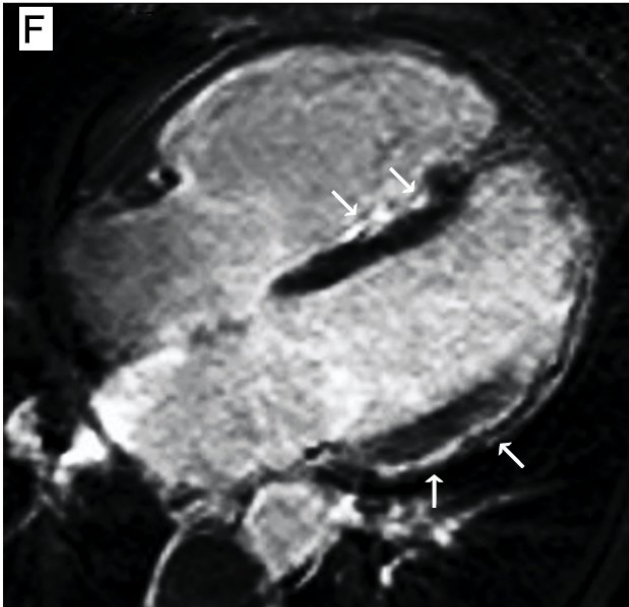
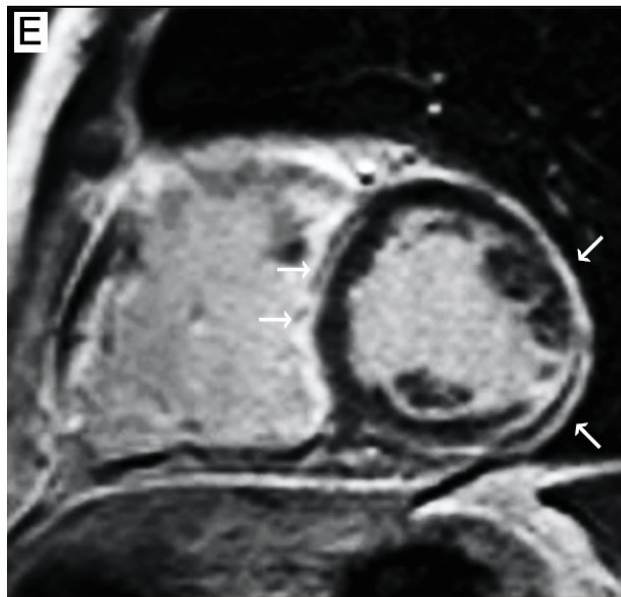
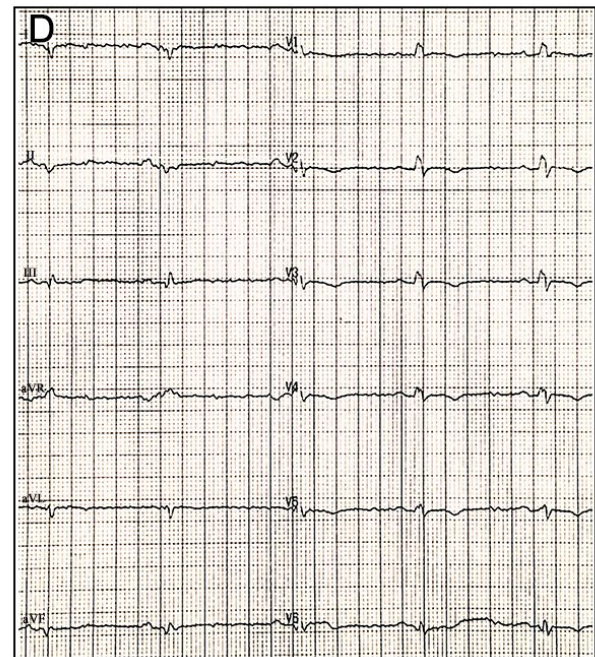
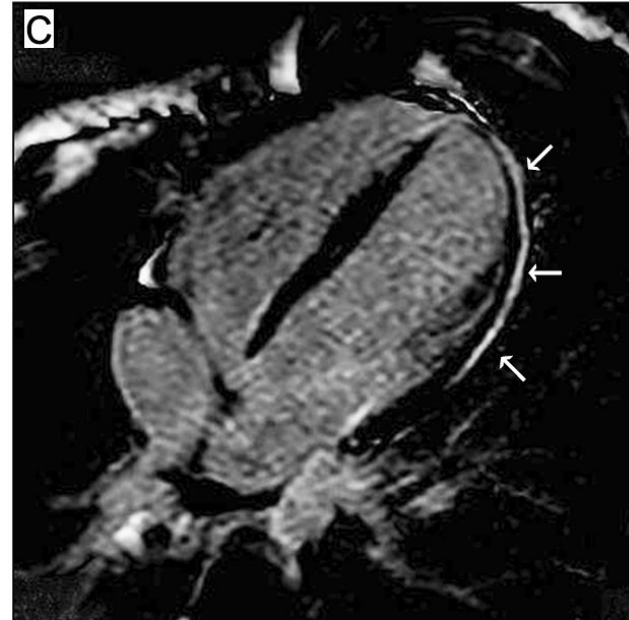
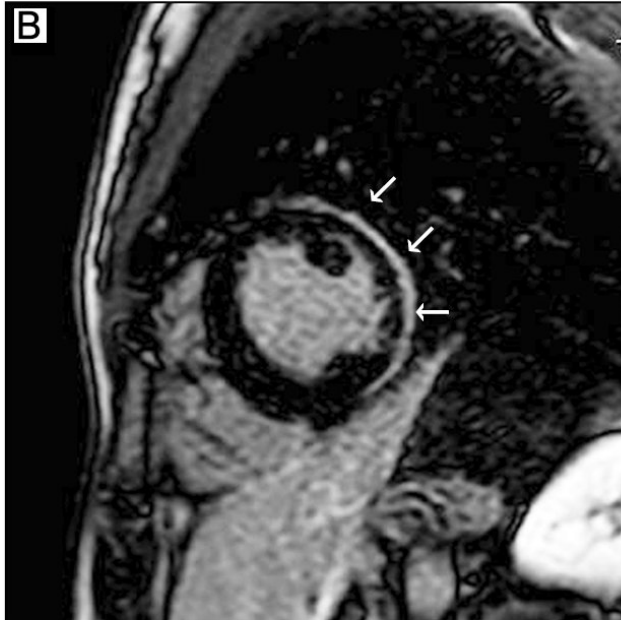
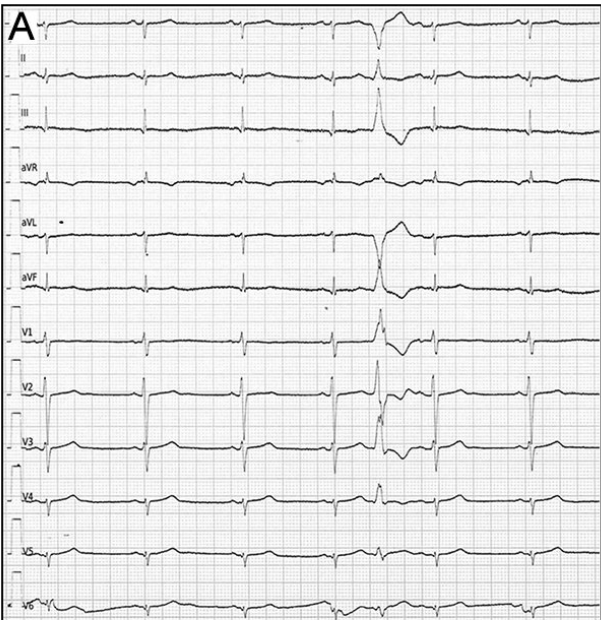






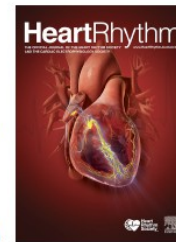












Fascicular heart blocks and risk of adverse cardiovascular outcomes: results from a large primary care population.

Benjamin Chris Nyholm, MD, Jonas Ghouse, MD, PhD, Christina Ji-Young Lee, MD, PhD, Peter Vibe Rasmussen, MD, Adrian Pietersen, MD, Steen Møller Hansen, MD, PhD, Christian Torp-Pedersen, MD, DMSci, Lars Køber, MD, DMSci, Stig Haunsø, MD, DMSci, Morten Salling Olesen, MSc, PhD, Jesper Hastrup Svendsen, MD, DMSci, Claus Graff, MSc, PhD, Anders Gaarsdal Holst, MD, PhD, Jonas Bille Nielsen, MD, PhD, Morten Wagner Skov, MD, PhD

PII: S1547-5271(21)02216-5

DOI: <https://doi.org/10.1016/j.hrthm.2021.09.041>

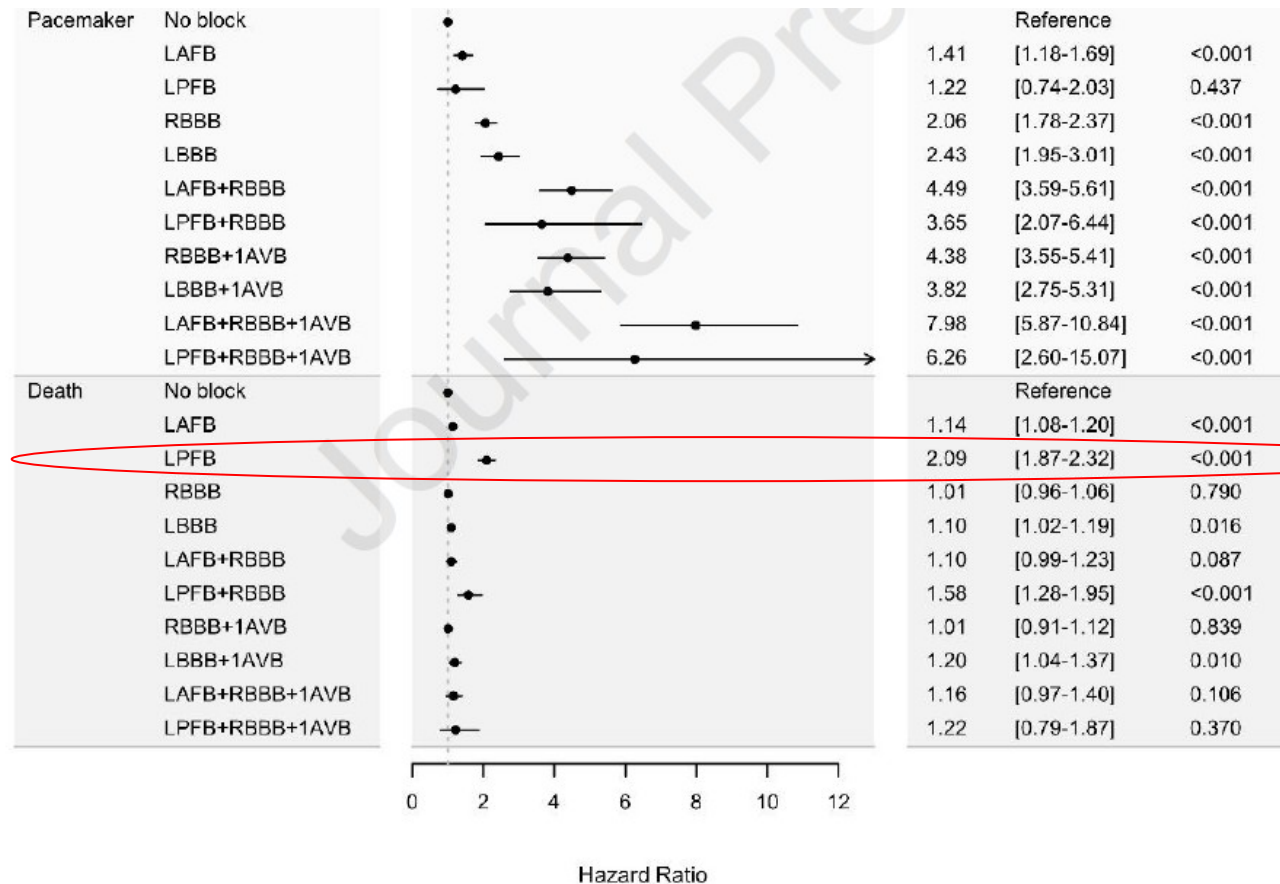


Table 1. Baseline characteristics

Fascicular block subtype n (%)	No conduction defects		LAFB		LPFB		RBBB		LBBB		RBBB + LAFB		RBBB + LPFB		RBBB + 1AVB		LBBB + 1AVB		RBBB + LAFB + 1AVB		RBBB + LPFB + 1AVB	
	345,315	(96.2)	3,526	(0.98)	2,889	(0.80)	3,910	(1.09)	1,390	(0.39)	570	(0.16)	196	(0.05)	643	(0.18)	304	(0.08)	176	(0.05)	32	(0.01)
Age, years, median (IQR)	54	(41-66)	71	(60-80)	35	(26-51)	69	(58-79)	75	(64-82)	76	(68-83)	66	(53 -78)	77	(70-84)	80	(72-86)	79	(70-86)	78	(71-84)
Women, n (%)	190,796	55	1,463	41	1,441	50	1,349	35	949	68	169	30	79	40	158	25	136	45	32	18	6	19
Medical history, n (%)																						
Hypertension	66,316	(19)	1,139	(32)	198	(7)	1,349	(35)	625	(45)	241	(42)	48	(25)	333	(52)	174	(57)	101	(57)	15	(47)
Syncope	9,355	(2.7)	135	(3.8)	83	(2.9)	148	(3.8)	60	(4.3)	26	(4.6)	6	(3.1)	37	(5.8)	13	(4.3)	16	(9.1)	<4	(<12.5)*
Atrial fibrillation	5,041	(1.5)	134	(3.8)	38	(1.3)	121	(3.1)	66	(4.8)	20	(3.5)	9	(4.6)	35	(5.4)	27	(8.9)	12	(6.8)	5	(15.6)
Valvular heart disease	1,442	(0.4)	46	(1.3)	10	(0.4)	50	(1.3)	25	(1.8)	12	(2.1)	<4	(<2)*	15	(2.3)	12	(4.0)	<4	(<3)	<4	(<12.5)*
Beta blocker therapy	52,809	(15.3)	736	(20.9)	242	(8.4)	845	(21.6)	408	(29.4)	132	(23.2)	31	(15.8)	193	(30.2)	111	(36.5)	58	(33.0)	11	(34.4)
Charlson Comorbidity Index																						
0 points	265,361	(77)	2,078	(59)	2,413	(84)	2,429	(62)	802	(58)	296	(52)	124	(63)	319	(50)	144	(47)	71	(40)	14	(44)
1 point	41,598	(12)	648	(18)	271	(9)	632	(16)	237	(17)	109	(19)	31	(16)	121	(19)	66	(22)	34	(19)	8	(25)
≥ 2 points	38,356	(11)	800	(23)	205	(7)	849	(22)	351	(25)	165	(29)	41	(21)	203	(31)	94	(31)	71	(40)	10	(31)
ECG variables																						
QRS duration, median (IQR)	92	(84-100)	102	(96-110)	96	(88-104)	136	(128-146)	146	(136-156)	144	(136-154)	140	(130-148)	144	(134-152)	154	(144-164)	151	(142-160)	150	(134-159)
PR interval, median (IQR)	156	(144-172)	168	(152-186)	154	(140-170)	162	(148-178)	168	(154 -180)	170	(156-184)	162	(146-178)	220	(208-242)	218	(208-238)	228	(211-251)	221	(207-242)
Heart rate (IQR)	69	(62-79)	72	(63-82)	71	(62-82)	70	(62-80)	73	(65-83)	71	(64-80)	74	(66-84)	68	(60-78)	70	(62-80)	69	(60-77)	76	(68-86)

TABLE 1: LAFB = left anterior fascicular block; LPFB = left posterior fascicular block; LBBB = left bundle branch block; RBBB = right bundle branch block; 1AVB = first degree atrioventricular block;

\*Due to the Act on Processing of Personal Data, we are not allowed to report any number less than four observations.



## From Argentina to Denmark—The wine is still good

Reginald T. Ho, MD, FHRS

*From the Division of Cardiology, Department of Medicine, Thomas Jefferson University Hospital, Philadelphia, Pennsylvania.*

In 1968, Dr Mauricio Rosenbaum published a book dedicated entirely to the intraventricular conduction system.<sup>1</sup> In this classic monograph and its subsequent English version, he coined the term “hemiblock” and introduced the concept of a trifascicular conduction system after analyzing electrocardiograms from a 58-year-old man who had suffered an anterior myocardial infarction and demonstrated right bundle branch block (RBBB) with alternating left anterior fascicular block (LAFB) and left posterior fascicular block (LPFB) (now called Rosenbaum’s syndrome).<sup>2</sup> He referred to the conduction system as a “detector” of the heart, showing the association between various conduction blocks and heart disease (commonly coronary artery disease and Chagas cardiomyopathy in his home country of Argentina). He described the unequal “anatomic vulnerability” of the bundle branches (right more than left; left anterior more than posterior) and the relative “immunity” of the left posterior fascicle because of its thick structure and dual blood supply (indicating that the presence of LPFB generally signified more severe heart disease). His book was followed by a flurry of studies in the mid-1970s and early 1980s evaluating the value of His-ventricular intervals in predicting impending atrioventricular block (AVB) in patients with bifascicular block—research that today remain the foundation for our current pacemaker guidelines.<sup>3</sup> Since then, however, research on the natural history of fascicular block and its progression to AVB has been relatively quiet.

In this issue of *Heart Rhythm Journal*, Nyholm et al<sup>4</sup> breathe new life into the study of fascicular blocks by providing the largest population-based study on its natural progression to AVB. Among 358,958 primary care patients in a large Danish registry (Copenhagen ECG Study), the authors studied 13,636 patients with fascicular block (3.8%) and compared them with a reference group of patients without block. Not surprisingly, RBBB and isolated LAFB were most common. With the longest follow-up approaching 16 years, they found that syncope, pacemaker implantation, and third AVB increased with increasing complexity of

fascicular block. Depending on gender and age, the 10-year absolute risk of developing third-degree AVB increased from 0% to 2% (hazard ratio [HR] 1.60) for isolated LAFB to 23% (HR 10.98) for multicomination block (first-degree AVB + RBBB + LAFB). While this dose-response relationship between worsening fascicular block and AVB is not unexpected, their data provide clearer granularity about the long-term risk of developing AVB among 10 different block subtypes. True bilateral BBB (eg, alternating BBB and Rosenbaum’s syndrome) was not represented. However, this subtype is already an established high-risk group carrying a class I indication for pacemaker implantation. While a higher burden of comorbidity occurred with increasing block complexity, LAFB was not associated with worse mortality. This has been observed in another study from the same group but not by others.<sup>5–7</sup> Curiously, isolated LPFB was associated with the youngest age group (median age 35 years) and the highest risk of death (HR 2.09). A recent case-control study of 10 young patients (median age 27.5 years) with LPFB and aborted cardiac arrest/sudden cardiac death found left ventricular fibrosis (particularly along the inferolateral wall) in all patients undergoing cardiac magnetic resonance imaging (n = 6) or histopathological analysis/autopsy (n = 4).<sup>8</sup> Further investigation is required into this small but worrisome group of young patients.

In the preface to his book, Dr Rosenbaum wrote “Like good wines, some research improves after resting for a while.” By allowing many years for their registry to mature, Nyholm et al have produced an excellent bottle of wine for a slowly aging cellar.

### References

1. Rosenbaum MB, Elizari MV, Lazzari JO. *Los Hemibloques*. Buenos Aires, Argentina: Editorial Paidós; 1968.
2. Rosenbaum MB, Elizari MV, Lazzari JO. The Hemiblocks: New Concepts of Intraventricular Conduction Based on Human Anatomical, Physiological and Clinical Studies. Oklawaha, FL: Tampa Tracing; 1970.
3. Kusumoto FM, Schoenfeld MH, Barrett C, et al. 2018 ACC/AHA/HRS guideline on the evaluation and management of patients with bradycardia and cardiac conduction delay: executive summary. *J Am Coll Cardiol* 2019;74:932–987.
4. Nyholm BC, Ghouse J, Lee CJ, et al. Fascicular heart blocks and risk of adverse cardiovascular outcomes: results from a large primary care population. *Heart Rhythm* 2021;XX:XX–XX.
5. Nielsen JB, Strandberg SE, Pietsen A, et al. Left anterior fascicular block and the risk of cardiovascular outcomes. *JAMA Int Med* 2014;174:1001–1003.
6. Mandyam M, Soliman EZ, Heckbert S, et al. Long-term outcomes of left anterior fascicular block in the absence of overt cardiovascular disease. *JAMA* 2013; 309:1587–1588.

but not by others.<sup>5–7</sup> Curiously, isolated LPFB was associated with the youngest age group (median age 35 years) and the highest risk of death (HR 2.09). A recent case-control study of 10 young patients (median age 27.5 years) with LPFB and aborted cardiac arrest/sudden cardiac death found left ventricular fibrosis (particularly along the inferolateral wall) in all patients undergoing cardiac magnetic resonance imaging (n = 6) or histopathological analysis/autopsy (n = 4).<sup>8</sup> Further investigation is required into this small but worrisome group of young patients.

# **OUR EXPERIENCE**

**54 subjects with typical LV subepicardial LGE distribution**

**5 with fibro-fatty infiltration at histological analysis (biopsy)  
and 1 autopsy with negative or presence of VUS**

**48 with positive genetic testing for pathogenic/likely  
pathogenic variants associated with ARVC with LV involvement  
affected by left dominant AC**

- 35 (72.9%) gene DSP; 7 (14.6 %) gene DSG; 3 gene PKP, 3  
JUP**



	<b>ALVC (n=54)</b>
Age at diagnosis, years	39±15
Male, n (%)	32 (59.3)
Probands, n (%)	40 (74.1)
Family history of ACM/DCM, n (%)	23 (42.6)
Family history of SCD, n (%)	18 (33.3)
NYHA class I-II, n (%)	52 (96.3)
NYHA class III, n (%)	2 (3.7)
Atrial fibrillation, n (%)	4 (7.4)
Unexplained syncope, n (%)	8 (14.8)
NSVT, n (%)	26 (48.1)
<b><i>Cardiac magnetic resonance</i></b>	
LVEDVi (ml/m2)	97.6±24.5
LVEF, %	49.5±10.0
LV WMA, %	35 (64.8)
RVEDVi (ml/m2)	85.8±18.8
RVEF, %	54.3±9.3
RV WMA, %	13 (24.1)
Intramyocardial fat signal, n (%)	22 (40.7)
Segments with LGE	6±3; 6 (4-8)
<b><i>LGE pattern</i></b>	
- Ringlike, n (%)	28 (51.9)
<b><i>LGE distribution</i></b>	
- Subepicardial, n (%)	35 (64.8)
- Midmural, n (%)	10 (18.5)
- Transmural, n (%)	9 (16.7)
<b><i>Genetic testing</i></b>	
Pathogenic/likely pathogenic variant, n (%)	48/54 (88.9)
DSP, n (%)	35/48 (72.9)
Non-DSP, n (%) *	13/48 (27.1)

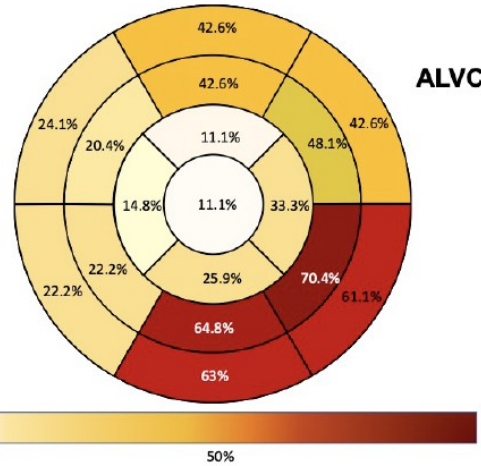
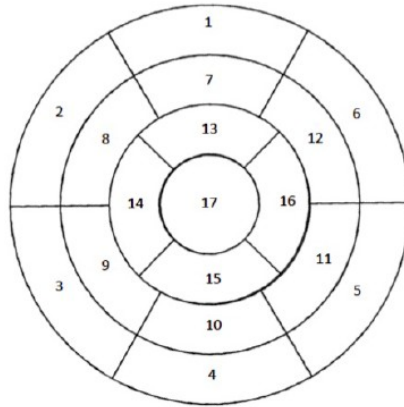
	Pedigree	Gene	ACMG Variant Criteria	Deoxyribonucleic acid change	Amino acid change
1	Proband	PKP2	LP	c.1216delG	p.Val406fs
2	Proband	DSP	P	c.1707-1708insAC	p.Met571Glnfs*8
3	Proband	DSP	LP	c.7180delA	p.Arg2394fs*ter
4	Proband	DSG2	LP	c.1912G>A	p.Gly638Arg
5	Proband	DSG2	LP	c.445G>T	p.Val149Phe
6	Proband	DSC2	LP	c.977A>C	p.Gln326Pro
7	Proband	DSP	LP	c.3932_3936del	p.Gln1311Profs*13
8	Family member	DSP	P	c.5851 C>T	p.Arg1951Ter
9	Family member	DSP	P	c.5851 C>T	p.Arg1951Ter
10	Proband	DSG2	LP	c.1003A>G	p.Thr335Ala
11	Family member	DSP	LP	c.2848delA	p.Ile950Leu
12	Proband	DSP	P	c.2497 C>T	p.Gln833ter
13	Family member	DSP	LP	c.1351C>T	p.Arg451Cys
14	Proband	DSP	LP	c.2584C>T	p.Gln862Ter
15	Family member	DSP	LP	c.1351C>T	p.Arg451Cys
16	Family member	PKP2	P	c.2447_2448del	p.Thr816Argfs*10
17	Proband	DSP	LP	c.1352G>C	p.Arg451Pro
18	Proband	DSP	P	c.3203_3204delAG	p.Glu1068ValfsTer19
19	Proband	DSP	P	c.5210delG	p.Gly1737AspfsTer16
20	Proband	DSP	P	c.5210delG	p.Gly1737AspfsTer16
21	Family member	DSP	P	c.3465G>A	p.Trp1155Ter
22	Proband	JUP	P	c.2069A>G	p.Arg690Ser

23	Proband	JUP	P	c.2069A>G	p.Arg690Ser
24	Proband	DSP	LP	c.6478C>T	p.R2160X
25	Proband	DSP	LP	c.G3793T	p.Glu1265X
26	Proband	DSP	LP	c.356dupA	p.I120Nfs*16
27	Proband	DSP	LP	c.1891C>T	p.(Gln631*)
28	Family member	DSP	LP	c.3793G>T	p.E1265X
29	Proband	DSP	LP	c.7248dupT	p.D2417X
30	Family member	DSP	LP	c.3337C>T	p.R1113X
31	Proband	DSP	LP	c.3465G>A	p.Trp1155*
32	Proband	DSP	P		6p25.1-p24.3
33	Proband	DSC2	LP	c.2078G>T	p.Gly693Val
34	Proband	DSP	LP	c.537_554del	p.Arg2334*
35	Proband	DSG2	P	c.1912G>A	p.Gly638Arg
36	Family member	DSG2	P	c.1912G>A	p.Gly638Arg
37	Proband	DSP	LP	c.448C>T	p.Arg150*
38	Proband	DSP	P	c.6852C>T	p.Arg2284*
39	Proband	DSP	LP	c.860A>G	p.Asn287Ser
40	Proband	DSP	VUS	c.212T>G	p.Ile71Ser
41	Proband	DSC2	VUS	c.907G>A	p.Val303Met
42	Proband	DSP/DSG2	LP	DSP: c.212T>G ; DSG2: c.561T>G	DSP: p.Ile71Ser; DSG2 p.Asp187Glu
43	Proband	JUP	LP	c.1359G>T	p.Glu453Asp
44	Proband	DSP	LP	c.2000delG	p.Trp667fs*0
45	Family member	DSP	LP	c.860A>G	p.Asn287Ser
46	Family member	DSP	LP	c.860A>G	p.Asn287Ser
47	Family member	DSP	P	c.1267-2A>G	
48	Proband	DSP	LP	c.448C>T	p.Arg150
49	Family member	DSG2	P	c.271G>T	p.Gly91Ter
50	Proband	DSP	P	c.4198C>T	p.Arg1400*

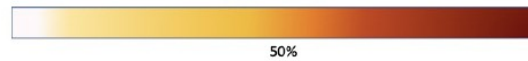
# Distribution of late gadolinium enhancement

AHA 17-segment model

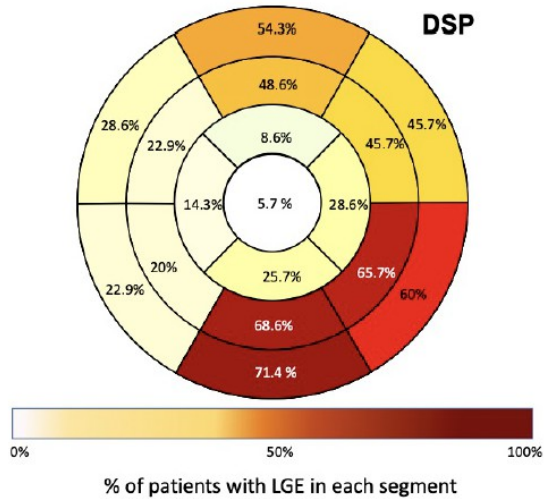
1. Basal anterior
2. Basal anteroseptal
3. Basal inferoseptal
4. Basal inferior
5. Basal inferolateral
6. Basal anterolateral
7. Mid anterior
8. Mid anteroseptal
9. Mid inferoseptal
10. Mid inferior
11. Mid inferolateral
12. Mid anterolateral
13. Apical anterior
14. Apical septal
15. Apical inferior
16. Apical lateral
17. Apex



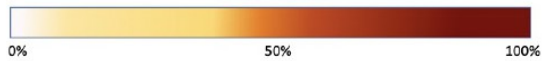
ALVC



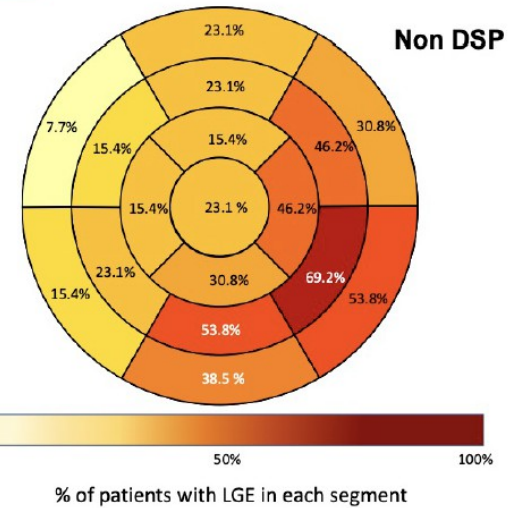
% of patients with LGE in each segment



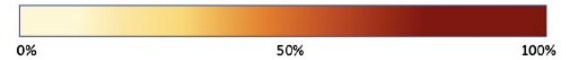
DSP



% of patients with LGE in each segment



Non DSP



% of patients with LGE in each segment



## VOLTAGES IN LIMB LEADS

	Controls (n=84)	ALVC (n=54)	P Value
Lead I QRS	7 (5-8.5)	4.5 (3-6)	<0.0001
Lead I r wave	6 (4-7)	3 (1.9-4.1)	<0.0001
Lead I s wave	0.1 (0-1.5)	1 (0-2)	0.07
Lead II QRS	10.4 (8-12.5)	6.5 (4.2-9.1)	<0.0001
Lead II r wave	9.5 (6.6-12)	4 (2-6.5)	<0.0001
Lead II s wave	1 (0-2)	1 (0-2)	0.11
Lead aVF QRS	8 (5.1-10.5)	5 (4-7.6)	0.0004
Lead aVF r wave	7 (3.3-9)	3.5 (2-6.1)	<0.0001
Lead aVF s wave	1 (0-2)	1 (0-2)	0.70
Lead III QRS	7 (5-8.5)	6 (3.5-8)	0.028
Lead III r wave	5 (2-7.4)	3 (1-5.5)	0.0055
Lead III s wave	1 (0-2.4)	0.5 (0-2.3)	0.83
Lead aVR QRS	8 (7-9.5)	5 (4-6.1)	<0.0001
Lead aVR r wave	1 (0.3-1.5)	1 (0.5-1.3)	0.35
Lead aVR s wave	0 (0-7)	0 (0-1.3)	0.0001
Lead aVL QRS	4.1 (3-6.2)	4 (2.5-5)	0.28
Lead aVL r wave	2 (1-4)	2 (0.5-3.5)	0.38
Lead aVL s wave	1 (0-2.5)	0.8 (0-2.6)	0.39

## VOLTAGES IN PRECORDIAL LEADS

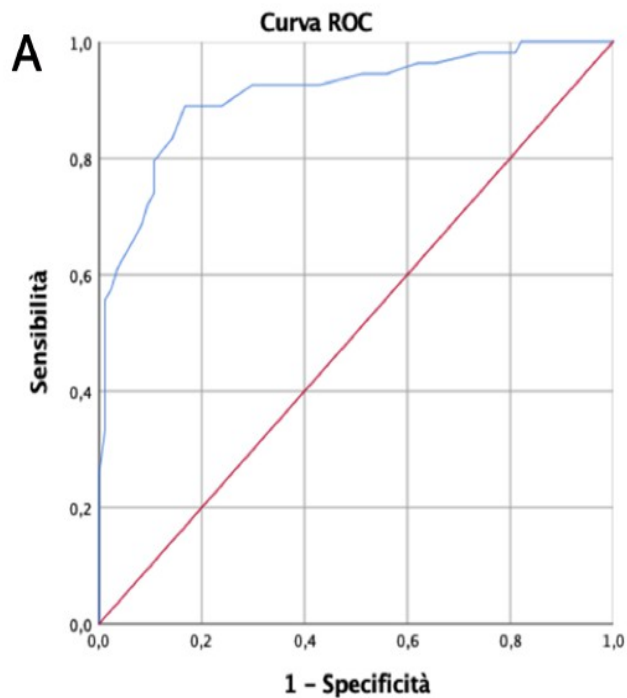
	Controls (n=84)	ALVC (n=54)	P Value
Lead V1 QRS	9.3 (7-12.9)	6.8 (4.5-9)	<b>0.0007</b>
Lead V1 r wave	1.5 (1-2)	1 (1-2.6)	0.40
Lead V1 s wave	8 (6-10)	5 (3-7.1)	<b>&lt;0.0001</b>
Lead V2 QRS	13 (9-17.5)	11 (7.5-16.6)	0.24
Lead V2 r wave	2.8 (1.8-4.4)	3 (1.9-5)	0.68
Lead V2 s wave	9 (6.1-14)	8.3 (5-11.8)	0.07
Lead V3 QRS	15.3 (12-19)	11.8 (7.4-16)	<b>0.0003</b>
Lead V3 r wave	6 (4-10)	4 (2.4-6.3)	<b>0.003</b>
Lead V3 s wave	7.3 (4-11.4)	7 (4-9)	0.17
Lead V4 QRS	16 (10.6-19.8)	11.3 (9-16.6)	<b>0.0026</b>
Lead V4 r wave	11 (8-16)	8 (5.9-11.1)	<b>0.0002</b>
Lead V4 s wave	4 (1.5-5.9)	4 (2-6.3)	0.39
Lead V5 QRS	14.5 (10.6-18)	11 (8-14.3)	<b>0.0011</b>
Lead V5 r wave	12.5 (8.6-16)	8.5 (6.5-11)	<b>&lt;0.0001</b>
Lead V5 s wave	2 (0.1-3)	2 (0.9-4)	0.18
Lead V6 QRS	11.1 (9-15.5)	8.9 (6.9-11.1)	<b>0.0001</b>
Lead V6 r wave	10 (7.5-14)	7 (5-9)	<b>&lt;0.0001</b>
Lead V6 s wave	1 (0-1.9)	1 (0-2)	0.27
RI + RII	15 (13-17.5)	7 (5-10.6)	<b>&lt;0.0001</b>
SV1 + RV6	18.8 (15.5-23)	12 (9-17)	<b>&lt;0.0001</b>

**CONTROLS**

**ALVC**

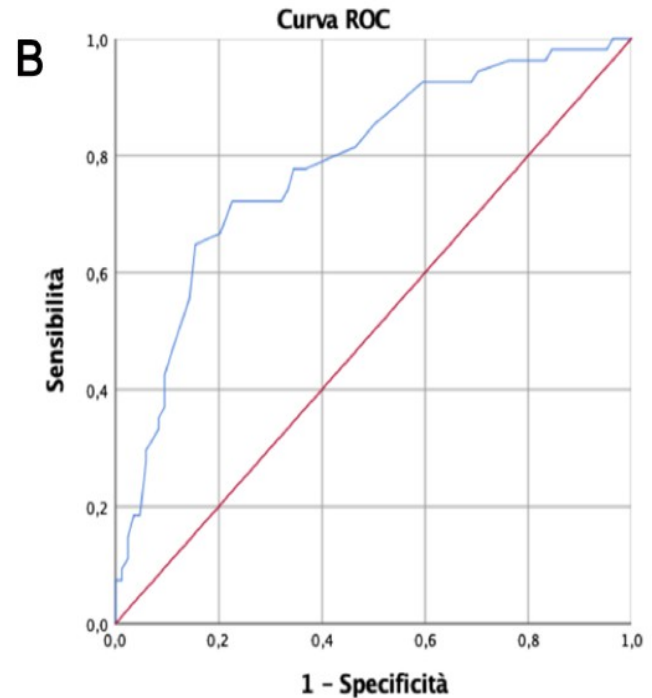
<b>RI + RII</b>	15 (13-17.5)	7 (5-10.6)	<b>&lt;0.0001</b>
<b>SV1 + RV6</b>	18.8 (15.5-23)	12 (9-17)	<b>&lt;0.0001</b>





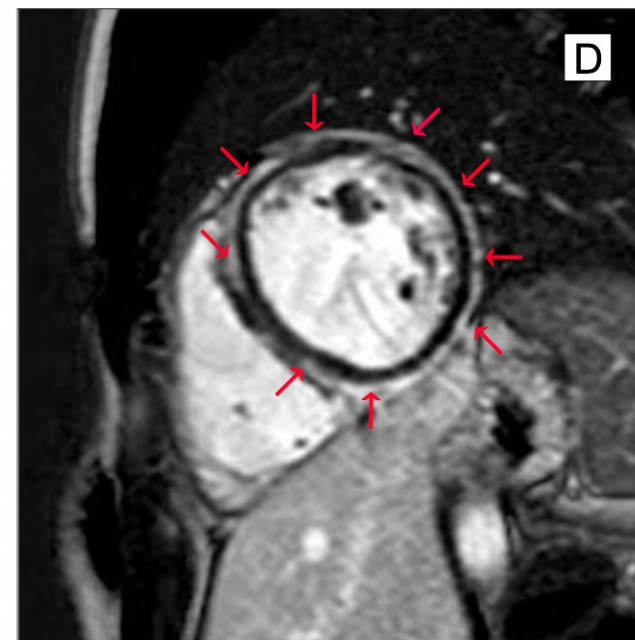
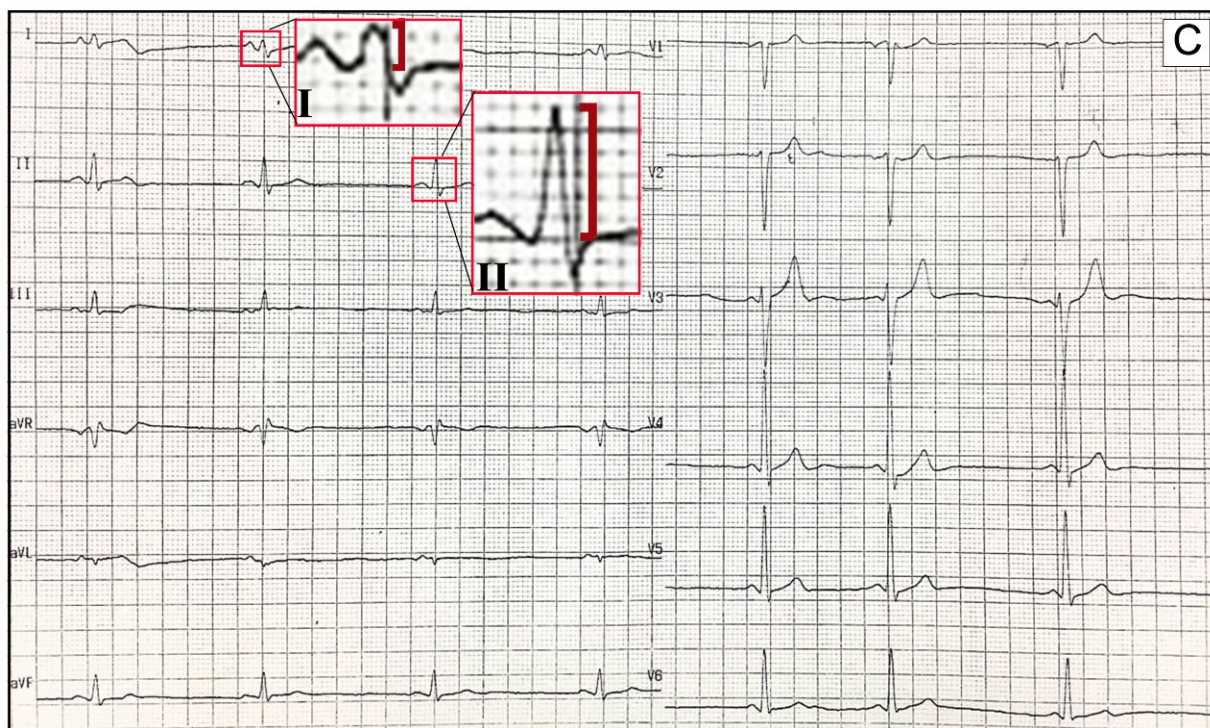
**Sum of R-wave in I-II**

A, Area under curve = 0.909 (0.856-0.962),  $p < 0.0001$ . The cut-off value for the sum of R-wave in I-II that best identified ALVC pts was **8 mm** (sensitivity 57.4%, specificity 97.6%).

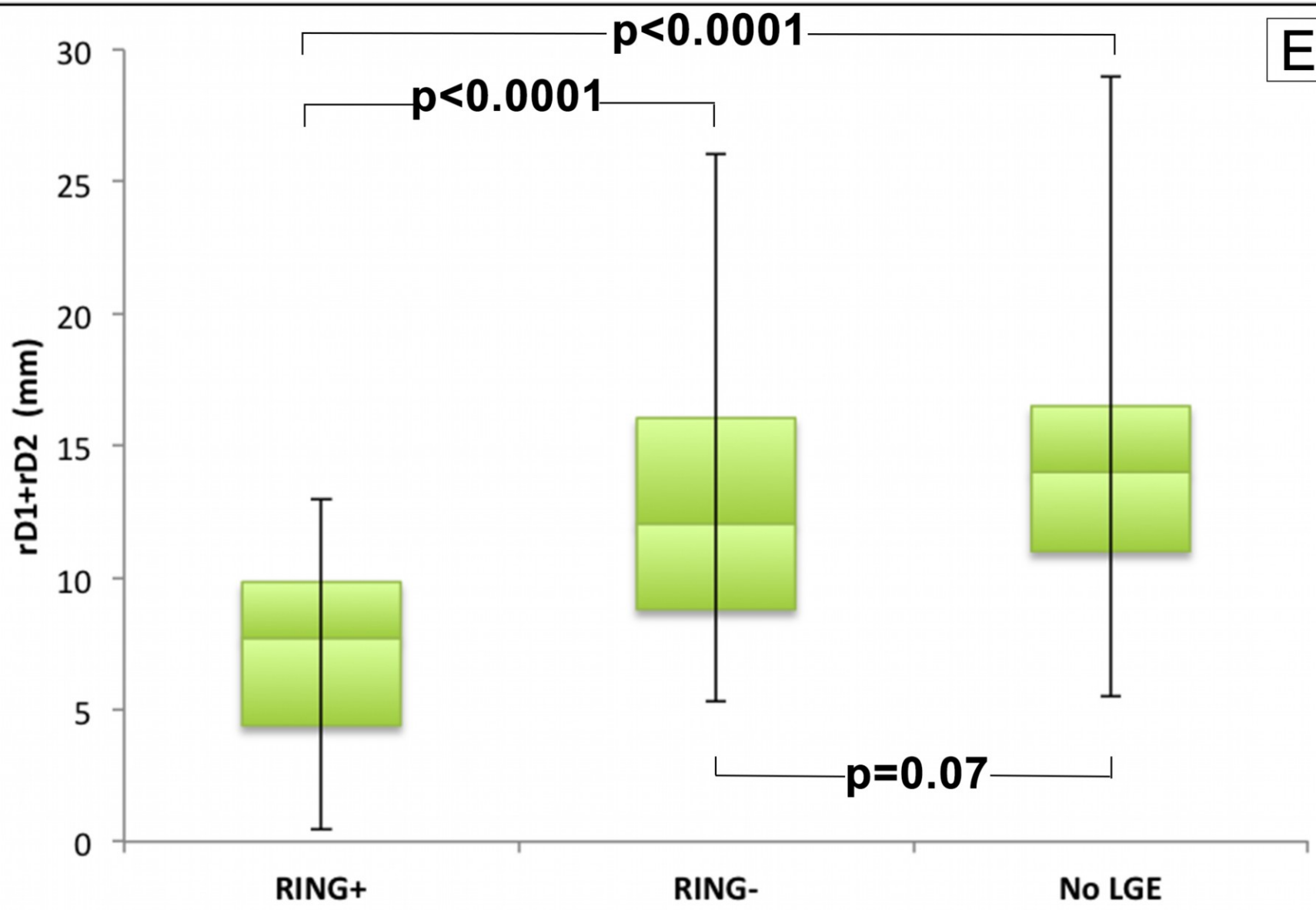


**Sum of S wave in V1 and R in V6**

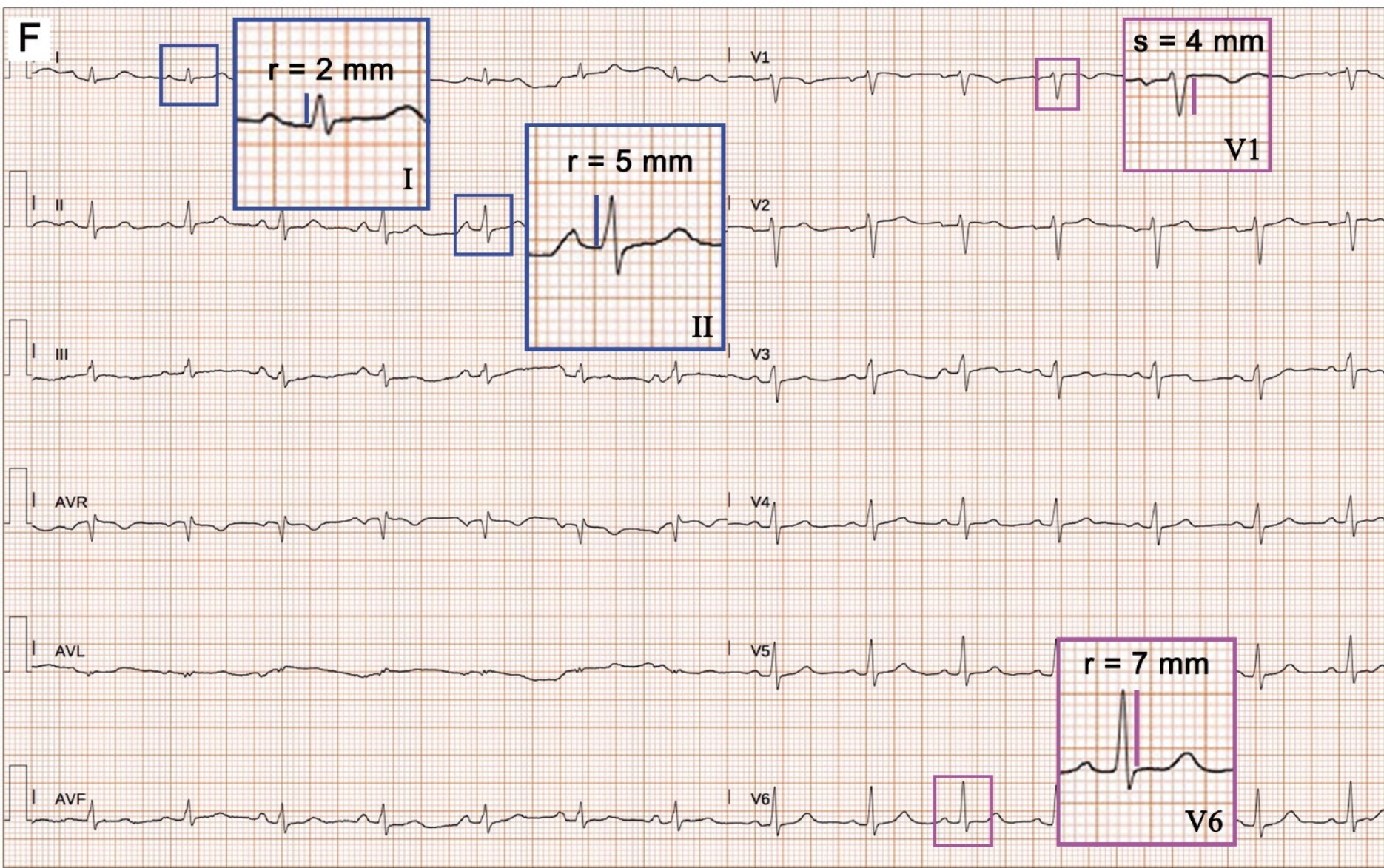
B, Area under curve = 0.784 (0.704-0.863),  $p < 0.0001$ . The cut-off value for the sum of S wave in V1 and R in V6 that best identified ALVC pts was **12 mm** (sensitivity 55.5%, specificity 85.7%).



E







Patient #20, 23-year-old woman with a pathogenic variant in desmoplakin (c.5210del, p.Gly1737AspfsTer16)





# ECG characteristics of the control group and study population

	Controls (n=84)	ALVC (n=54)	P Value
QRS (msec)	91±10	95±14	0.15
First degree AV block	3 (3.6)	5 (9.3)	0.42
NSICD	0	2 (3.7)	0.30
RBBB	1 (1.2)	0	0.99
LAFB	1 (1.2)	4 (7.4)	0.15
LPFB	0	11 (20.4)	<0.0001
LBBB	0	0	0
Pathological Q waves	0	18 (33.3)	<0.0001
Lateral distribution	0	7 (13.0)	0.003
Inferior distribution	0	8 (14.8)	0.0012
Precordial distribution	0	1 (1.9)	0.82
More 2 localizations	0	2 (3.7)	0.30
Fragmented QRS	9 (10.7)	19 (35.2)	0.001
Lateral distribution	0	1 (1.9)	0.82
Inferior distribution	9 (10.7)	10 (18.5)	0.31
Precordial distribution	0	1 (1.9)	0.82
More 2 localizations	0	7 (13.0)	0.003
TWI	1 (1.2)	31 (57.4)	<0.0001
Inferolateral TWI	0	6 (11.1)	0.007
Anterior TWI	1 (1.2)	6 (11.1)	0.028
Inferior TWI	0	4 (7.4)	0.044
Lateral TWI	0	6 (11.1)	0.007
Anterolateral TWI	0	6 (11.1)	0.007
Inferior-anterior-lateral TWI	0	3 (5.6)	0.11
<b>NEW ECG CRITERIA</b>			
SV1+RV6 ≤12 (mm)	12 (14.3)	30 (55.6)	<0.0001
RI + RII ≤8 (mm)	2 (2.4)	31 (57.4)	<0.0001
SV1+RV6 ≤12 and RI + RII ≤8 (mm)	0	24 (44.4)	<0.0001

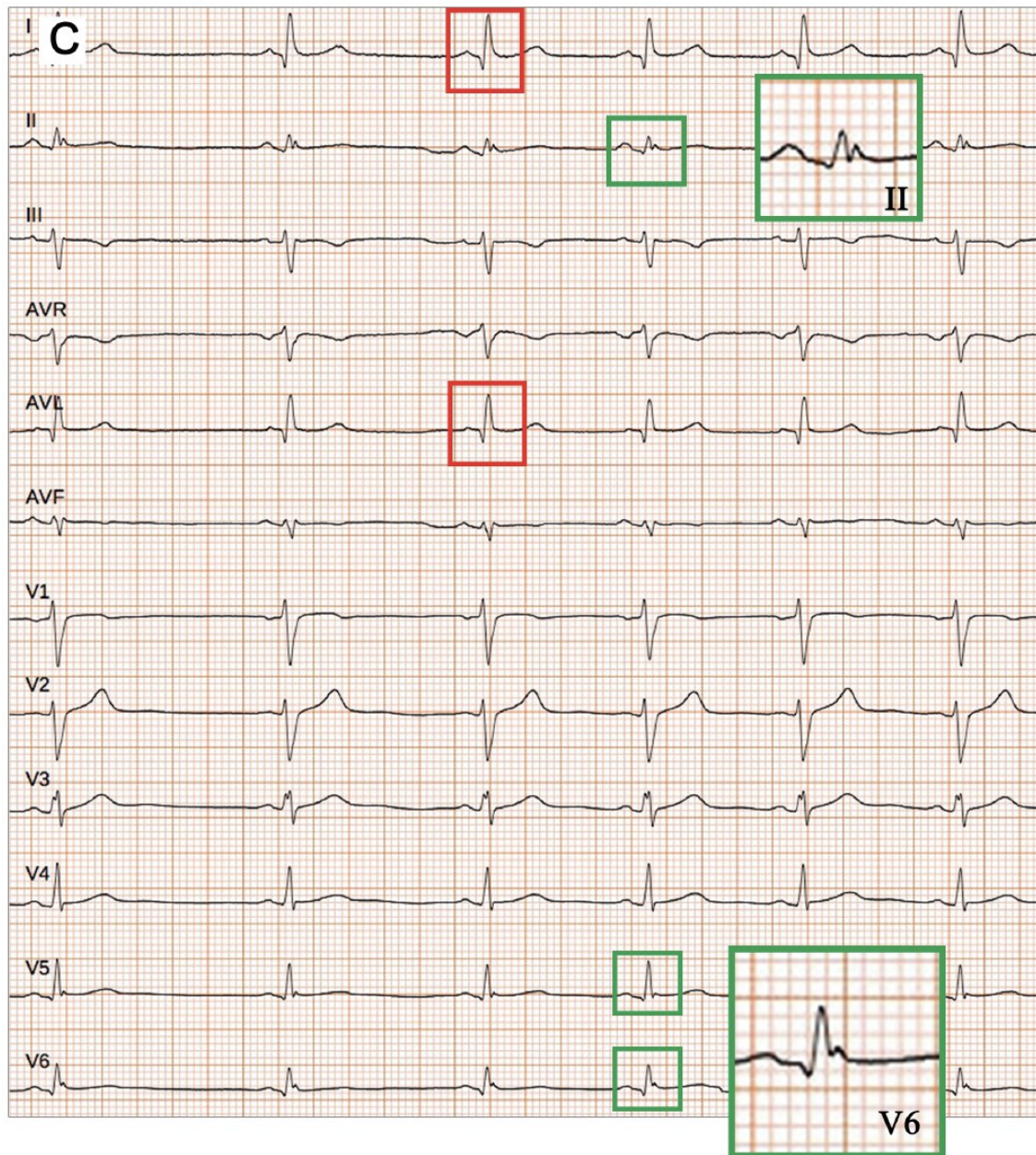
Global LQRSV	0	4 (7.4)	0.044
LQRSV in limb leads	0	8 (14.8)	0.0011
Local LQRSV			
Lateral distribution	16 (18.8)	13 (24.1)	0.52
Inferior distribution	11 (12.9)	8 (14.8)	0.75
Inferolateral distribution	0	3 (5.6)	0.11
Precordial and local distribution	3 (3.5)	8 (14.8)	0.017
Epsilon Wave	0	1 (1.9)	0.82
Epsilon-like Wave in inferior leads	0	3 (5.6)	0.11
QTc (msec)	405±19	407±26	0.49
QTc ≥440 msec	0	4 (7.4)	0.044
Tzou criteria *	15 (17.6)	10 (18.5)	0.89
R >3 mm V1	1 (1.2)	6 (11.1)	0.028
R/S ratio ≥0.5 in V1	1 (1.2)	13 (24.1)	<0.0001
R/S ratio ≥1 in V1	0	6 (11.1)	0.007
Bayés de Luna criteria †	1 (1.2)	3 (5.6)	0.33



## Sensitivity, specificity, PPV and NPV value of new and known ECG parameters for ALVC diagnosis

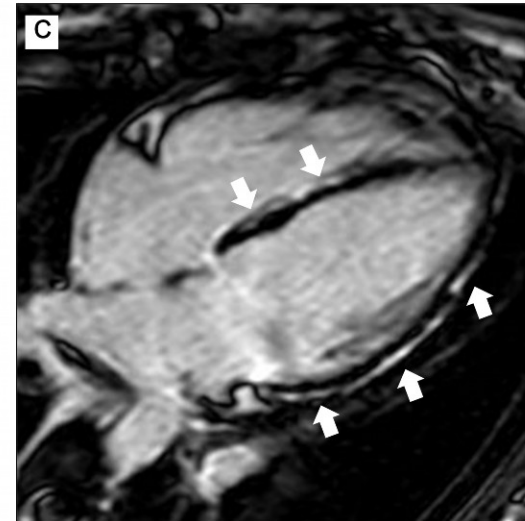
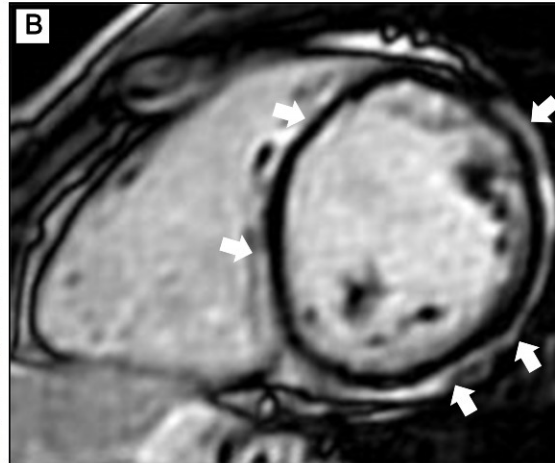
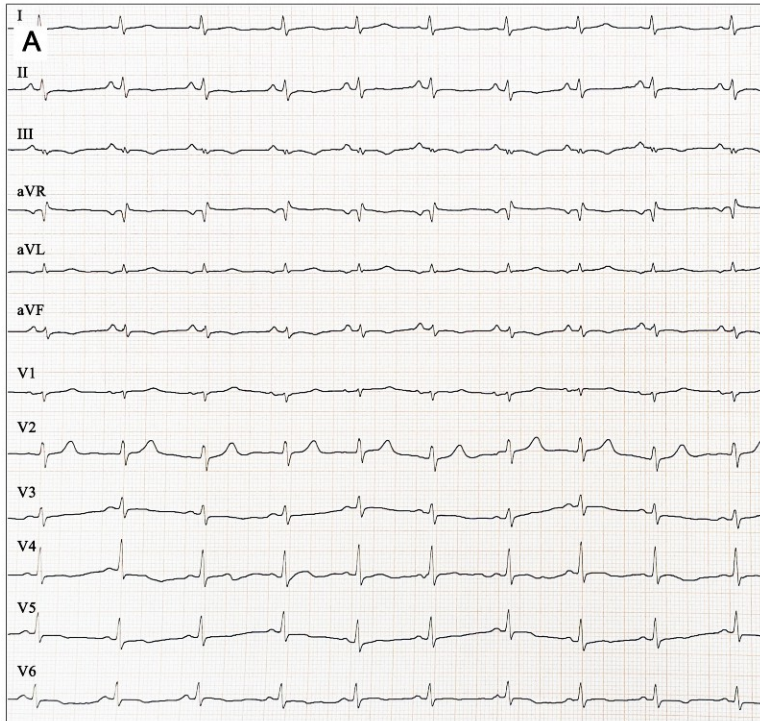
	ALVC (n=54)	Controls (n=84)	Sensitivity (%)	Specificity (%)	PPV (%)	NPV (%)	Accuracy (%)
<b>Single ECG Parameters</b>							
LPFB	11	0	20.4	100	100	66.1	68.8
Pathologic Q waves	18	0	33.3	100	100	70.0	73.9
TWI	31	1	57.4	98.8	96.9	78.3	82.6
LQRSV in limb leads	8	0	14.8	100	100	64.6	66.7
Global LQRSV	4	0	7.4	100	100	62.7	63.8
R >3 mmV1	6	1	11.1	98.8	85.7	63.4	64.5
R/S ratio $\geq 0.5$ in V1	13	1	24.1	98.8	92.9	66.9	69.6
SV1+RV6 $\leq 12$	30	12	55.6	85.7	71.4	75.0	73.9
RI+ RII $\leq 8$	31	2	57.4	97.6	93.9	78.1	81.9
<b>Combined ECG Parameters</b>							
<i>Known ECG criteria</i>							
TWI or LQRSV in limb leads	35	1	64.8	98.8	97.2	81.4	85.5
TWI or LQRSV (limb leads and global)	37	1	68.5	98.8	97.4	83.0	86.9
<i>New ECG criteria</i>							
SV1+RV6 $\leq 12$ and RI + RII $\leq 8$	24	0	44.4	100	100	73.7	78.3
LPFB or Q or R/S ratio $\geq 0.5$ in V1	30	1	55.6	98.8	96.8	77.6	81.9
LPFB or Q or R/S ratio $\geq 0.5$ in V1 or [SV1+RV6 $\leq 12$ and RI + RII $\leq 8$ ]	35	1	64.8	98.8	97.2	81.4	85.5
<i>Know and New ECG criteria</i>							
TWI or LPFB or Q	38	1	70.4	98.8	97.4	83.8	87.7
TWI or LPFB or Q or [SV1+RV6 $\leq 12$ and RI + RII $\leq 8$ ]	44	1	81.5	98.8	97.8	89.3	92.0
TWI or LPFB or Q or R/S ratio $\geq 0.5$ in V1 or [SV1+RV6 $\leq 12$ and RI + RII $\leq 8$ ] or LQRSV in limb leads	47	2	87.0	97.6	95.9	92.1	93.5





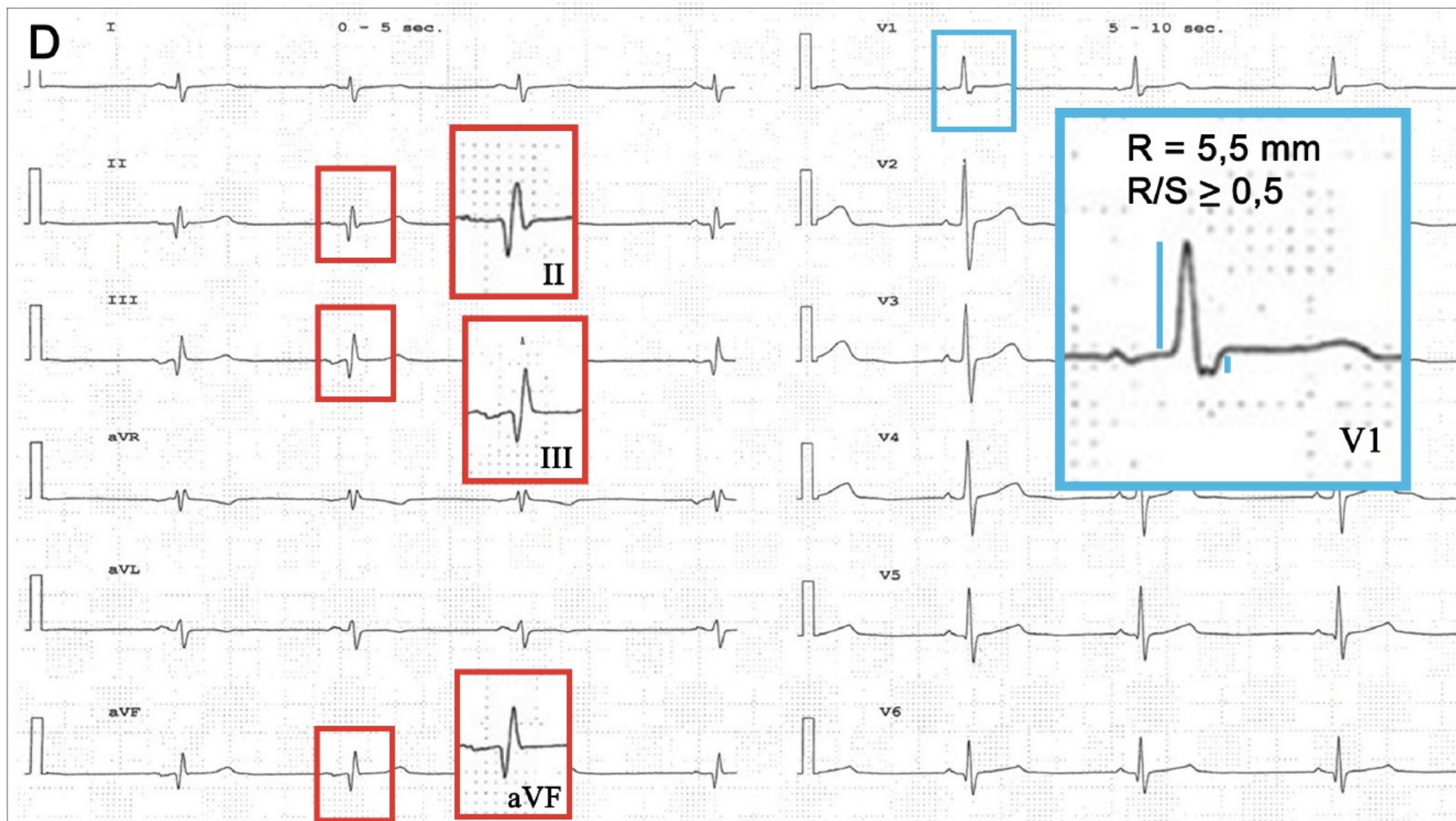
Patient #8, 20-year-old man, pathogenic variant in desmoplakin (c.5851 C>T, p.Arg1951Ter)





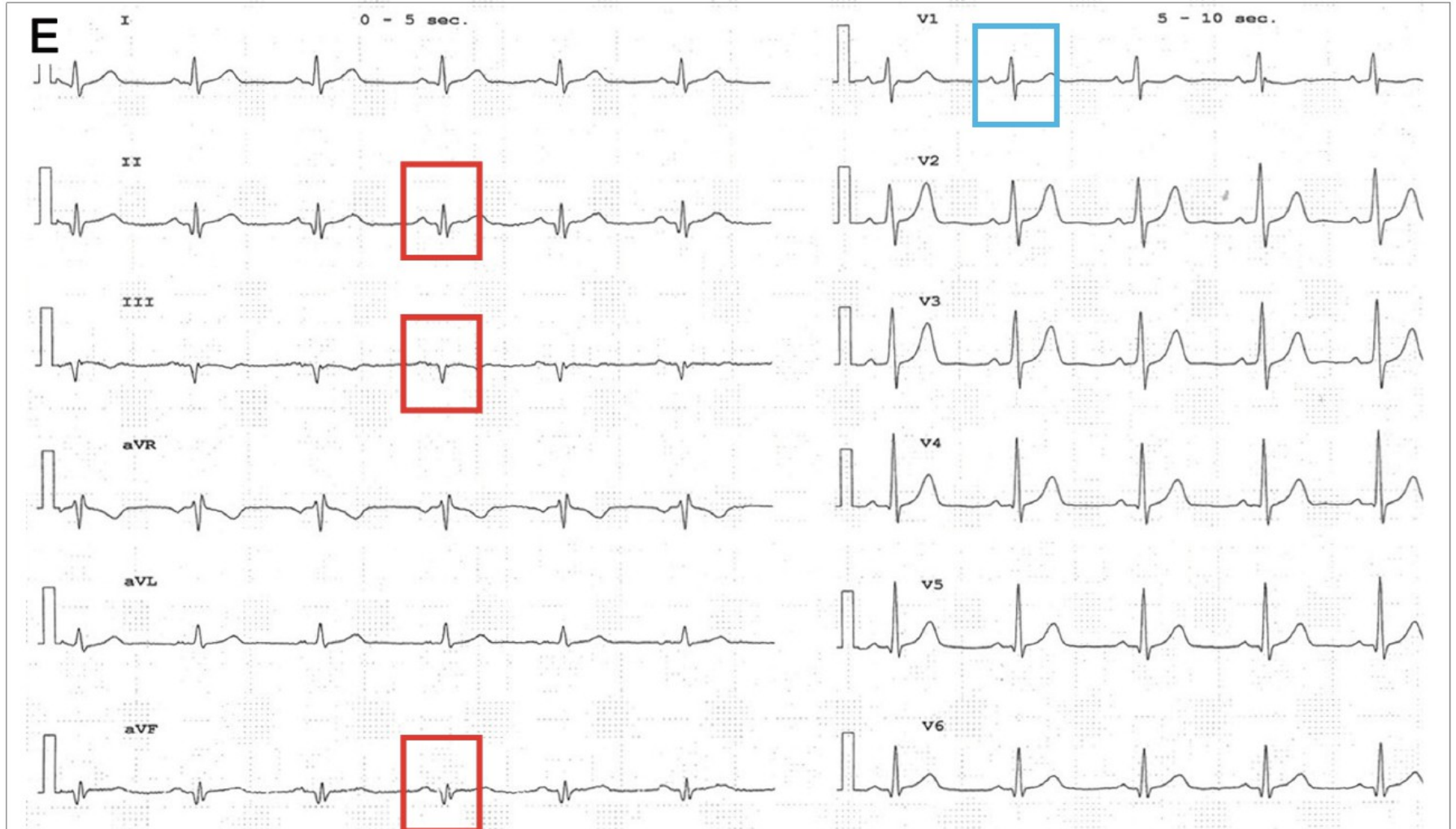
Patient #15 is a 18-year-old woman with a likely pathogenic variant in desmoplakin (c.1351C>T, p.Arg451Cys).



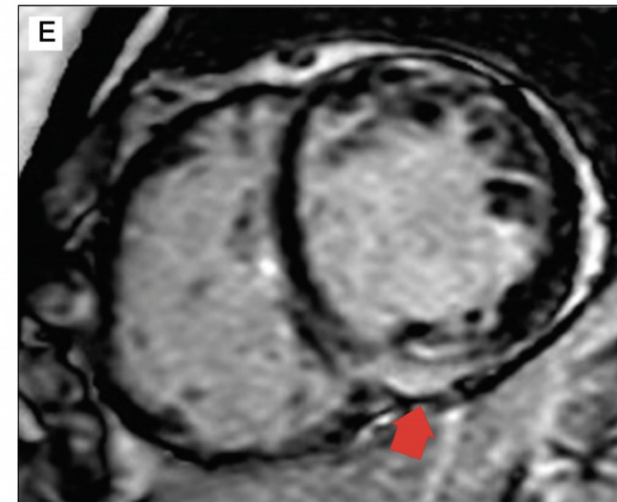
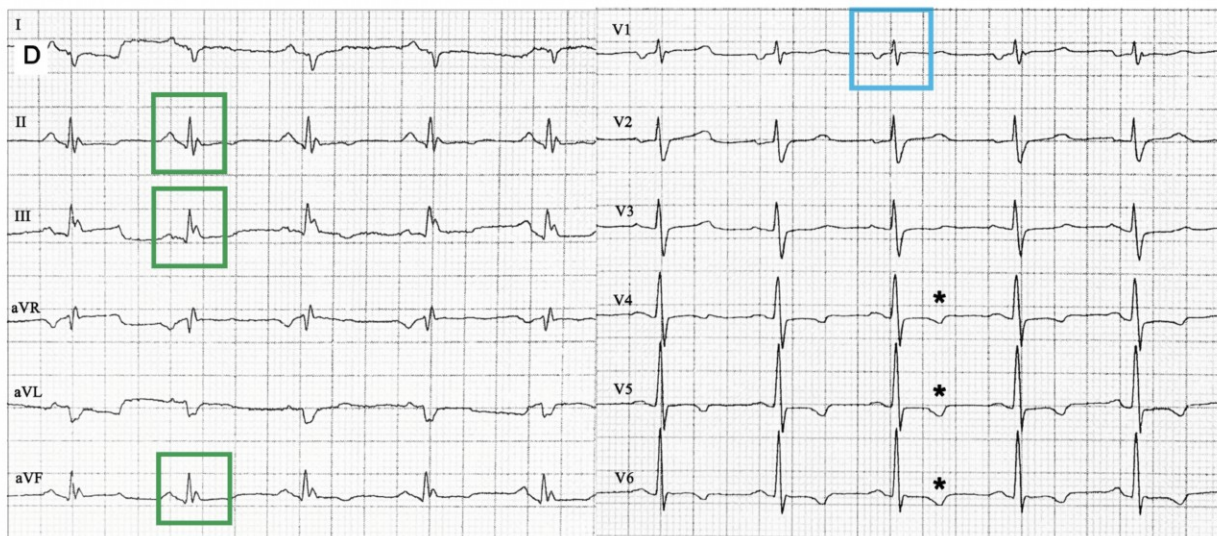


Patient #35, 42-year-old man), pathogenic variant in desmoglein-2 (c.1912G>A, p.Gly638Arg)





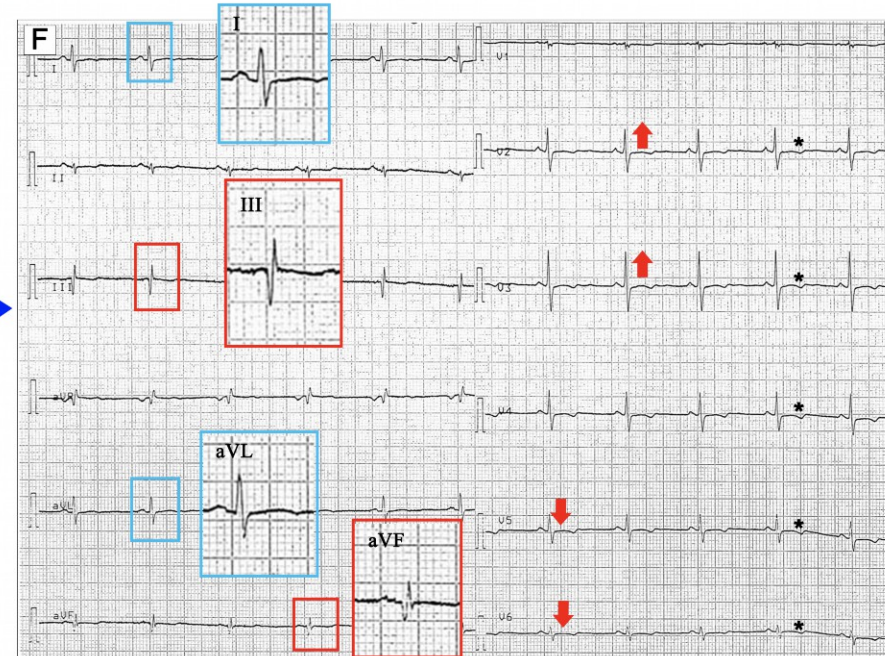
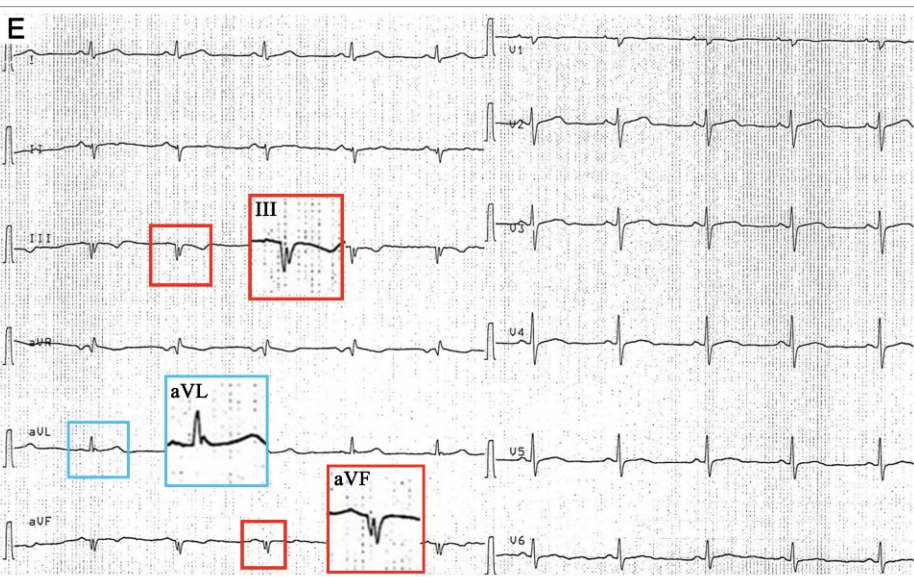
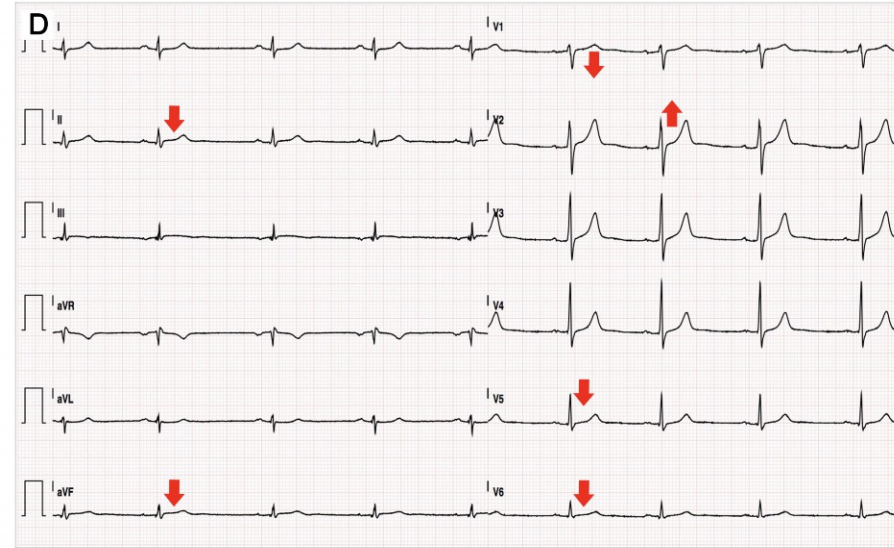
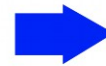
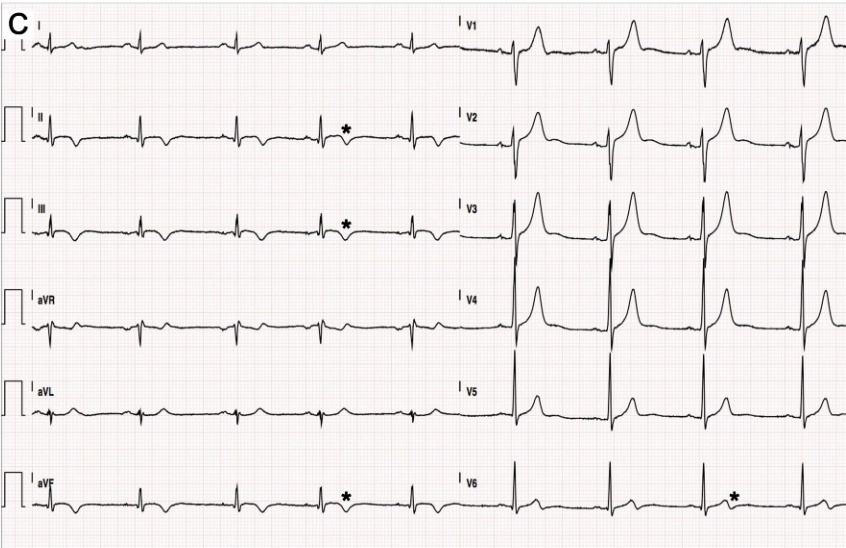
The family member (Patient #36, 37-year-old man) has the same pathogenic variant in desmoglein-2 (c.1912G>A, p.Gly638Arg)



Patient #9 is a 33-year-old woman with a pathogenic variant in desmoplakin (c.5851 C>T, p.Arg1951Ter).









	Major Arrhythmic Events (n=15)	No Major Arrhythmic Events (n=39)	P Value
Age at diagnosis, years	43±15	38±15	0.28
Male gender	13 (86.7)	19 (48.7)	<b>0.011</b>
Proband	13 (86.7)	27 (69.2)	0.19
Family history of DCM	5 (33.3)	18 (46.2)	0.39
Family history of SCD	3 (20.0)	15 (38.5)	0.20
NYHA class I-II	13 (86.7)	39 (100)	0.22
NYHA class III	2 (13.3)	0	<b>0.0215</b>
Atrial fibrillation	2 (13.3)	2 (5.1)	0.31
Unexplained syncope	6 (40.0)	2 (5.1)	<b>0.001</b>
NSVT	8 (53.3)	18 (46.2)	0.64
<b>Cardiac magnetic resonance</b>			
LVEDVi (ml/m <sup>2</sup> )	99.9±19.7	96.8±26.1	0.68
LVEF, %	46.3±6.1	50.8±10.9	0.14
LVEF <50%	10 (66.7)	13 (33.3)	<b>0.0276</b>
RVEDVi (ml/m <sup>2</sup> )	87.2±20.9	85.4±18.4	0.76
RVEF, %	52.6±9.8	54.9±9.2	0.42
Segments with LGE	6±3; 6 (4-7)	6±4; 6 (4-8)	1.0
<b>LGE pattern</b>			
- Ringlike	8 (53.3)	20 (51.3)	0.89
<b>LGE distribution</b>			
- Subepicardial	7 (46.7)	28 (71.8)	<b>0.09</b>
- Midmural	2 (13.3)	8 (20.5)	0.55
- Transmural	6 (40.0)	3 (7.7)	<b>0.0047</b>
<b>Genetic testing</b>			
Pathogenic/likely pathogenic variant	12/15 (80.0)	36/39 (92.3)	0.20
DSP	6/12 (50.0)	29/36 (80.6)	0.64
Non-DSP *	6/12 (50.0)	7/36 (19.4)	<b>0.026</b>
<b>ECG</b>			
QRS (msec)	97±13	95±13	0.61
First degree AV block	1 (6.7)	4 (10.3)	0.68
NSICD	0	2 (5.1)	0.37
RBBB	0	0	-
LAFB	0	4 (10.3)	0.20
LPFB	6 (40.0)	5 (12.8)	<b>0.028</b>
LBFB	0	0	-



	Major Arrhythmic Events (n=15)	No Major Arrhythmic Events (n=39)	P Value
<b>Pathological Q waves</b>	5 (33.3)	13 (33.3)	1.0
Lateral distribution	2 (13.3)	5 (12.8)	0.96
Inferior distribution	2 (13.3)	6 (15.4)	0.84
Precordial distribution	0	1 (2.6)	0.53
More 2 localizations	1 (6.7)	1 (2.6)	0.48
<b>Fragmented QRS</b>	4 (26.7)	15 (38.5)	0.42
Lateral distribution	0	1 (2.6)	0.53
Inferior distribution	1 (6.7)	9 (23.1)	0.17
Precordial distribution	1 (6.7)	0	0.11
More 2 localizations	2 (13.3)	5 (12.8)	0.96
<b>Global LQRSV</b>	1 (6.7)	3 (7.7)	0.90
<b>LQRSV in limb leads</b>	1 (6.7)	7 (17.9)	0.31
<b>Local LQRSV</b>			
Lateral distribution	4 (26.7)	9 (23.1)	0.78
Inferior distribution	2 (13.3)	6 (15.4)	0.84
Inferolateral distribution	2 (13.3)	1 (2.6)	0.13
Precordial and local distribution	1 (6.7)	4 (10.3)	0.69
<b>QTc (msec)</b>	401±27	409±26	0.32
<b>QTc ≥440 msec</b>	0	4 (10.3)	0.20
<b>Tzou criteria †</b>	6 (40.0)	4 (10.3)	<b>0.01</b>
<b>R &gt;3 mm V1</b>	3 (20.0)	3 (7.7)	0.20
<b>R/S ratio ≥0.5 in V1</b>	9 (60.0)	4 (10.3)	<b>0.0002</b>
<b>R/S ratio ≥1 in V1</b>	6 (40.0)	0	<b>&lt;0.0001</b>
<b>Bayés de Luna criteria ‡</b>	3 (20.0)	0	<b>0.0044</b>
<b>TWI</b>	11 (73.3)	20 (51.3)	0.15
Inferolateral TWI	4 (26.7)	2 (5.1)	<b>0.025</b>
Anterior TWI	2 (13.3)	4 (10.3)	0.76
Inferior TWI	2 (13.3)	2 (5.1)	0.31
Lateral TWI	2 (13.3)	4 (10.3)	0.76
Anterolateral TWI	1 (6.7)	5 (12.8)	0.53
Inferior-anterior-lateral TWI	0	3 (7.7)	0.27
<b>NEW ECG CRITERIA</b>			
<b>SV1+RV6 ≤12 (mm)</b>	10 (66.7)	20 (51.3)	0.31
<b>RI + RII ≤8 (mm)</b>	7 (46.7)	24 (61.5)	0.33
<b>SV1+RV6 ≤12 and RI + RII ≤8 (mm)</b>	7 (46.7)	17 (43.6)	0.84

## Probability of major arrhythmic events in relation to clinical, electrocardiographic and structural parameters

	Univariate analysis			Multivariate analysis		
	OR	95% CI	<i>P value</i>	OR	95% CI	<i>P value</i>
<b><i>Clinical parameters</i></b>						
Age	1.0	0.9-1.1	0.317			
Sex	6.8	1.4-34.4	<b>0.020</b>			
Unexplained syncope	12.3	2.1-71.5	<b>0.005</b>	<b>8.9</b>	<b>1.1-70.6</b>	<b>0.037</b>
<b><i>Structural parameters</i></b>						
Transmural LGE	8.0	1.7-38.2	<b>0.009</b>			
LVEF <50%	4.0	1.1-14.1	<b>0.031</b>			
<b><i>ECG parameters</i></b>						
LPFB	4.5	1.1-18.3	<b>0.034</b>			
R/S ratio in V1 $\geq 0.5$	13.1	3.0-56.6	<b>0.001</b>	<b>6.8</b>	<b>1.4-34.4</b>	<b>0.020</b>
Inferolateral TWI	6.7	1.1-41.8	<b>0.041</b>			
SV1+RV6 $\leq 12$ mm	1.9	0.5-6.6	0.312			
RI+ RII $\leq 8$ mm	0.6	0.2-1.8	0.325			





# Unrecognized cases of prominent R-wave in V1 detected in the iconography of published papers

Case ID	References	Figure	12 lead ECG findings	Genetic analysis	CMR data	Endomyocardial biopsy data/ Histologic data
Case 1	Rubino M et al <sup>1</sup> <i>Genes</i> 2021	Fig.1	Prominent R V1 (>3mm) Inferolateral TWI Pathological Q in I-aVL	DSP (c.5428C>T, p.Gln1810Ter)	Subepicardial circumferential LGE involving the entire LV	Not available
Case 2	Zorzi A et al <sup>2</sup> <i>Circ Arrhythm Electrophysiol</i> 2016	Fig. 4	LPFB Inferolateral TWI Pathological Q II-III-aVF Prominent R V1 (>3 mm) LQRSV in left precordial leads	Not performed	Sub/midmyocardial LGE with a stria pattern involving the inferolateral LV wall	Extensive fibrosis in the sub- and midmyocardial layers (inferolateral LV), focal and patchy fatty infiltration. Cardiomyocytes hypertrophic with dysmetric and dysmorphic nuclei, with cytoplasmic vacuolization.
Case 3	Oloriz T et al <sup>3</sup> <i>Europace</i> 2016	Fig. 1- right panel	LPFB - R/S ratio V1 ≥0.5	Not performed	Infero-lateral scar	Not performed
Case 4	Sakamoto N et al <sup>4</sup> <i>Circ Cardiovasc Imaging</i> 2019	Fig.1	R/S ratio V1 ≥1 Inferolateral TWI LQRSV in limb leads	DSP (c.4650delTG, p.V1551E fs74X) and MYBPC3 (c.2459G>A, p.R820Q)	LGE in the mid-myocardial septum and subepicardial anterolateral LV myocardium.	Fibrofatty replacement, mild hypertrophy, and disarrangement of the myocytes. Electron microscopy of the intercalated discs showed disarrangement of the filaments and widening of the fascia adherens gap
Case 5	Tsuruta Y et al <sup>5</sup> <i>Heart Fail</i> 2020	Fig.1	R/S ratio V1 ≥1 Inferolateral TWI LQRSV in limb leads	Nonsense mutation in DSP (c.5212C > T, p.R1738*)	Fat signals LGE in the mid-wall to subepicardial layers in the LV myocardium	Moderate fibrofatty replacement and mild hypertrophy
Case 6	Groeneweg JA et al <sup>6</sup> <i>Heart Rhythm</i> 2013	Fig.4	R/S ratio V1 ≥1 TWI in II and anterolateral leads	PKP2 variant c.419C4T and the PLN mutation c.40_42delAGA	LGE in the lateral wall of the LV	Normal myocardium, with locally some (<10%) subendocardial fibrosis.

Case 7	Blom LJ et al <sup>7</sup> <i>Heart Rhythm Case Rep</i> 2018	Fig.2	LPFB TWI V5-V6, I, II, aVF R/S ratio V1 ≥1	Unclassified variant PKP2 gene and a pathogenic c.4042delAGA mutation in the PLN gene.	Not performed	Normal
Case 8	Singh SM et al <sup>8</sup> <i>JACC Case Rep</i> 2021	Fig.3 (C)	LPFB - R/S ratio V1 ≥1	Not performed	Biventricular apical and anterolateral LGE in the epi- to mid-myocardium	Not performed
Case 9	Norman M et al <sup>9</sup> <i>Circulation</i> 2005	Fig.3	R/S ratio V1 ≥0.5 Inferolateral TWI	DSP gene identified insertion of a single adenine base (2034insA)	Not performed	Not performed
Case 10	Chen P et al <sup>10</sup> <i>Int J Cardiol</i> 2020	Fig. 2 (A)	LPFB. TWI V1-V3. R/S ratio V1 ≥1	DSG2 p.Leu237Ter mutation	Dilation of both ventricles	Not performed
Case 11	Pilichou K et al <sup>11</sup> <i>Circulation</i> 2014	Fig.3	R/S ratio V1 ≥1	DSP c.448C>T mutation	Focal bulging on anterolateral RV apex. LGE (midepicardial stria) in the inferior LV wall	Not performed

# The end of an electrocardiographic dogma: a prominent R wave in V<sub>1</sub> is caused by a lateral not posterior myocardial infarction—new evidence based on contrast-enhanced cardiac magnetic resonance—electrocardiogram correlations

Antonio Bayés de Luna<sup>1\*</sup>, Daniele Rovai<sup>2</sup>, Guillem Pons Llado<sup>1</sup>, Anton Gorgels<sup>3</sup>,  
 Francesc Carreras<sup>1</sup>, Diego Goldwasser<sup>1</sup>, and Raymond J. Kim<sup>4</sup>

<sup>1</sup>Institut Català Ciències Cardiovasculars (ICCC), Sant Pau Hospital, S. Antoni M. Claret 167, Barcelona 08025, Spain; <sup>2</sup>CNR, Institute of Clinical Physiology, Pisa, Italy;

<sup>3</sup>Maastricht University, Maastricht, The Netherlands; and <sup>4</sup>Duke University, Durham, NC, USA

Received 6 February 2014; revised 16 October 2014; accepted 6 January 2015

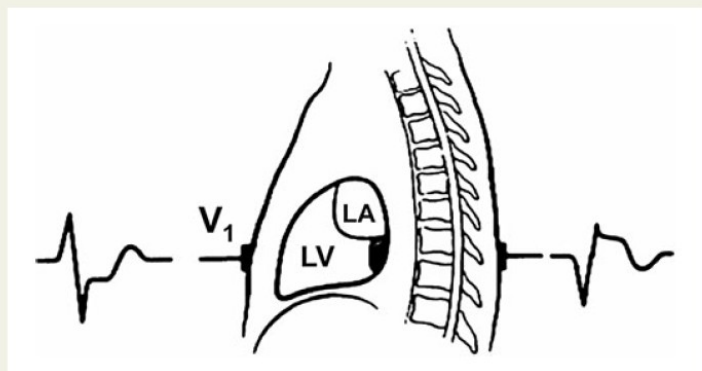


**Figure 1** Original drawing of true posterior infarction with the QRS morphology according to Perloff.<sup>1</sup>

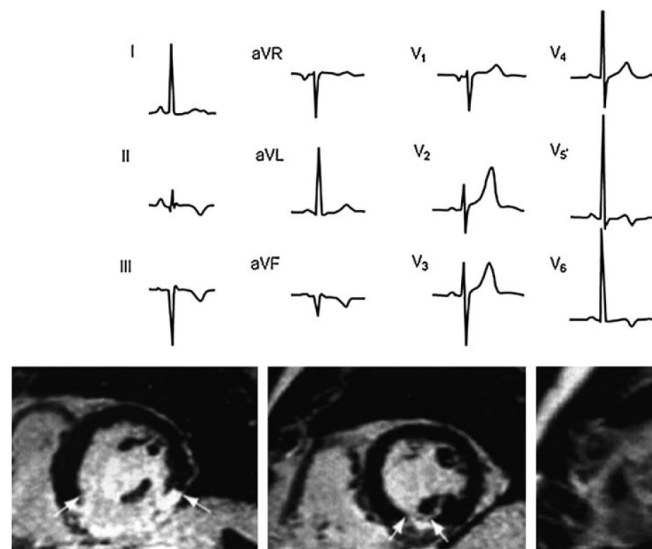


**Figure 2** Electrocardiographic and cardiac magnetic resonance images of an inferior infarct. Despite the clear infero-basal location of infarction at contrast-enhanced cardiac magnetic resonance (left-hand panel, between the white arrows), lead V<sub>1</sub> does not show a prominent R wave but an rS morphology.

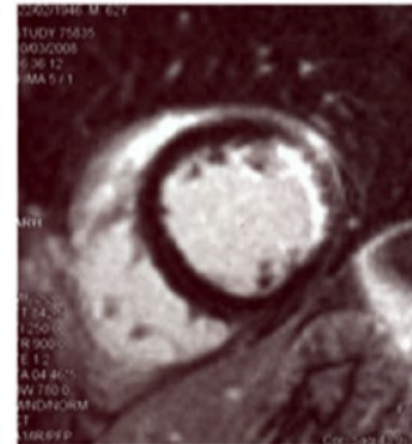
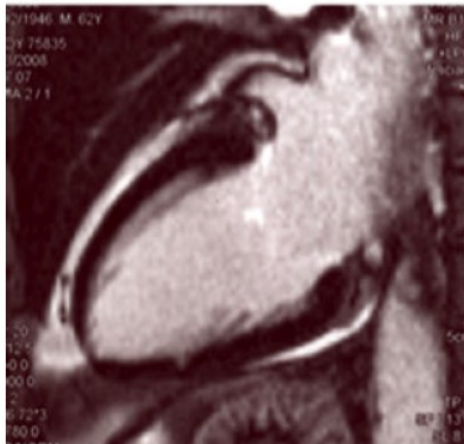
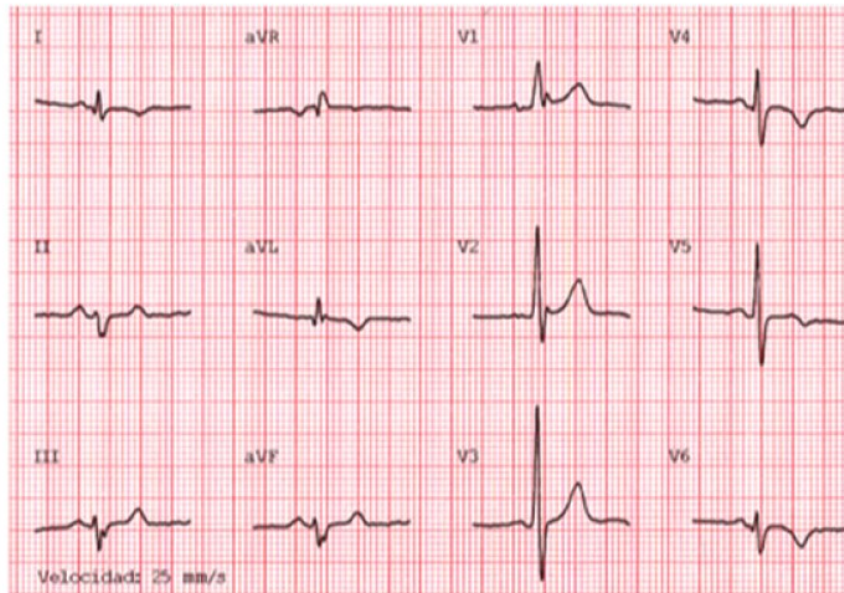
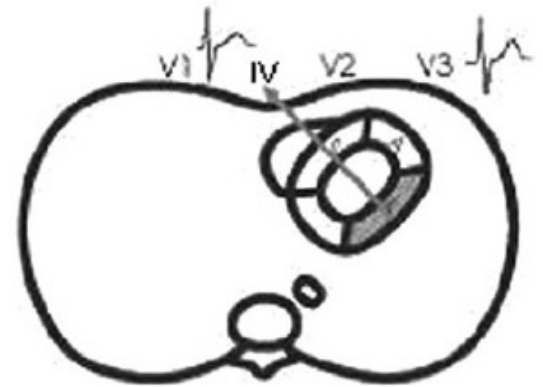
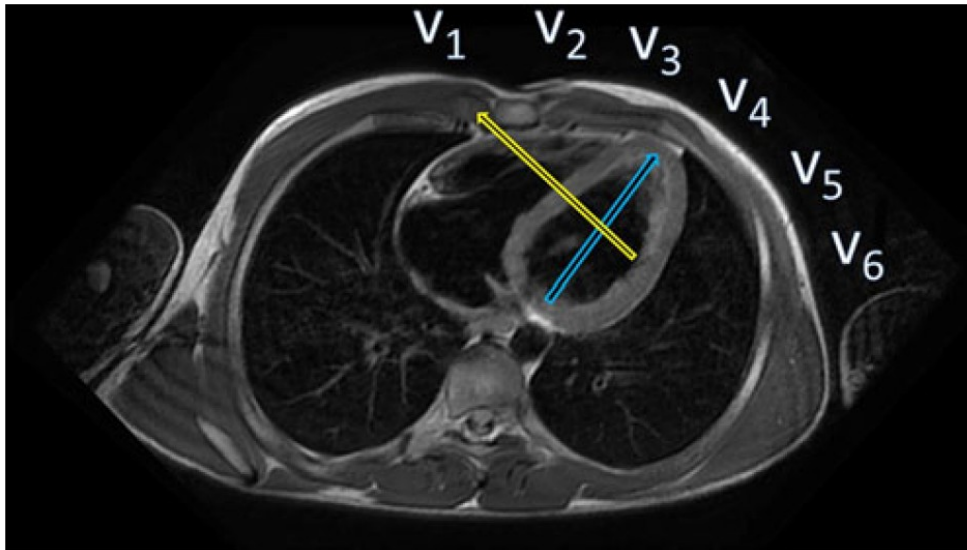


**Figure 3** Electrocardiographic and cardiac magnetic resonance images of a lateral infarct. A tall R wave in V<sub>1</sub> corresponds to a lateral infarct at contrast-enhanced cardiac magnetic resonance (lower central and right-hand panels). Of note, the infero-basal segment (segment 4) does not present any sign of necrosis (lower left and right panels).



## Transverse plane of the thorax at cardiac magnetic resonance



The infarction vector produced by involvement of the wall formerly termed posterior (blue arrow) is directed towards V3–V4, while the infarction vector generated by the lateral wall (yellow arrow) is directed towards V1



# Left-Dominant Arrhythmogenic Cardiomyopathy With Heterozygous Mutations in *DSP* and *MYBPC3*

Sakamoto N. et al. Circ Cardiovasc Imaging. 2019;12:e008913

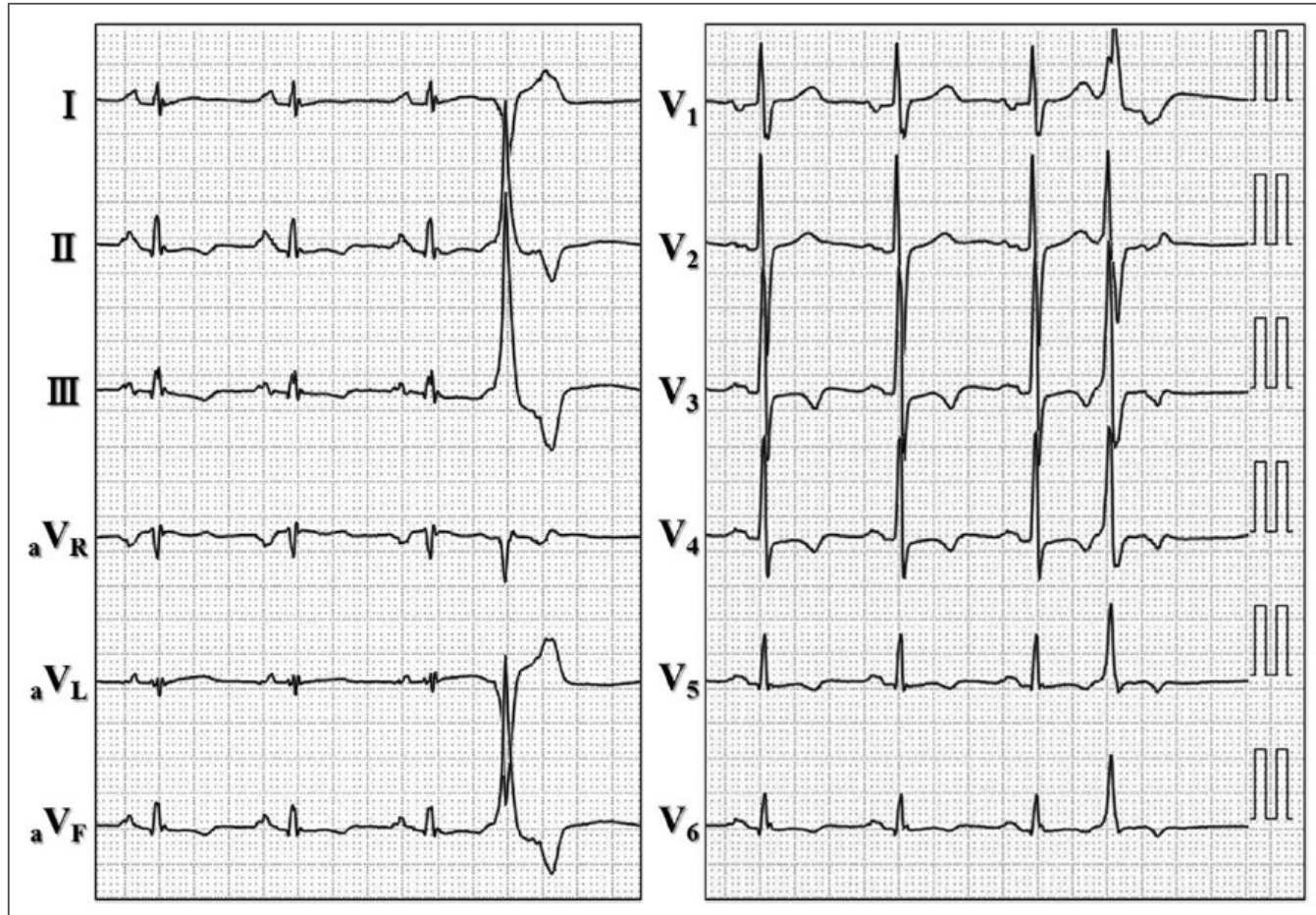


**Figure 1.** ECG showing T-wave inversion in the left-sided leads and a premature ventricular complex of left ventricular origin.

Pathogenic mutations in desmoplakin (c.4650delTG, p.V1551E fs74X) and myosin-binding protein C gene (c.2459G>A, p.R820Q)



## LETTER TO THE EDITOR

# Letter by Pérez-Riera et al Regarding Article, "Left-Dominant Arrhythmogenic Cardiomyopathy With Heterozygous Mutations in *DSP* and *MYBPC3*"

*To the Editor:*

We have read with interest the recent exceptional case report from Dr Sakamoto et al<sup>1</sup> who presented a 46-year-old woman whose main complaint was dyspnea on exertion and in whom the final diagnosis was left-dominant arrhythmogenic cardiomyopathy (ALVC). Genetic screening showed a mutation not reported previously consisting of heterozygous pathogenic mutation in the desmoplakin and myosin-binding protein C.

In their description of the 12-lead ECG, the authors wrote literally: "T-wave inversion in the left-sided leads and a premature ventricular complex of left ventricular origin." We would like to add some additional ECG features of Figure 1,

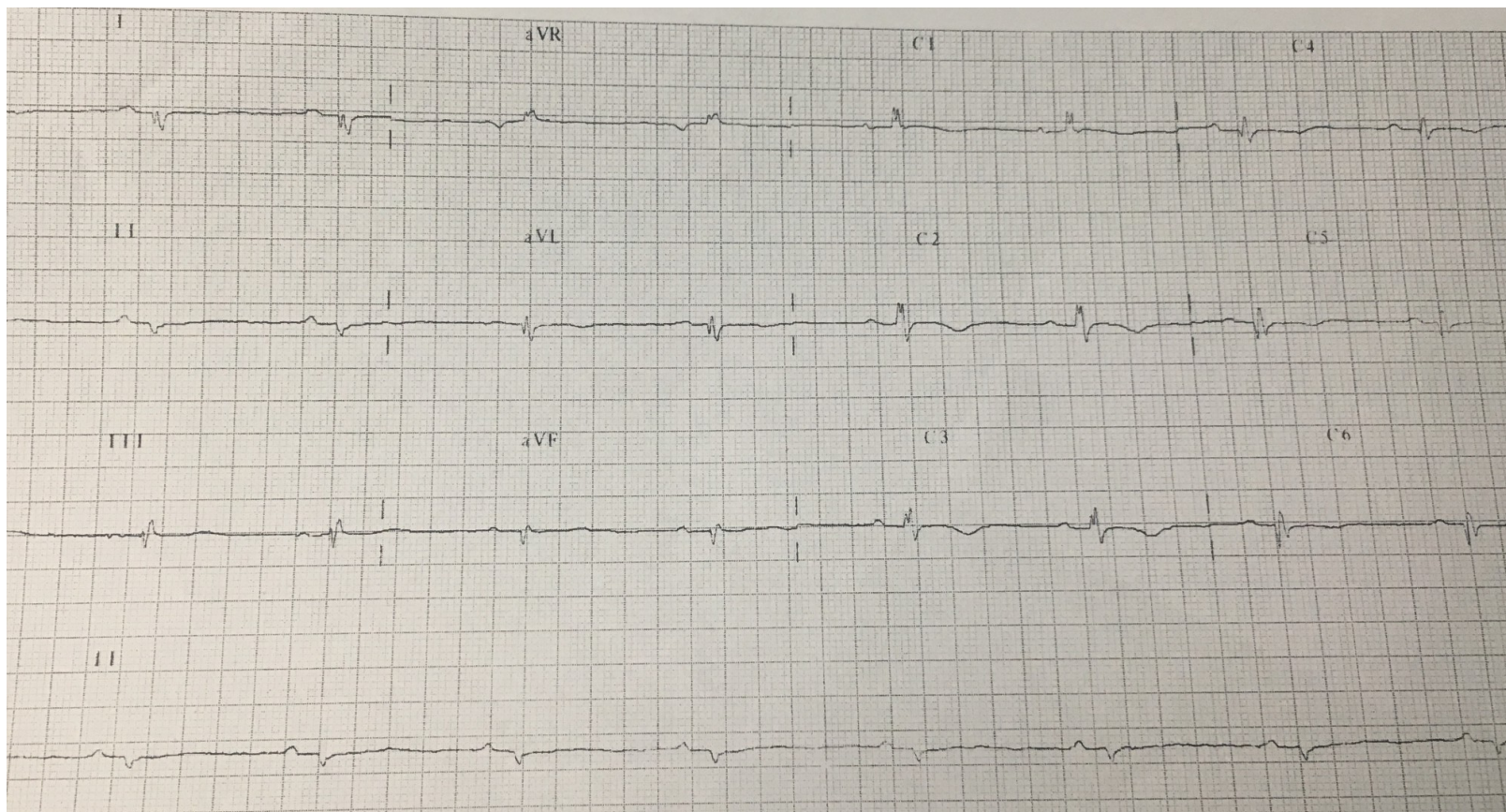
Andrés Ricardo  
Pérez-Riera, MD, PhD  
Raimundo Barbosa-Barros,  
MD  
Bernard Belhassen, MD

Finally, early precordial transition was observed in the precordial leads (R/S ratio >1 in V1-V2).

Such prominent anterior QRS forces can be observed in numerous scenarios: normal variant, athlete's heart, misplaced precordial leads, lateral myocardial infarction (previously named dorsal myocardial infarction), right ventricular hypertrophy, left ventricular hypertrophy, biventricular hypertrophy, right bundle branch block, **left septal fascicular block**, ventricular preexcitation with accessory pathway located in the posterior wall, hypertrophic cardiomyopathy, Duchenne's cardiomyopathy, endomyocardial fibrosis, dextroposition, and ALVC.

In the latter case, **early precordial transition indicates fibrosis in the basal-lateral wall of the LV.**







# The tetrafascicular nature of the intraventricular conduction system

Andrés R. Pérez-Riera<sup>1</sup>  | Raimundo Barbosa-Barros<sup>2</sup> | Rodrigo Daminello-Raimundo<sup>1</sup> | Luiz C. de Abreu<sup>1</sup> | Kjell Nikus<sup>3</sup>

<sup>1</sup>Design of Studies and Scientific Writing Laboratory, ABC Faculty of Medicine, São Paulo, Brazil

<sup>2</sup>Coronary Center of the Hospital de Messejana Dr. Carlos Alberto Studart Gomes, Fortaleza, Brazil

<sup>3</sup>Heart Center, Tampere University Hospital and Faculty of Medicine and Life Sciences, University of Tampere, Tampere, Finland

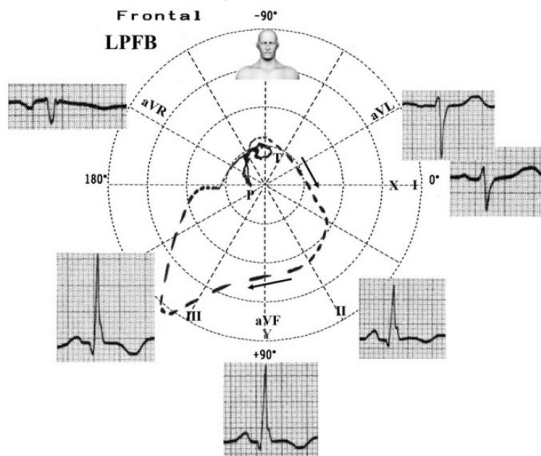
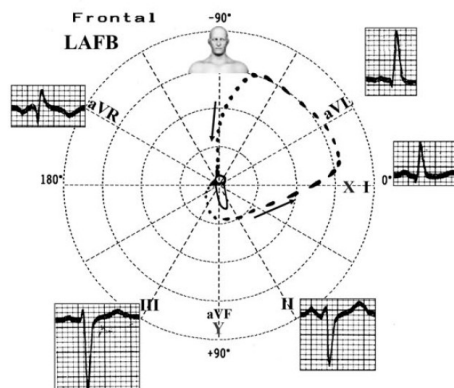
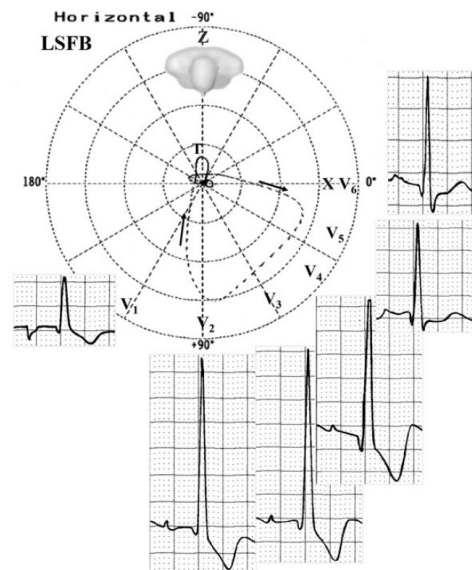
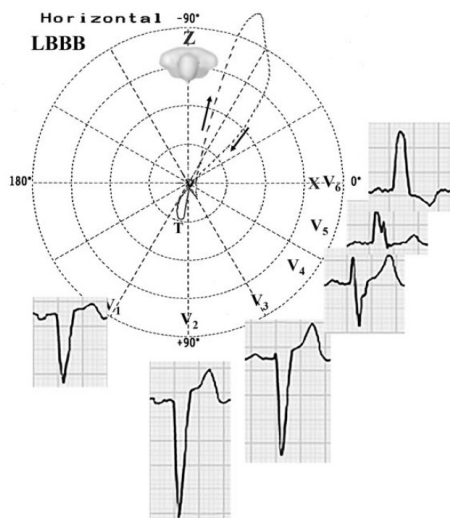
## Correspondence

Andrés Ricardo Pérez-Riera, Rua Sebastião Afonso, 885 Zip code: 04417-100 Jardim Miriam, São Paulo-SP, Brazil.  
Email: riera@uol.com.br

The existence of a tetrafascicular intraventricular conduction system remains debatable. A consensus statement ended up with some discrepancies and, despite agreeing on the possible existence of an anatomical left septal fascicle, the electrocardiographic and vectorcardiographic characteristics of left septal fascicular block (LSFB) were not universally accepted. The most important criteria requested to confirm the existence of LSFB is its intermittent nature. So far, our group has published cases of transient ischemia-induced LSFB and phase 4 or bradycardia-dependent LSFB. Finally, anatomical, anatomopathological, histological, histopathological, electrocardiographic, vectorcardiographic, body surface potential mapping, and electrophysiology studies support the fact that the left bundle branch divides into three fascicles or a “fan-like interconnected network.”

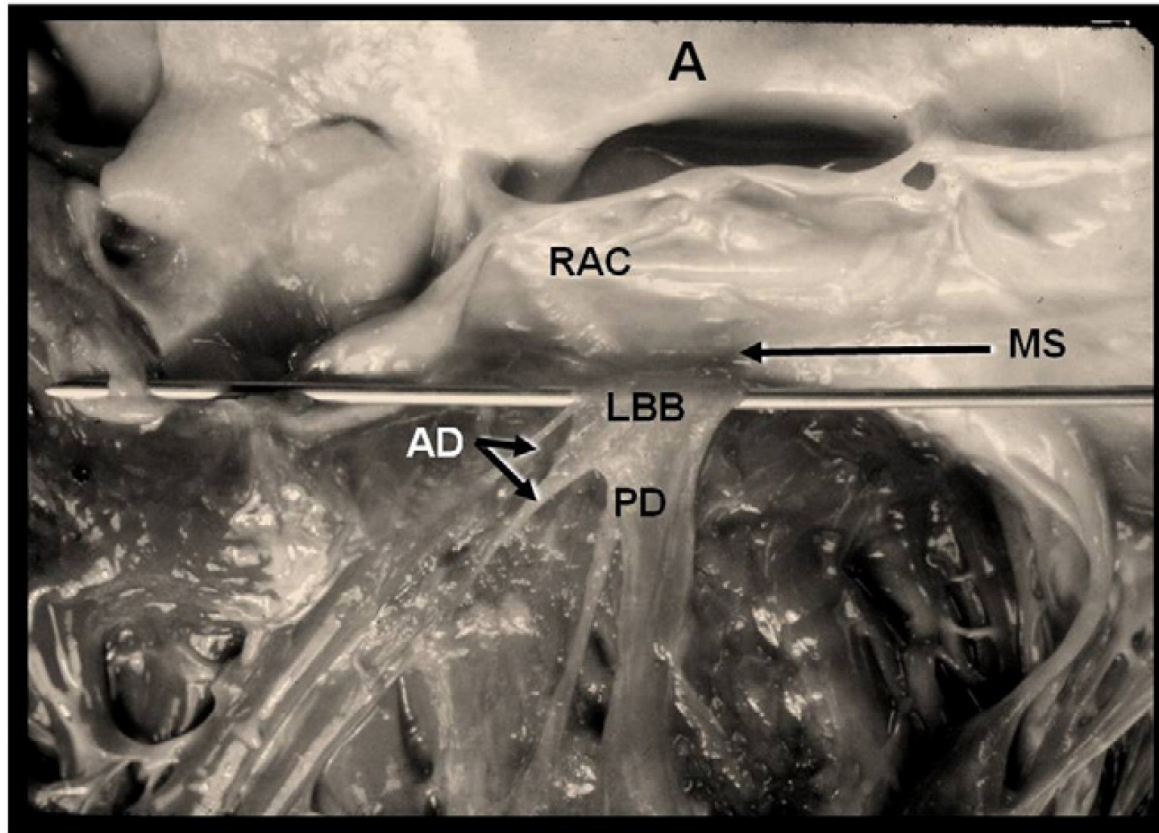
## KEYWORDS

intraventricular conduction system, left septal fascicle, left septal fascicular block









Human heart. The LBB (LBB) emerges in the subaortic region. The membranous septum (MS) is almost absent and the aortic valve lies directly over the LBB, which gives off the anterior division (AD) and posterior division (PD) from its very beginning. The membranous septum is strikingly small or practically absent in this case. The distance between the branching portion of the bundle of His from the aortic valve depends on the size of the MS. The larger the MS, the lesser the possibility that the aortic valve pathology involves this crucial part of the conducting system. A: aorta; RAC right aortic cusp.

# Unrecognized LPFB cases noted in the iconography of published papers

Case ID	References	Figure	12 lead ECG findings	Genetic analysis	CMR data	Endomyocardial biopsy data/ Histologic data
Case 1	Protonotarios A et al <sup>1</sup> <i>J Electrocardiol.</i> 2013	Fig. 1	LPFB, LQRSV in limb and left precordial leads, TWI V5-V6, fQRS in lead V1.	Not performed	Not performed	Fibrotic subepicardial and midwall bands on anterolateral and posterolateral LV walls and on the interventricular septum. Myocyte loss with fibro-fatty replacement and myocyte abnormalities
Case 2	Zorzi A et al <sup>2</sup> <i>Circ Arrhythm Electrophysiol.</i> 2016	Fig. 4	LPFB Inferolateral TWI Pathological Q in II-III-aVF Prominent R wave V1 LQRSV in left precordial leads	Not performed	Sub/midmyocardial LGE with a stria pattern involving the infero-lateral LV wall	Extensive fibrosis in the sub- and midmyocardial layers (inferolateral LV), focal and patchy fatty infiltration. Cardiomyocytes hypertrophic with dysmetric and dysmorphic nuclei, with cytoplasmic vacuolization.
Case 3	Oloriz T et al <sup>3</sup> <i>Europace.</i> 2016	Fig. 1 -right panel	LPFB - R/S ratio V1 $\geq 0.5$	Not performed	Infero-lateral scar	Not performed
Case 4	Miles C et al <sup>4</sup> <i>Circulation.</i> 2019	Fig. 4	LPFB – fQRS in-septal leads First-degree AV block, Inferolateral TWI – LQRSV in limb leads, prolonged terminal activation duration in V1	Not performed	Extensive LV LGE, including near transmural LGE of lateral wall and midwall of anterior wall.	Myocyte degeneration and fibrofatty infiltration within the posterolateral wall of the LV (extending transmurally).
Case 5	Saguner AM et al <sup>5</sup> <i>Circulation.</i> 2015	Fig. 2	LPFB Early repolarization in the inferior leads and QRS fragmentation in aVL	Heterozygous pathogenic variant in the plakophilin-2 (c.2392A>G, p.T798A) and desmoglein-2 (c.877A>G, p.I293V) genes.	Fibrofatty infiltration involving epi- and midmyocardial layers of the inferolateral, anterolateral, and septal LV wall.	Unremarkable
Case 6	d'Amati G et al <sup>6</sup> <i>Int J Cardiol.</i> 2016	Fig. 1	LPFB	Not pathogenic mutation	Not performed	Fibro-adipose replacement (LV postero-lateral wall). Myocytes enlarged, dysmorphic nuclei

Case 7	Blom LJ et al <sup>7</sup> <i>Heart Rhythm Case Rep.</i> 2018	Fig. 1	LPFB - Intra-ventricular conduction delay, J-point elevation in inferior leads	Unclassified variant in the DSG2 gene and a p.Leu729del mutation in the gene SCN5A.	Not performed	Normal
Case 8	Blom LJ et al <sup>7</sup> <i>Heart Rhythm Case Rep.</i> 2018	Fig.2	LPFB TWI V5-V6, I, II, aVF R/S ratio V1 $\geq 1$	Unclassified variant plakophilin-2 gene and a pathogenic c.40-42delAGA mutation in the phospholamban (PLN) gene.	Not performed	Normal
Case 9	Singh SM et al <sup>8</sup> <i>JACC Case Rep.</i> 2021	Fig.3 (C)	LPFB - R/S ratio V1 $\geq 1$	Not performed	Biventricular apical and anterolateral LGE in the epi- to mid-myocardium	Not performed
Case 10	Pirou N et al <sup>9</sup> <i>ESC Heart Fail.</i> 2020	Fig.2 (B)	LPFB - TWI V4-V6 LQRSV in limb leads	Pathogenic variant in desmoplakin c.3924del	High T2 Intensity and subepicardial circumferential LGE.	Not performed
Case 11	Reichl K et al <sup>10</sup> <i>Circ Genom Precis Med.</i> 2018	Fig.1 (A)	LPFB	Heterozygous variant was identified in exon 23 of the DSP gene—c.3415_3417del TATinsG.	Epi- and midmyocardial LGE and fatty replacement in anterior, lateral and inferior LV and basal inferior RV segments.	Not performed
Case 12	Chmielewski P et al <sup>11</sup> <i>Diagnostics</i> 2020	Fig.2 (A)	LPFB TWI V1-V3 LQRSV, prolonged terminal activation duration in V1, fQRS II-III- aVF.	DSP NM_004415.4:c.3737dupA (p.Asn1246Lysfs Ter7) PKP2 NM_004572.3:c.2636T>C (p.Leu879Pro) NLRP3 NM_004895.4:c.1469G>A (p.Arg490Lys)	Moderate subepicardial and midwall areas of LGE with a ringlike pattern	
Case 13	Poller W et al <sup>12</sup> <i>J Am Heart Assoc.</i> 2020	Fig.3 (C)	LPFB TWI inferolateral leads	Dystrophin c.3970C>T, p.Arg1324Cys, desmoplakin c.4372C>T, p.Arg1458Ter,	Multifocal subepicardial posteroseptal and lateral LGE.	Low-level immune cell infiltration in the absence of intramyocardial virus genomes
				nexilin F-actin-binding protein c.154G>C, p.Asp52His		
Case 14	Vahidinezhad H et al <sup>13</sup> <i>Sci Rep.</i> 2020	Fig.2 (A)	LPFB, TWI V1-V3 Prolonged V3 terminal QRS duration- LQRSV limb leads	JUP mutation	Normal	Not performed
Case 15	Chen P et al <sup>14</sup> <i>Int J Cardiol.</i> 2020	Fig. 2 (A)	LPFB, TWI V1-V3. R/S ratio V1 $\geq 1$	DSG2 p.Leu237Ter mutation	Dilation of both ventricles	Not performed
Case 16	Protonotarios N et al <sup>15</sup> <i>Br Heart J.</i> 1986	Fig. 3 (A)	LPFB, QRS prolongation, LQRSV, TWI precordial leads.	Not performed (JUP mutation?)	Not performed	Not performed
Case 17	Chen V et al <sup>16</sup> <i>Eur Heart J Case Rep</i> 2022	Fig 2	LPFB	Pathogenic heterozygous DSP gene truncation variant (p.R1951X) and the pathogenic HFE variant (p.H63D).	Subepicardial basal-anterior, basal anterolateral, mid-inferior and mid-anteroseptal areas of LGE.	Mild lymphocytic myocarditis, interstitial fibrosis, and myocyte hypertrophy



Europace  
doi:10.1093/europace/euv360

Europace Advance Access published November 20, 2015

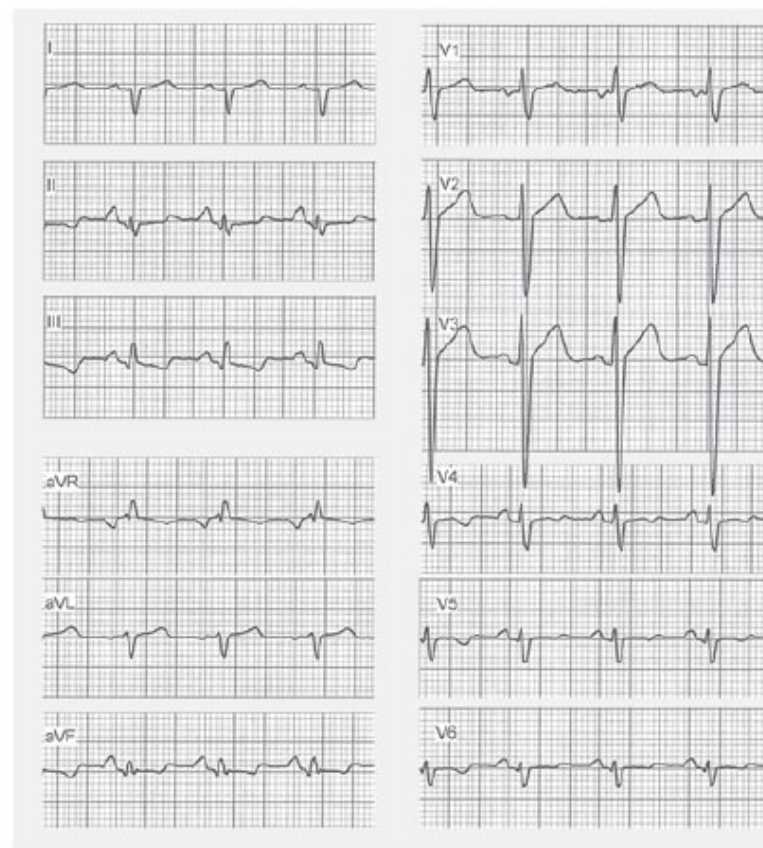
## CLINICAL RESEARCH

# The value of the 12-lead electrocardiogram in localizing the scar in non-ischaemic cardiomyopathy

**Teresa Oloriz<sup>1</sup>, Hein J.J. Wellens<sup>2</sup>, Giulia Santagostino<sup>1</sup>, Nicola Trevisi<sup>1</sup>, John Silberbauer<sup>1</sup>, Giovanni Peretto<sup>1</sup>, Giuseppe Maccabelli<sup>1</sup>, and Paolo Della Bella<sup>1\*</sup>**

<sup>1</sup>Arrhythmia Units and Electrophysiology Laboratories, Ospedale San Raffaele, Via Olgettina 60, Milan, Italy; and <sup>2</sup>Cardiovascular Research Center, Maastricht, The Netherlands

Received 16 June 2015; accepted after revision 7 September 2015





## Original Article

OPEN

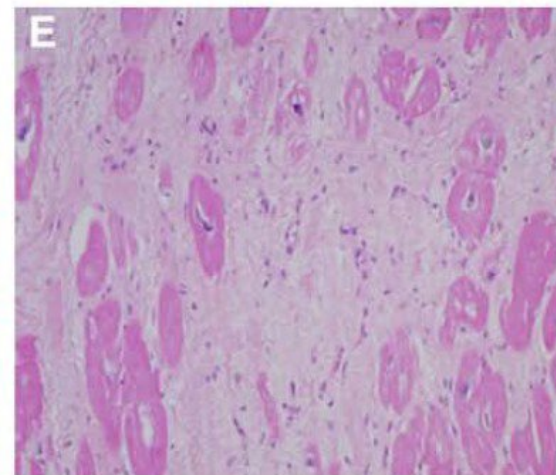
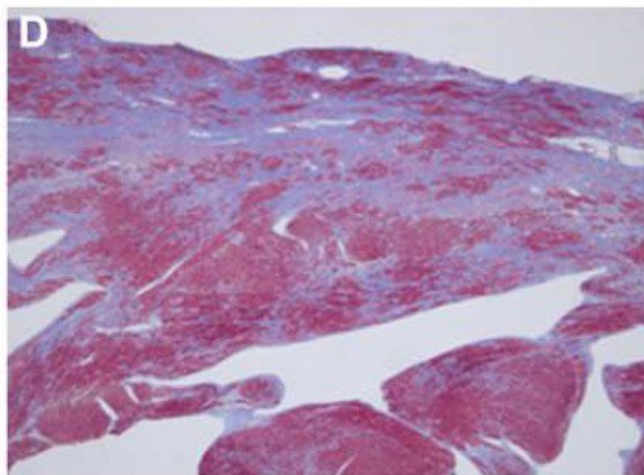
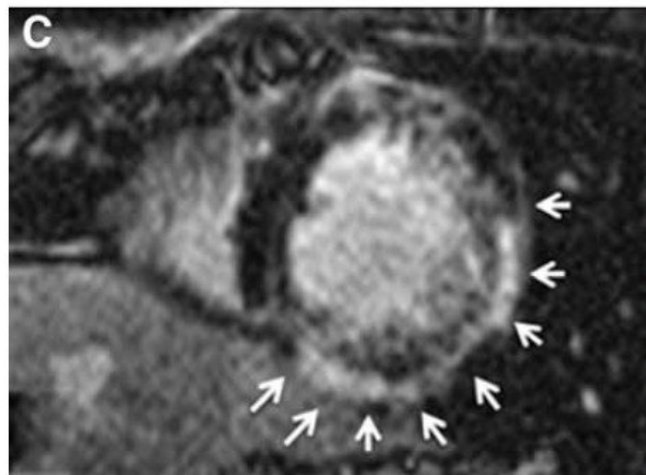
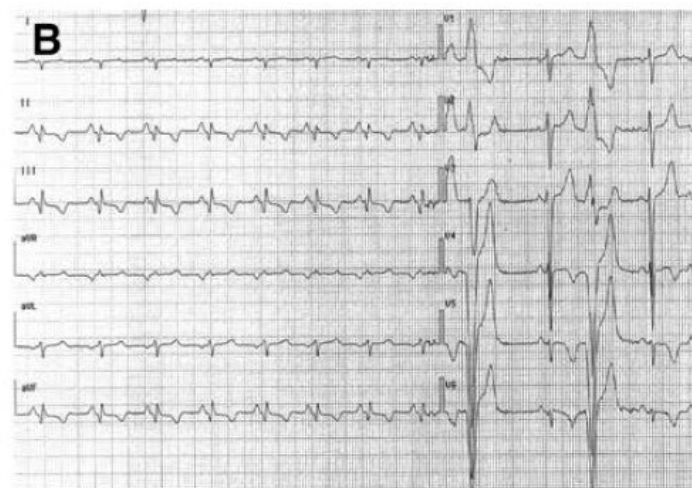
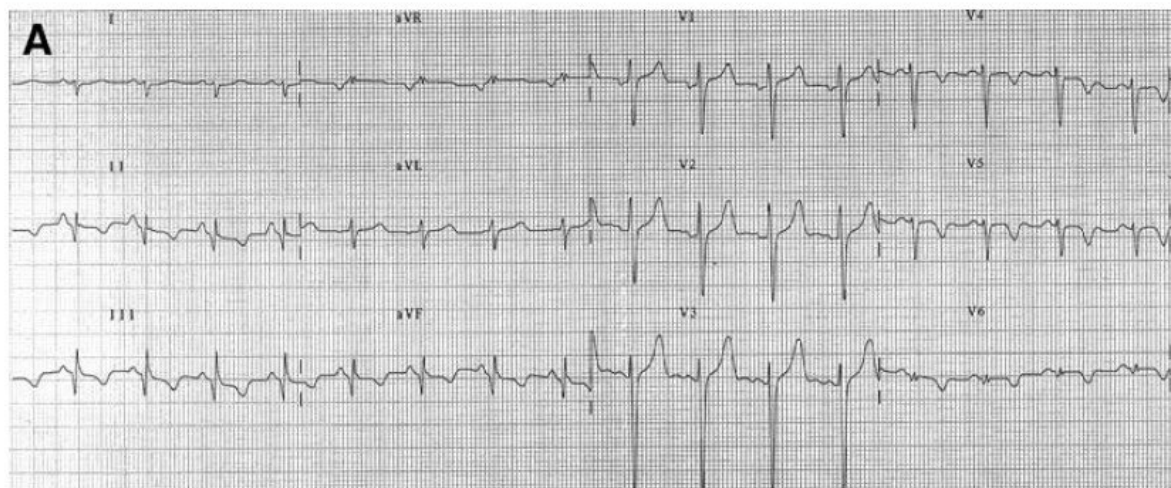
### Nonischemic Left Ventricular Scar as a Substrate of Life-Threatening Ventricular Arrhythmias and Sudden Cardiac Death in Competitive Athletes

Alessandro Zorzi, MD\*; Martina Perazzolo Marra, MD, PhD\*; Ilaria Rigato, MD, PhD;  
Manuel De Lazzari, MD; Angela Susana, MD; Alice Niero, MD; Kalliopi Pilichou, BS, PhD;  
Federico Migliore, MD, PhD; Stefania Rizzo, MD, PhD; Benedetta Giorgi, MD;  
Giorgio De Conti, MD; Patrizio Sarto, MD; Luis Serratosa, MD; Giampiero Patrizi, MD;  
Elia De Maria, MD; Antonio Pelliccia, MD; Cristina Basso, MD, PhD;  
Maurizio Schiavon, MD; Barbara Bauce, MD, PhD; Sabino Iliceto, MD;  
Gaetano Thiene, MD; Domenico Corrado, MD, PhD

**Background**—The clinical profile and arrhythmic outcome of competitive athletes with isolated nonischemic left ventricular (LV) scar as evidenced by contrast-enhanced cardiac magnetic resonance remain to be elucidated.

**Methods and Results**—We compared 35 athletes (80% men, age: 14–48 years) with ventricular arrhythmias and isolated LV subepicardial/midmyocardial late gadolinium enhancement (LGE) on contrast-enhanced cardiac magnetic resonance (group A) with 38 athletes with ventricular arrhythmias and no LGE (group B) and 40 healthy control athletes (group C). A stria LGE pattern with subepicardial/midmyocardial distribution, mostly involving the lateral LV wall, was found in 27 (77%) of group A versus 0 controls (group C;  $P<0.001$ ), whereas a spotty pattern of LGE localized at the junction of the right ventricle to the septum was respectively observed in 11 (31%) versus 10 (25%;  $P=0.52$ ). All athletes with stria pattern showed ventricular arrhythmias with a predominant right bundle branch block morphology, 13 of 27 (48%) showed ECG repolarization abnormalities, and 5 of 27 (19%) showed echocardiographic hypokinesis of the lateral LV wall. The majority of athletes with no or spotty LGE pattern had ventricular arrhythmias with a predominant left bundle branch block morphology and no ECG or echocardiographic abnormalities. During a follow-up of  $38\pm 25$  months, 6 of 27 (22%) athletes with stria pattern experienced malignant arrhythmic events such as appropriate implantable cardiac defibrillator shock ( $n=4$ ), sustained ventricular tachycardia ( $n=1$ ), or sudden death ( $n=1$ ), compared with none of athletes with no or LGE spotty pattern and controls.

**Conclusions**—Isolated nonischemic LV LGE with a stria pattern may be associated with life-threatening arrhythmias and sudden death in the athlete. Because of its subepicardial/midmyocardial location, LV scar is often not detected by echocardiography. (*Circ Arrhythm Electrophysiol*. 2016;9:e004229. DOI: 10.1161/CIRCEP.116.004229.)



## Images in Cardiovascular Medicine

### **Arrhythmogenic Left Ventricular Cardiomyopathy Suspected by Cardiac Magnetic Resonance Imaging, Confirmed by Identification of a Novel Plakophilin-2 Variant**

Ardan M. Saguner, MD; Beate Buchmann, MD; Daniel Wyler, MD; Robert Manka, MD;  
Alexander Gotschy, MD; Argelia Medeiros-Domingo, MD, PhD; Corinna Brunckhorst, MD;  
Firat Duru, MD; Kurt A. Mayer, MD

A 26-year-old man was referred for family screening and cardiologic workup by the Institute of Legal Medicine. His mother recently succumbed to sudden cardiac death at work at 49 years of age. Her macroscopic and microscopic autopsy revealed arrhythmogenic right ventricular (RV) cardiomyopathy/dysplasia (ARVC/D) with diffuse left ventricular (LV) involvement. The 26-year-old patient, who has never engaged in competitive sports, reported a history of syncope without injury while playing leisure soccer 7 years ago. Since then, he has rarely felt palpitations. There was no history of infection within the last 12 months before the cardiologic workup. Clinical findings were normal.

A 12-lead-surface ECG demonstrated notched early repolarization in the inferior leads and QRS fragmentation in aVL but no ECG criteria according to the 2010 ARVC/D Task Force. Signal-averaged ECG was unremarkable, and 24-hour Holter ECG revealed >1000 premature ventricular contractions with 3 different morphologies.

Laboratory parameters were within the normal range, particularly for C-reactive protein, brain natriuretic peptide, and troponin T. Transthoracic 2- and 3-dimensional echocardiography (transthoracic echocardiography), RV angiography, and 3-D electroanatomical endocardial RV voltage mapping were unremarkable.

Cardiac magnetic resonance imaging confirmed the absence of RV structural abnormalities but revealed diffuse fibrofatty infiltration (late gadolinium enhancement) within the LV wall, involving primarily the epicardial and midmyocardial layers of the inferolateral, anterolateral, and septal LV wall. Biventricular dimensions and global RV and LV function were normal but the LV inferior and anterolateral wall displayed localized hypokinesia, corresponding well with the regions with late gadolinium enhancement. Endomyocardial biopsy of the RV septum was unremarkable.

Genetic testing for desmosomal genes revealed a heterozygous pathogenic variant in the plakophilin-2 (c.2392A>G, p.T798A) and desmoglein-2 (c.877A>G, p.I293V) genes.

(Circulation. 2015;132:e38-e40. DOI: 10.1161/CIRCULATIONAHA.115.017284.)



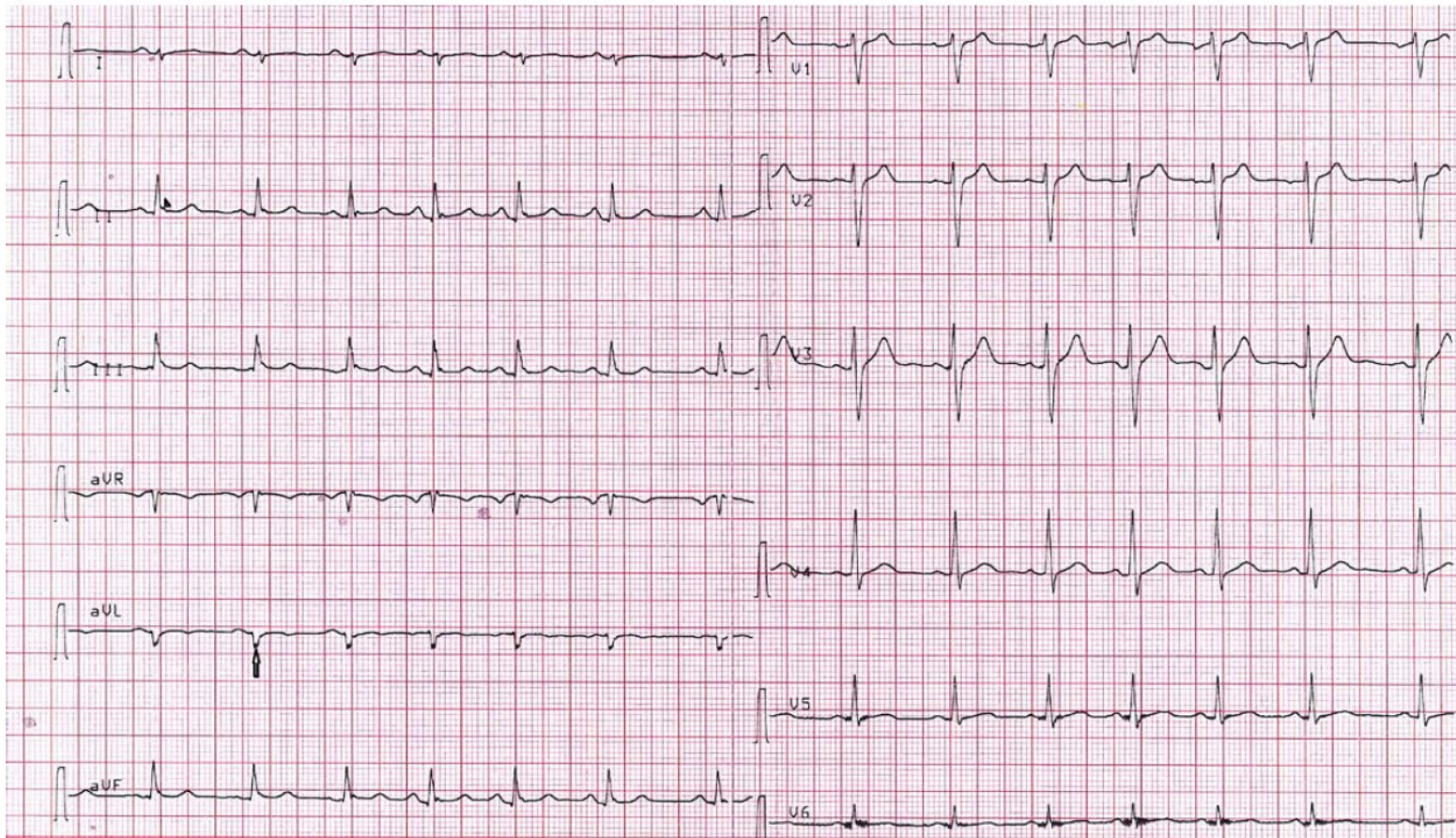
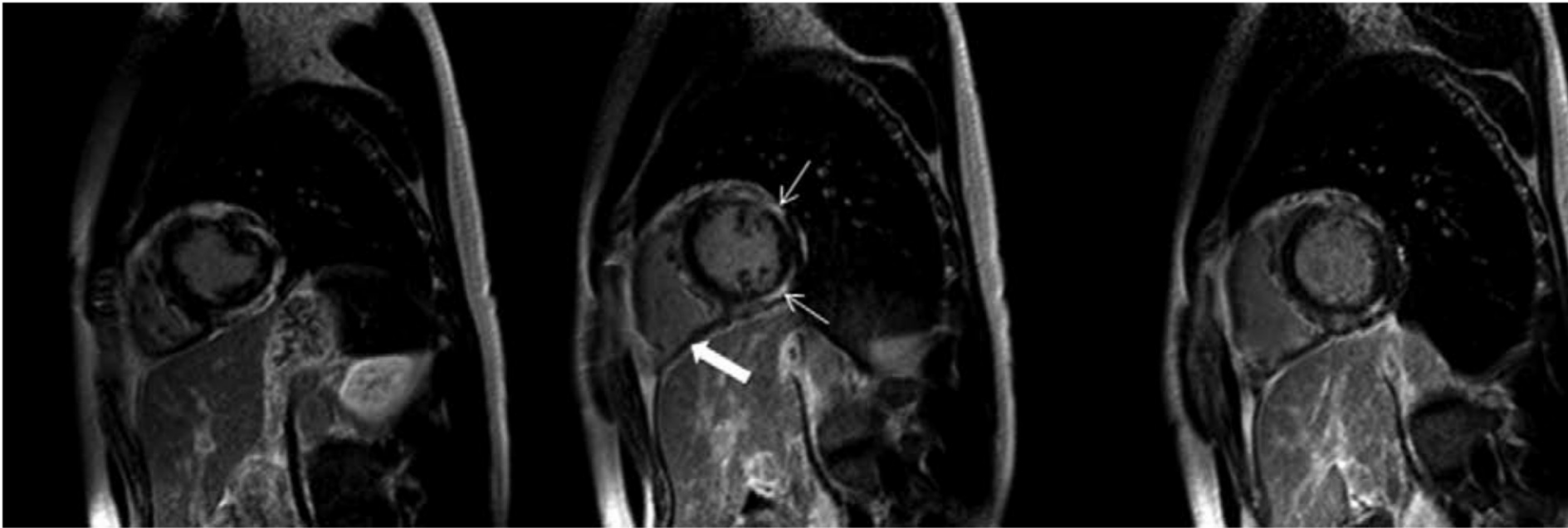
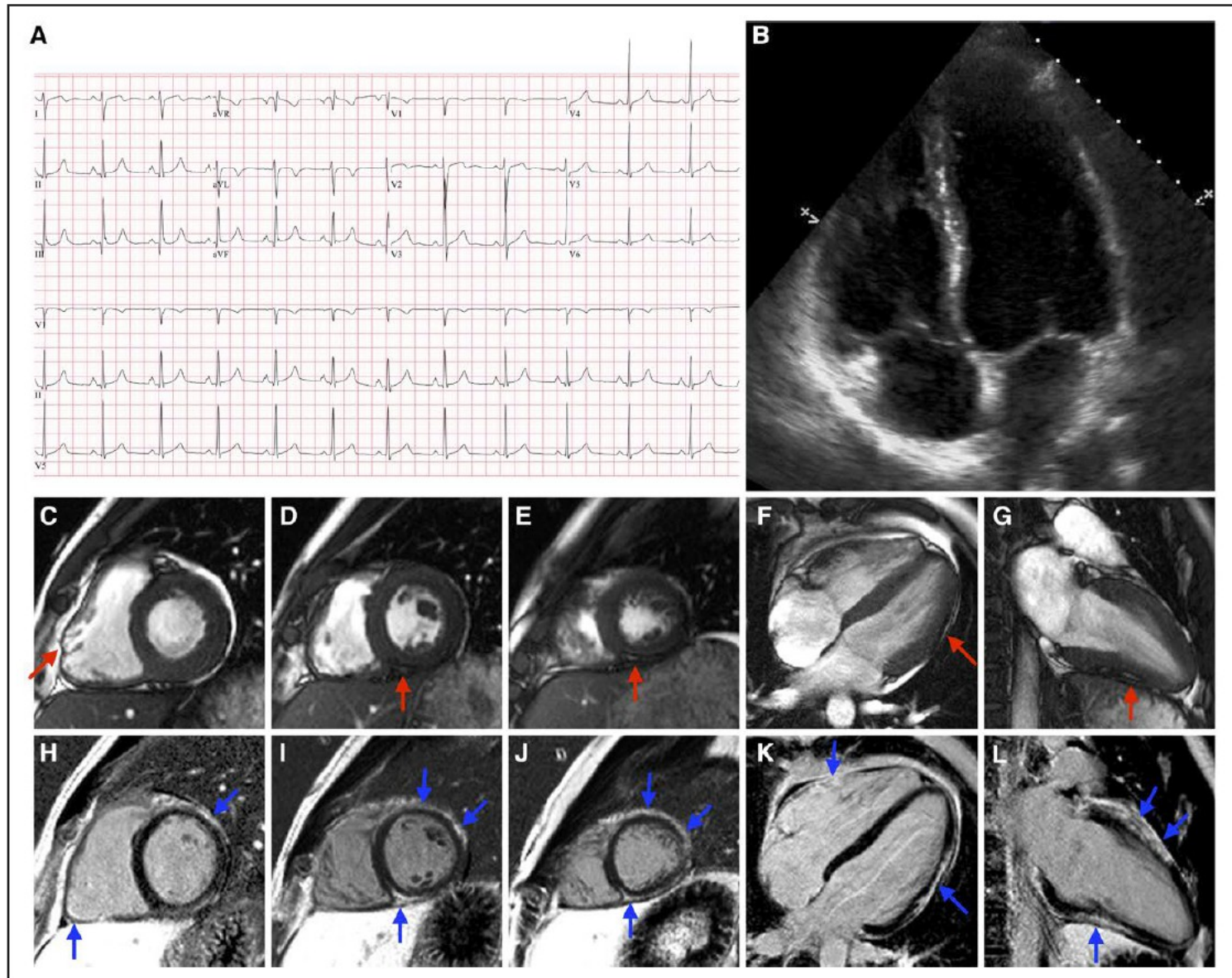


Figure 2. The 12-lead ECG (25 mm/s, 1 mm/mV) of a patient with arrhythmogenic left ventricular cardiomyopathy (ALVC) does not fulfill any diagnostic ECG criteria for arrhythmogenic right ventricular cardiomyopathy/dysplasia or ALVC. Of note, notched early repolarization in the inferior leads (II, III, and aVF; arrowhead in lead II) and QRS fragmentation in aVL (arrow) are visible, but the significance of these findings remains unclear.



Cardiac magnetic resonance imaging of the patient reveals late gadolinium enhancement (left to right: apical, midventricular, basal), mainly within the epicardial and midmyocardial layers of the left ventricle (LV), compatible with fibrofatty infiltration involving primarily the inferolateral, anterolateral, and septal LV segments (thin arrows). Note that right ventricular (RV) dimensions are normal, and no late gadolinium enhancement is visible within the RV wall (bold arrow). Biventricular function is preserved.





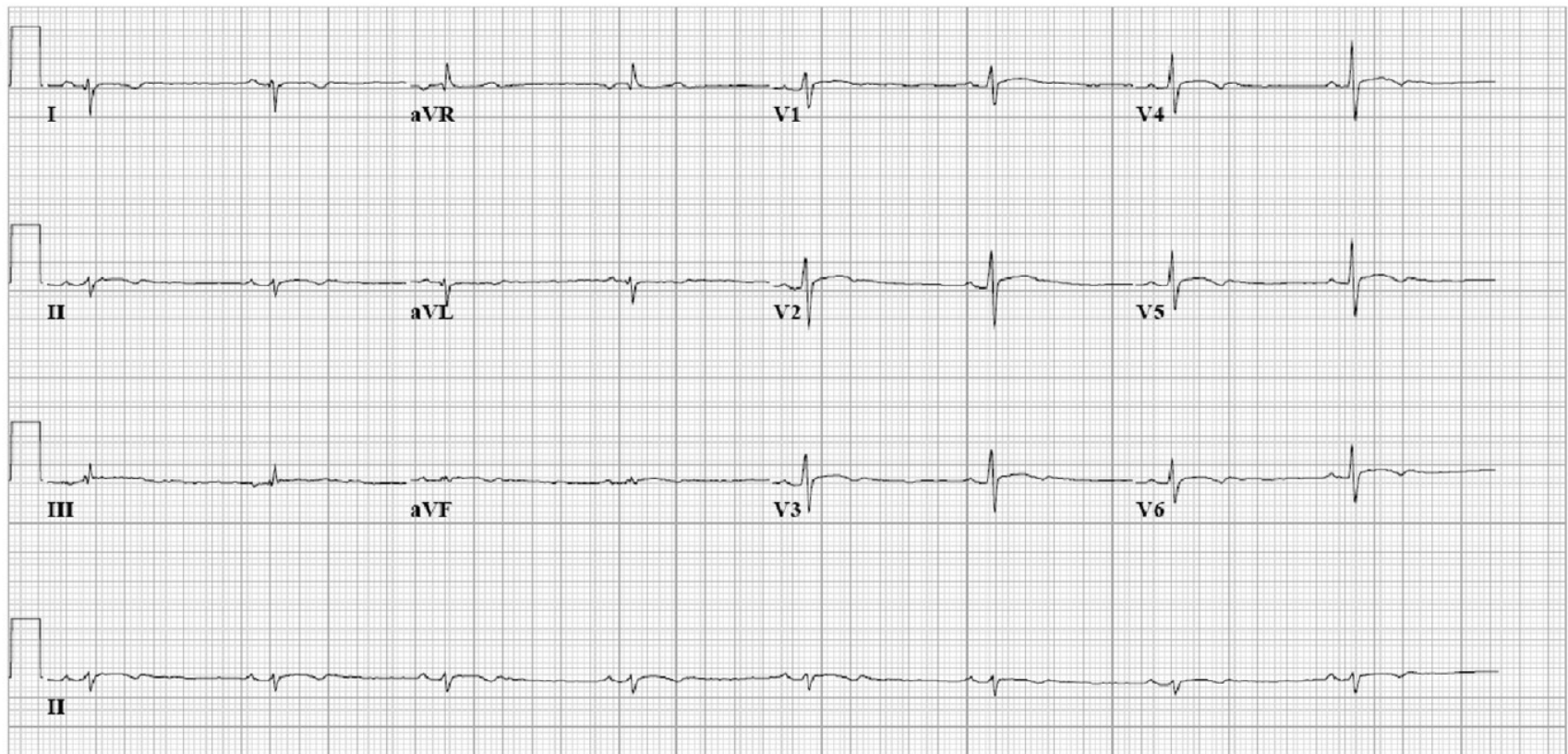


# Late evolution of arrhythmogenic cardiomyopathy in patients with initial presentation as idiopathic ventricular fibrillation

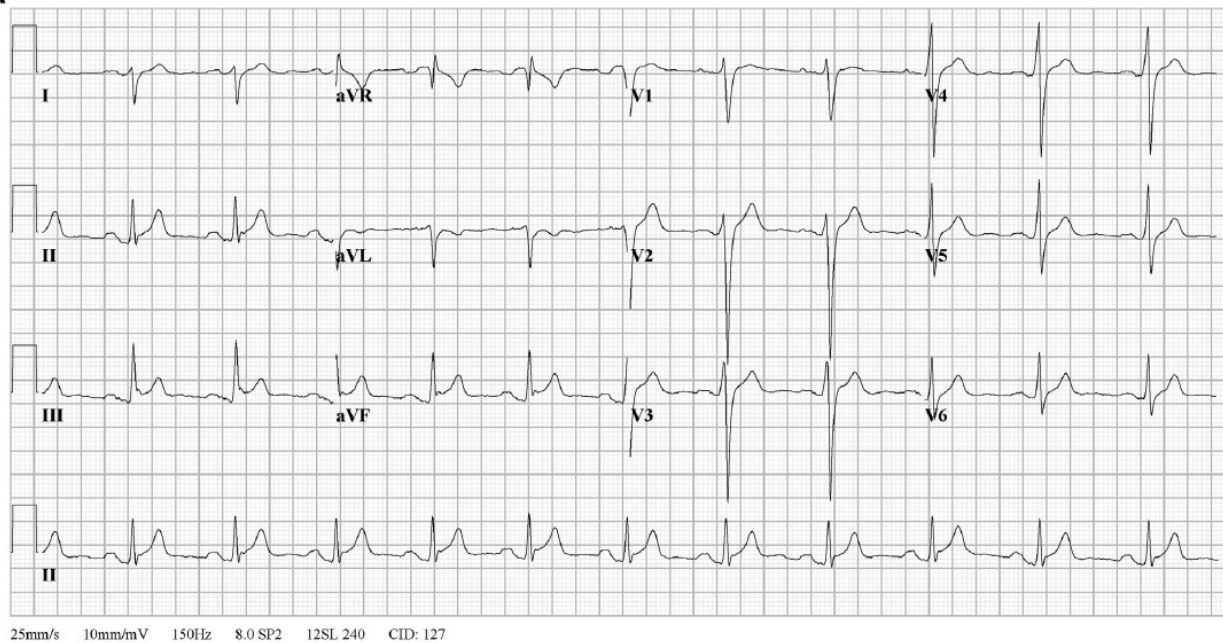
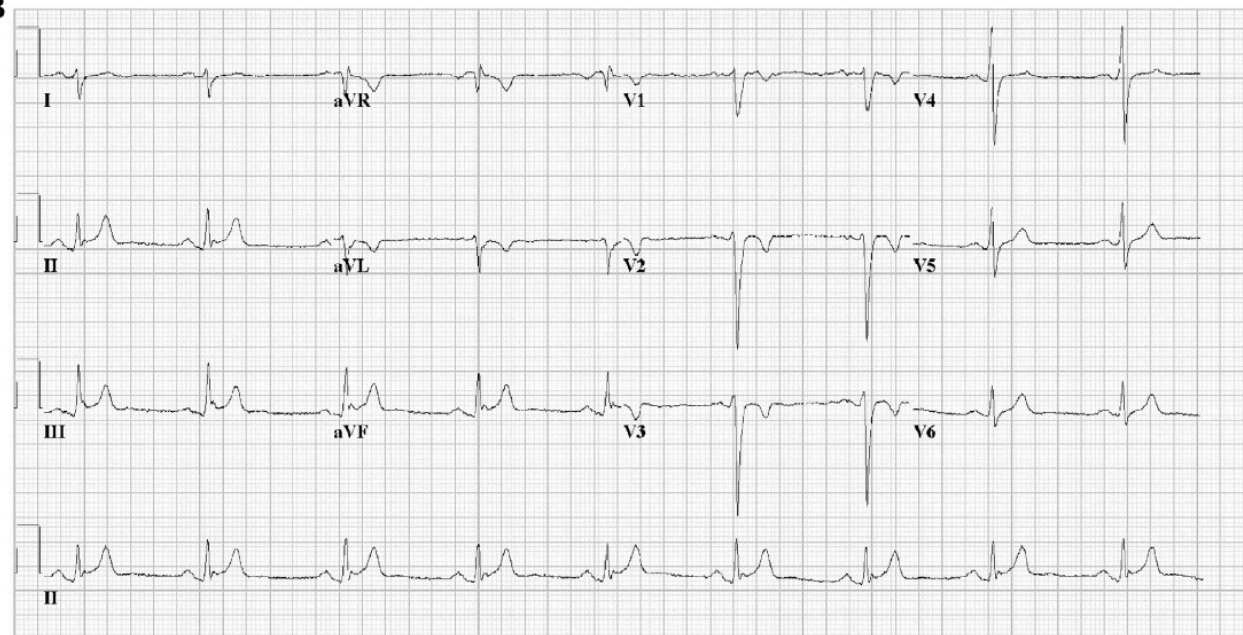


Lennart J. Blom, MD,<sup>\*</sup> Anneline S.J.M. Te Riele, MD, PhD,<sup>\*</sup> Aryan Vink, MD, PhD,<sup>†</sup>  
Richard N.W. Hauer, MD, PhD,<sup>\*</sup> Rutger J. Hassink, MD, PhD<sup>\*</sup>

**A**



25mm/s 10mm/mV 150Hz 8.0 SP2 12SL 240 CID: 127

**A****B**



## CASE REPORT

## CLINICAL CASE SERIES

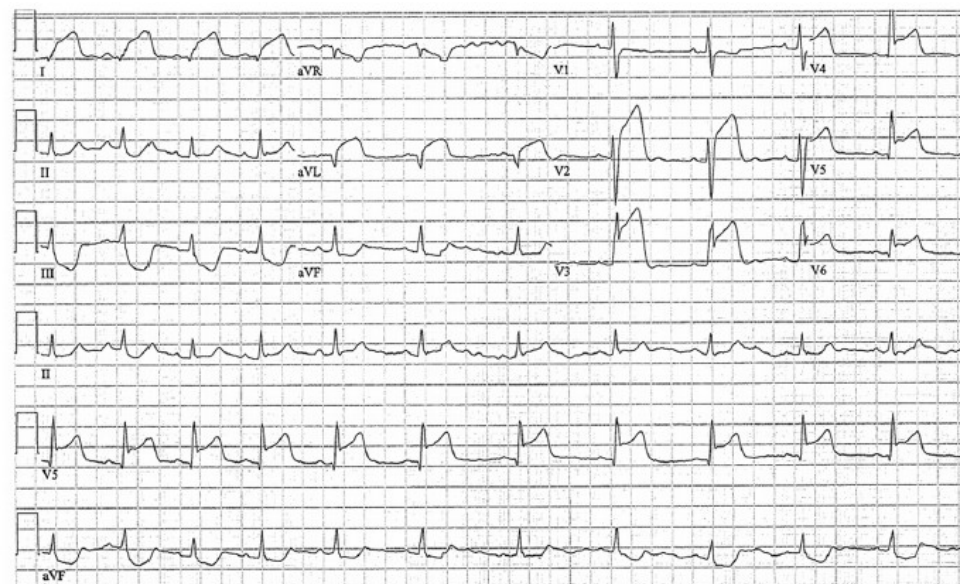
## Acute Myocardial Infarction-Like Events in Related Patients With a Desmoplakin-Associated Arrhythmogenic Cardiomyopathy

Sajya M. Singh, BS,<sup>a</sup> Scott W. Sharkey, MD,<sup>a</sup> Susan A. Casey, RN,<sup>a</sup> Kevin M. Harris, MD,<sup>a</sup> Christina M. Thaler, MD,<sup>a</sup>  
Mina Chung, MD,<sup>b</sup> Allison Berg, MS, CGC,<sup>c</sup> Mosi K. Bennett, MD,<sup>a</sup> Emily R. Ducanson, MD,<sup>a</sup>  
Shannon Mackey-Bojack, MD,<sup>d</sup> Jay D. Sengupta, MD<sup>a</sup>

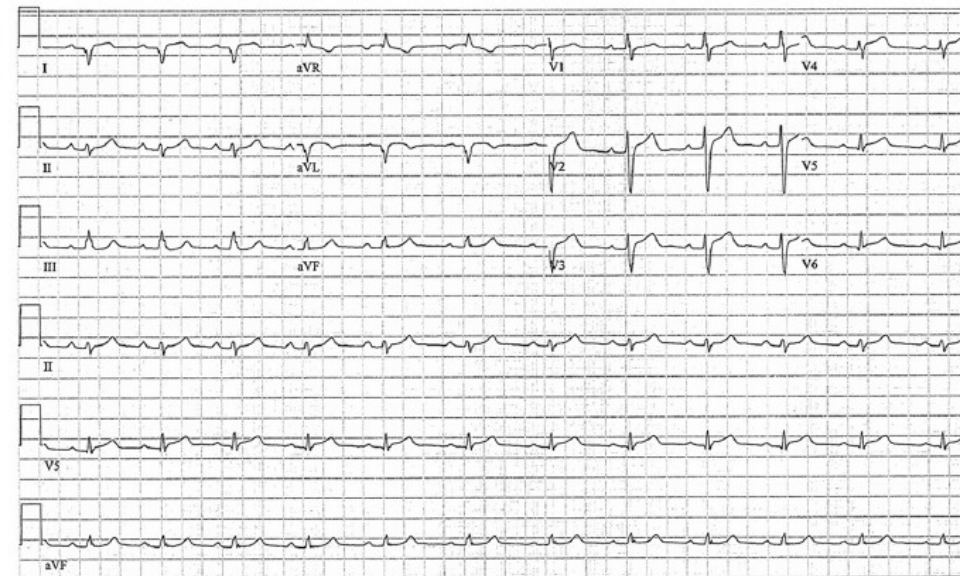
ADVANCED



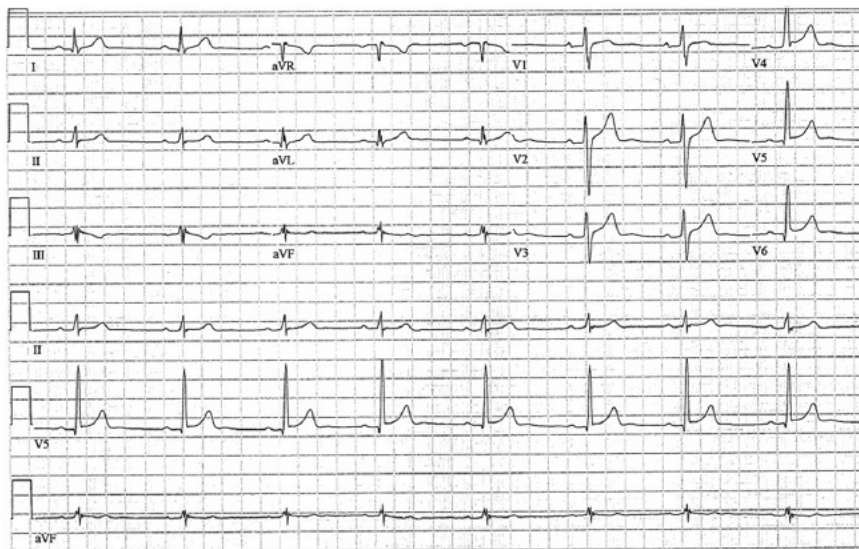
B



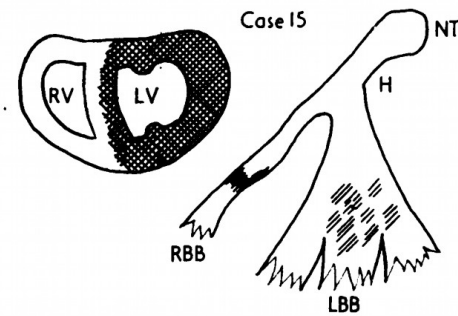
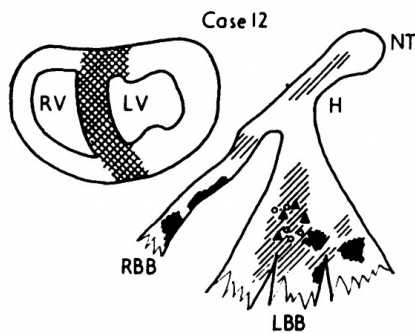
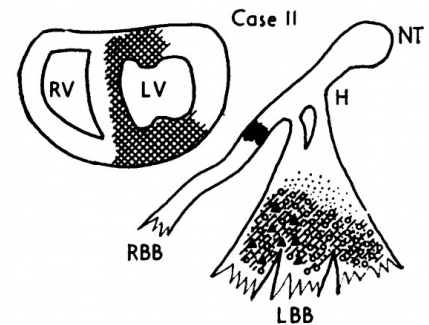
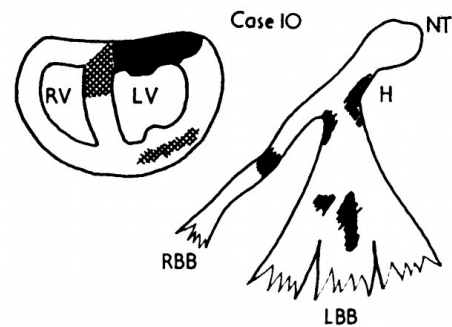
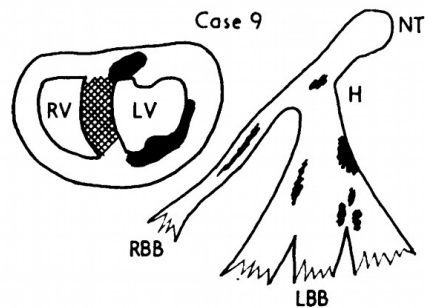
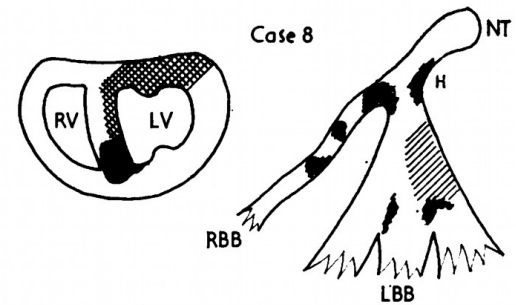
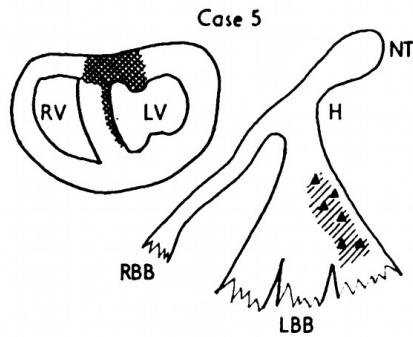
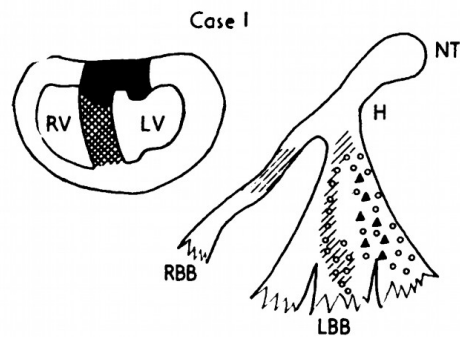
C



A







Conduction system lesions

Cloudy swelling, vacuolization

Leucocytic infiltration

Haemorrhage

Acute necrosis

Chronic (sclerosis, atrophy)

Myocardial infarction

Acute & subacute stage

Chronic stage

RV=Right ventricle; LV=Left ventricle

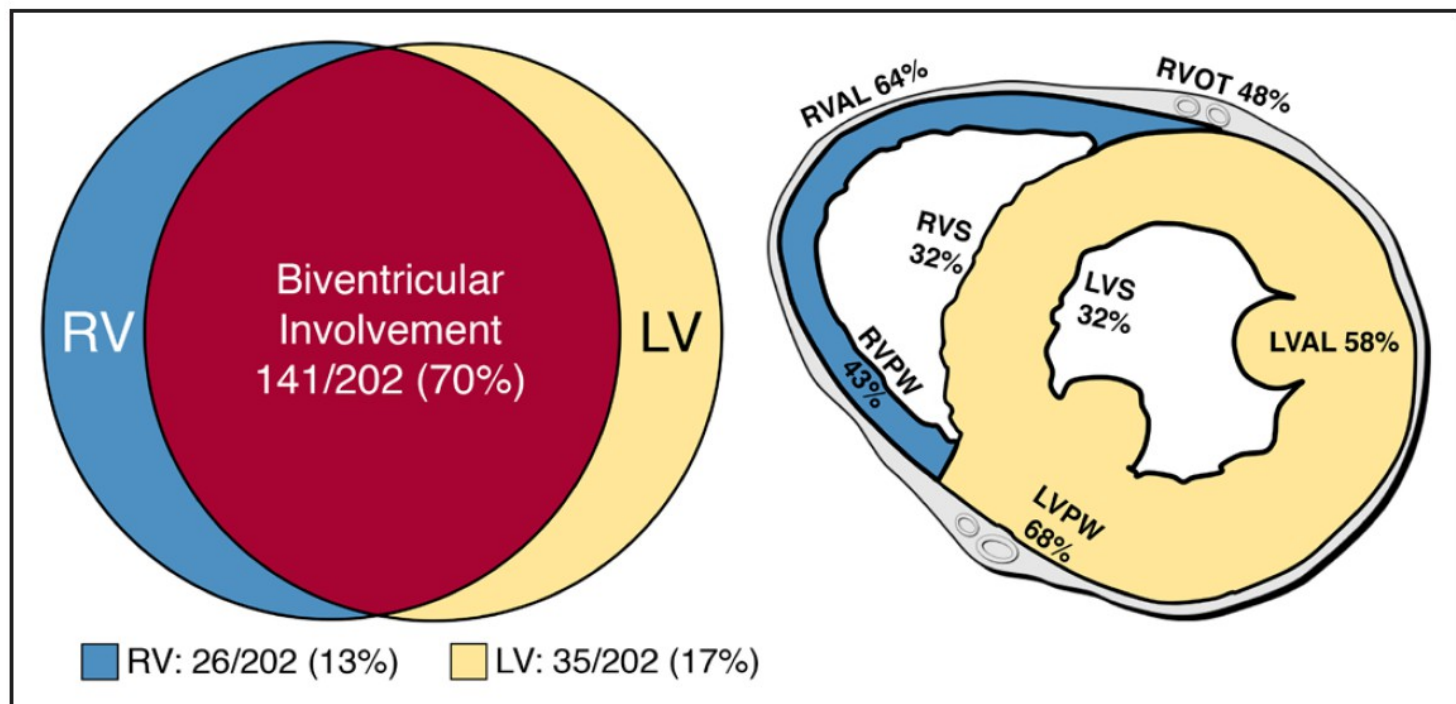
NT: Node of Tawara

H: His bundle

RBB: Right bundle-branch

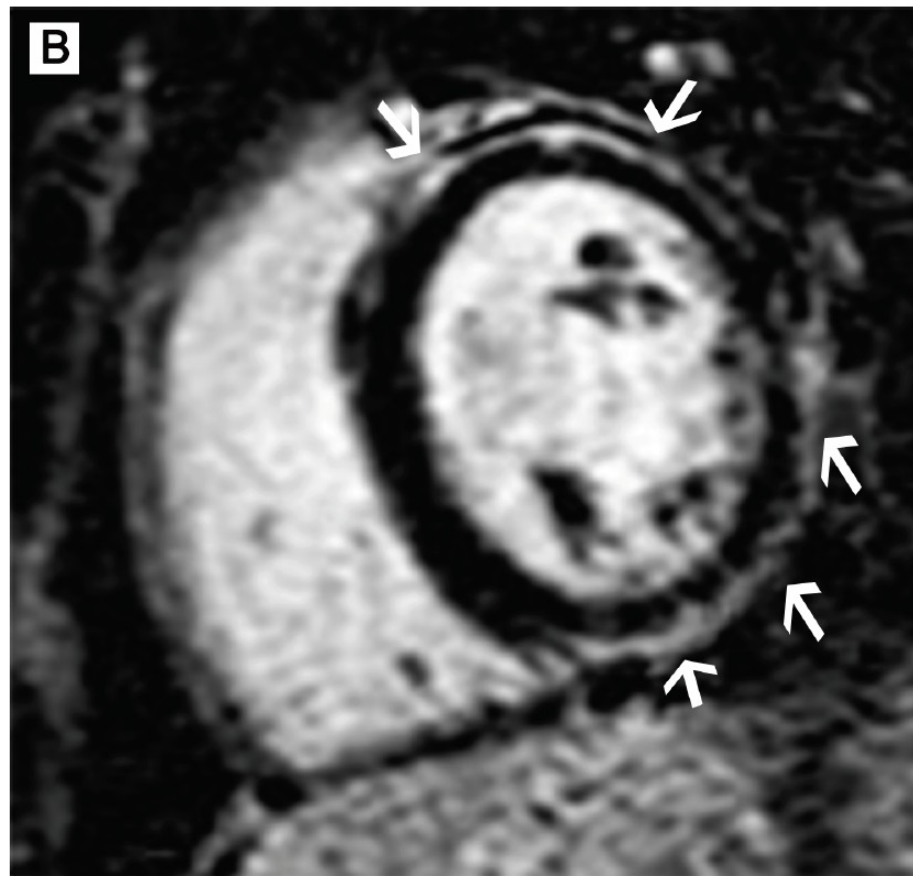
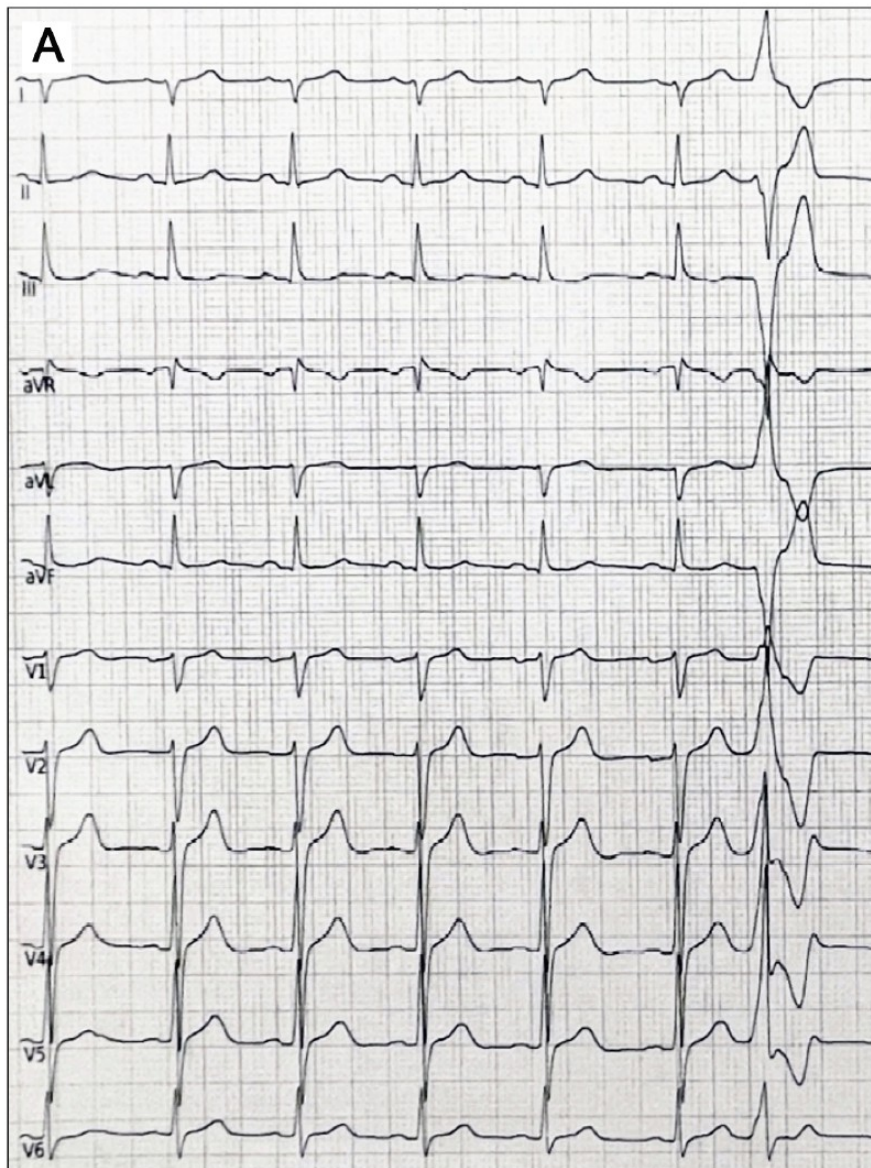
LBB: Left

## Distribution and location of disease involvement in arrhythmogenic cardiomyopathy









Patient #2, 19-year-old man, pathogenic variant in desmoplakin (c.1707-1708insAC,p.Met571Glnfs\*8)

**“Like good wines, some research  
improves after resting for a while”**

**Mauricio  
Rosenbaum**



Festina lente